

Variable Stars in Young Open Cluster NGC 2244

G. Michalska^{1*}

¹*Instytut Astronomiczny, Uniwersytet Wrocławski, Kopernika 11, 51-622 Wrocław, Poland*

Accepted ... Received ...; in original form ...

ABSTRACT

We present results of a $UBVI_C$ variability survey in the young open cluster NGC 2244. In total, we found 245 variable stars. Most of them, 211 stars, are variables with irregular variations. Furthermore, 23 periodic variables were found. We also detected four candidates for δ Scuti stars and 7 eclipsing binaries.

Based on the mid-infrared *Spitzer* and WISE photometry and near infrared JHK_S 2MASS photometry we classified 104 young stellar sources among our variables: 1 Class I object, 1 Class I/flat spectrum object, 4 flat spectrum objects, 91 Class II objects and 7 transition disk objects. This classification, together with $r'i'H\alpha$ IPHAS photometry and JHK UKIDSS photometry, were used for identification of pre-main sequence stars among irregular and periodic variables. In this way, 97 CTTS candidates (96 irregular and one periodic variable), 68 WTTS candidates (54 irregular and 14 periodic variables) and 6 Herbig Ae/Be stars were found.

For 223 variable stars we calculated membership probability based on proper motions from Gaia DR2 catalogue. Majority of them, 143 stars, are cluster members with probability greater than 70 percent. For only 36 variable stars the membership probability is smaller than 20 percent.

Key words: open clusters and associations: individual: NGC 2244 – photometric – stars: pre-main sequence, circumstellar matter – infrared: stars – stars: variables: T Tauri, Herbig Ae/Be, δ Scuti stars, eclipsing binaries.

1 INTRODUCTION

Stars in open clusters form in approximately the same chemical environment and have nearly the same age and distance. Multiwavelength photometry of young stellar clusters allows studying stars at the pre-main sequence (PMS) stage of evolution. The photometric variations in these stars are believed to originate from several mechanisms like rotation of a spotted star or obscuration by circumstellar matter (see Herbst et al. 1994, and references therein). PMS stars are usually divided into two main groups: low mass ($< 2.5 M_\odot$) T Tauri stars (TTSS) and more massive ($1.5 - 15 M_\odot$) Herbig Ae/Be (HAeBe) stars (Artemenko et al. 2010). Depending on the strength of the emission in the $H\alpha$ line, the TTSS are divided into weak line TTSS (WTTSS; with equivalent widths (EW), smaller than 10 \AA) and classical TTSS (CTTSS; with $\text{EW} > 10 \text{ \AA}$). Both WTTSS and CTTSS show brightness variations in X-ray, ultraviolet, optical and infrared domains.

Photometric variability of CTTSS is irregular. It may be attributed to unsteady accretion from the circumstellar disk as well as rotation of the surface hot and dark spots. The am-

plitudes range from few hundredths to several magnitudes in V band (Herbst et al. 2000). The light variations of WTTSS are periodic and related to the rotation of large dark spots on stellar surface. Typical periods of such changes range between 0.5 and 18 days with amplitudes between 0.03 and 0.3 mag in V band (Semkov 2011).

The HAeBe stars, defined by Herbig (1960), have spectral types earlier than F5 and are characterized by broad emission lines and infrared excess due to a circumstellar disk. They are often located in obscured regions, in the vicinity of bright nebulae. Their light variability is irregular, connected with accretion processes and dust clumps in the surrounding disk. Light curves of many HAeBe stars with spectral types later than A0 and some TTSS show 1–3 mag deep algol-like minima lasting several days to weeks. This class of variable is called UX Orionis stars (UXors), after the prototype star UX Ori (Herbst et al. 1994).

The other interesting group of variable PMS stars are low-mass FU Orionis stars (Herbig 1977) – FUors. The characteristic feature of these objects is an increase in brightness by about 3–6 mag, lasting several months, followed by a slow decay over several years. The brightening is caused by a sudden change in the accretion rate from about $10^{-7} M_\odot \text{ yr}^{-1}$ (typical for TTSS) to $10^{-4} M_\odot \text{ yr}^{-1}$. Their spectral types

* E-mail: michalska@astro.uni.wroc.pl

change from typical for TTS to F or K-type supergiant. The third group of irregularly variable PMS stars are EXors, after the prototype, EX Lupi (Herbig 1989). These stars repeatedly undergo increase in brightness by about 1–4 mag, and, after a few weeks or months, fade back to their original brightness.

The observations (in particular, of stars in very young open clusters) show that some PMS stars pulsate or at least some candidates for PMS pulsating stars can be indicated. In recent years, the number of known PMS pulsating stars increased largely. The most common are PMS δ Sct-type (Zwintz 2008; Díaz-Fraile et al. 2014) and γ Dor-type stars (Zwintz et al. 2013). A hybrid δ Sct/ γ Dor candidate was even found (Ripepi et al. 2011). By now, no confirmed SPB or β Cephei-type PMS star is known, however, although two suspected PMS SPB stars were discovered from the optical photometry obtained by MOST satellite in the region of NGC 2244 (Gruber et al. 2012).

In this paper, we present the results of the search for variable stars in the very young open cluster NGC 2244. The paper is organized as follows. First, we briefly introduce the cluster, our photometric observations, reduction process and transformation to the standard system (Sect. 2). Variable stars found in the field we observed and their membership probability are presented in Sect. 3 and Sect. 4, respectively. The identification of Young Stellar Objects based on *Spitzer* and 2MASS photometry is described in Sect. 5. The classification of PMS variables is discussed in Sect. 6. The results are summarized in Sect. 7.

2 THE CLUSTER AND ITS $UBVI_C$ PHOTOMETRY

2.1 The cluster

The very young open cluster NGC 2244 is associated with the famous Rosette Nebula and located in the Perseus Arm of the Galaxy. Its age, based on isochrone fitting, was estimated for 2–4 Myr, the distance for 1.4–1.7 kpc, and the reddening, in terms of the colour excess $E(B - V)$, for 0.47 mag (Ogura & Ishida 1981; Hensberge et al. 2000; Park & Sung 2002). The cluster is embedded in H II region and is rich in O and B-type stars. Its photometric $UBVI_C$ and $H\alpha$ study was performed by Park & Sung (2002). They classified about 30 O and B-type cluster members. They also discovered 21 PMS stars with $H\alpha$ in emission (four of them are massive H AeBe stars) and six PMS candidates with detectable X-ray emission. A large population of PMS stars in NGC 2244 was also reported by Bonatto & Bica (2009) and Berghöfer & Christian (2002).

The cluster contains O-type β Cephei type star (Briquet et al. 2011), double-lined eclipsing binary V578 Mon (Hensberge et al. 2000) and several other spectroscopic binaries. It also contains one known Ap star, NGC 2244-334 (Bagnulo et al. 2004), having strong magnetic field. This star, however, was outside the field we observed.

2.2 Observations and reductions

The photometric observations of NGC 2244 were carried out with the Yale SMARTS 1-m telescope at Cerro Tololo Inter-American Observatory (CTIO) in Chile. The telescope was equipped with Y4KCam CCD camera covering about $20' \times 20'$ area in the sky. Between December 24, 2008 and January 8,

2009, we collected about 2000 frames in V filter, 170 frames in I_C filter, 150 in B filter, and 70 in U filter. The exposure times ranged from 15 to 200 s, depending on the filter, seeing and sky transparency. All frames were calibrated with the use of Phil Massey scripts¹ designed to Y4KCam. Then, the images were reduced with the DAOPHOT II package (Stetson 1987, Stetson 1992).

2.3 Transformation to the standard system

Our photometry was transformed to the standard system. Since many observed stars show irregular variability, we decided to calculate mean instrumental magnitudes and colours applying 2σ clipping. Then, these mean values were tied to the $UBVI_C$ photometry of NGC 2244 published by Park & Sung (2002). The transformation was based on the photometry of about 400 stars common with these authors. The following transformation equations were obtained:

$$V - v = (0.009 \pm 0.003) \times (v - i) + (13.0030 \pm 0.0017), \quad (1)$$

$$V - I_C = (0.993 \pm 0.002) \times (v - i) + (0.9920 \pm 0.0009), \quad (2)$$

$$B - V = (0.855 \pm 0.003) \times (b - v) + (0.6754 \pm 0.0010), \quad (3)$$

$$U - B = (1.107 \pm 0.008) \times (u - b) + (0.104 \pm 0.003), \quad (4)$$

where u , b , v and i denote the mean instrumental magnitudes from our photometry, while U , B , V , and I_C , the standard magnitudes. The residual standard deviations for the transformation equations were equal to 0.030, 0.016, 0.014 and 0.034 mag for Eq. (1), (2), (3), and (4), respectively.

From the above equations, we computed V magnitudes and the $(V - I_C)$ colour indices for 4058 stars, and the $(U - B)$ and $(B - V)$ colour indices for 989 and 1347 stars, respectively. Standard photometry of the variable stars is given in Table A1² in Appendix. The equatorial coordinates shown in this Table A1, were determined by means of an astrometric transformation of mean stellar positions derived from images with the use of IRAF *cmap/cctran* tasks. As a reference catalogue, we used the UCAC4 catalogue (Zacharias et al. 2013).

2.4 $UBVI_C$ photometry

The magnitudes and colours derived in Sect. 2.3 are shown in the V vs. $(B - V)$ and V vs. $(V - I_C)$ colour-magnitude diagrams (Fig. 1), and in the $(U - B)$ vs. $(B - V)$ and $(U - B)$ vs. $(V - I_C)$ colour-colour diagrams (Fig. 2). The distance of 1.7 kpc, i.e. $(m - M)_0 = 11.1$ mag, the mean colour excesses $E(B - V) = 0.47$ mag, $E(V - I) = 0.6$ mag and the total absorption in V , $A_V = 1.46$ mag, were adopted from Park & Sung (2002). As can be seen in these figures, many stars are in their PMS phase of evolution and plenty of them are variable (coloured symbols). Their position spread between 0.5 and 10 Myr in the colour-magnitude diagrams may be caused by differential reddening towards NGC 2244, mentioned by Berghöfer & Christian (2002), or the stars were formed not at the same time. The variable reddening towards the early-type stars in NGC 2244 was reported by Massey et al. (1995) who

¹ <http://www2.lowell.edu/users/massey/obins/y4kcamred.html>.

² The full version of Table A1 is available in electronic form from the CDS.

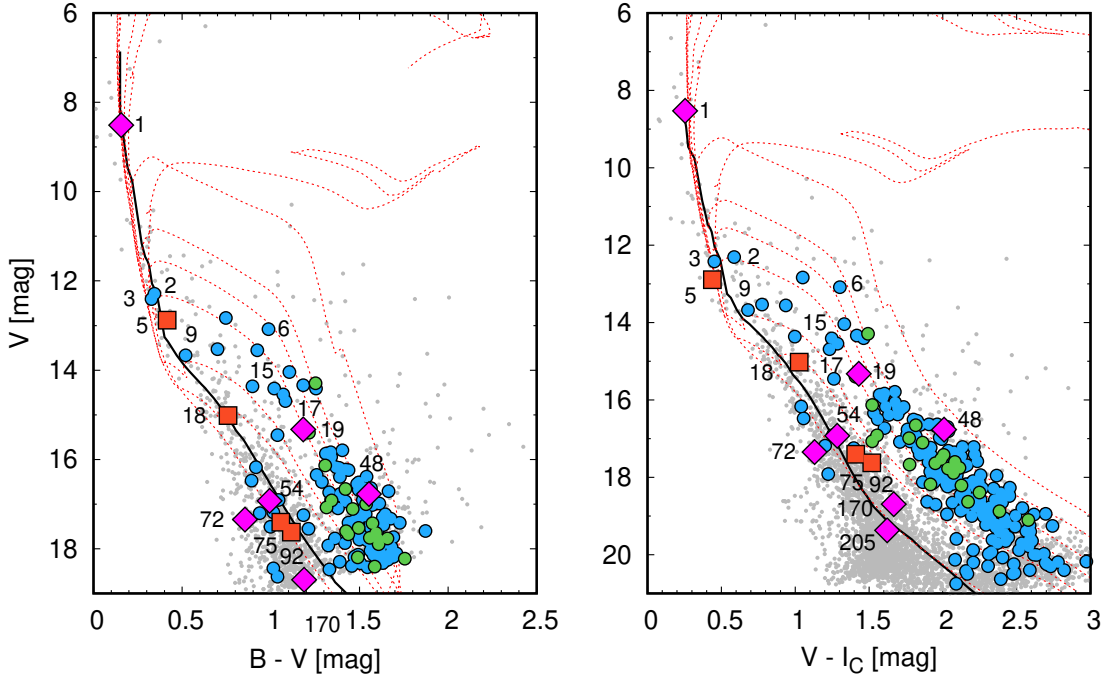


Figure 1. Variable stars in V vs. $(B - V)$ (left) and V vs. $(V - I_C)$ (right) colour-magnitude diagrams for the observed field. The symbols indicate variable stars found in this paper: pulsating stars (red squares), eclipsing stars (pink diamonds), other periodic variables (green) and remaining variables (blue). Some variables discussed in text are labeled. The ZAMS relation (thick line) was taken from Pecaut & Mamajek (2013). The isochrones (dotted lines) for 0.1, 0.5, 1, 2, 6, 10, and 100 Myr were taken from Bressan et al. (2012).

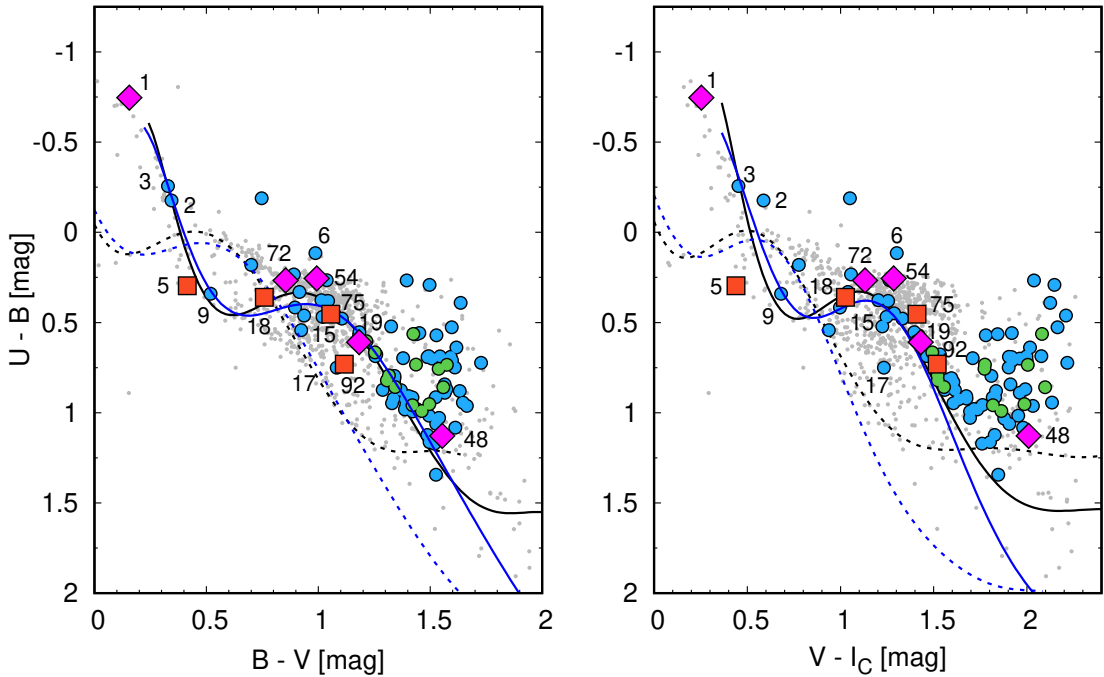


Figure 2. Variable stars in $(U - B)$ vs. $(B - V)$ (left) and $(U - B)$ vs. $(V - I_C)$ (right) colour-colour diagrams for the observed field. The symbols are the same as in Fig. 1. The dashed lines represent intrinsic relations for dwarfs (black) and for giants (blue) taken from Caldwell et al. (1993). The solid lines are the relations shifted adopting $E(B - V) = 0.47$ mag, $E(V - I_C) = 0.6$ mag and $E(U - B)/E(B - V) = 0.72$ (Massey et al. 1995).

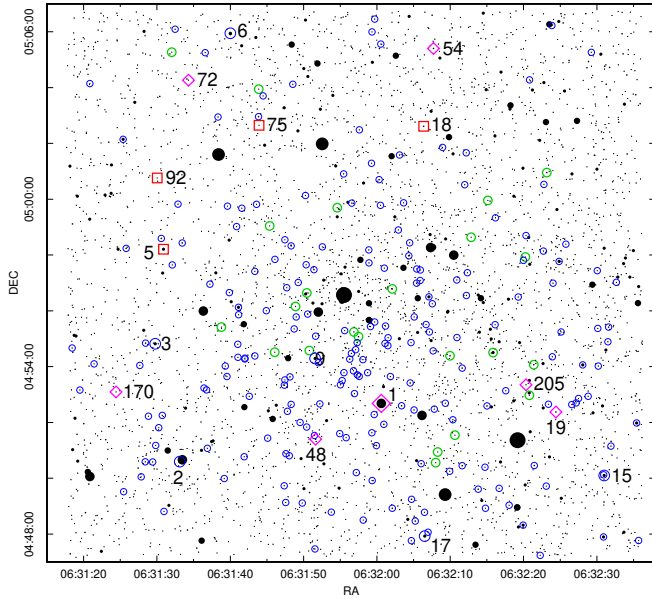


Figure 3. Schematic map of the observed field. Variable stars are marked with colours: pulsating stars (red squares), eclipsing stars (pink diamonds), other periodic variables (green circles) and remaining variables (blue circles). Some variables discussed in text are labeled.

obtained minimum and maximum values of $E(B - V)$ equal to 0.38 and 0.85, respectively. The estimation of masses and ages for PMS stars depends a lot on the adopted theoretical models of evolution (Bell et al. 2013).

As can be seen in Fig. 1, some stars lie close to or on the left side of ZAMS line. They are not cluster members. Among them, there are four eclipsing binaries, two δ Scuti candidates and several other variables. They are marked as “nm” in the last column in Table A1 in the Appendix.

3 VARIABLE STARS IN THE OBSERVED FIELD

The variability search was based mainly on the Fourier periodograms, calculated up to 80 d^{-1} . In addition, the light curves, periodograms and phased light curves for all stars were inspected by eye. Out of over 4000 stars in the observed field, 245 turned out to be variable. The brightest stars in our observations are strongly saturated. Since the Y4KCam is read out through four amplifiers, the saturation in one quadrant causes significant crosstalk, saturated in the remaining quadrants. This could have affected photometry of some stars.

In this section we present the main properties of the variable stars which we divided into four groups: pulsating stars, binary stars, other periodic variables and the remaining variables. Their location in schematic map of observed field is shown in Fig. 3. Some examples of variable stars in the cluster field were already announced by Michalska (2014).

3.1 Pulsating variables

There is one O-type star in NGC 2244, HD 46202 (Massey, Johnson & Degioia-Eastwood 1995), which was reported to be β Cephei type star (Briquet et al. 2011). Based on CoRoT data, the authors found eleven oscillations with frequencies

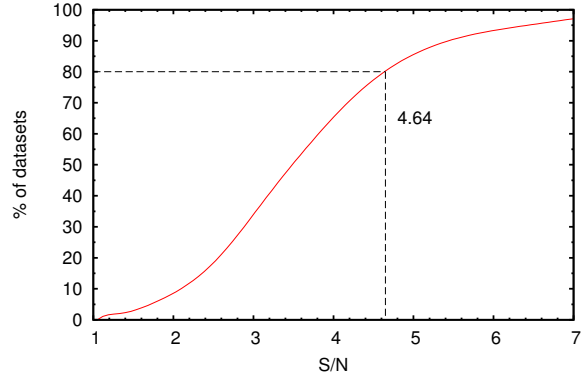


Figure 4. The percentage of correct frequency detections for time series of observed pulsating stars vs. signal to noise. Dashed line represents the confidence level equal to 80% which corresponds to $S/N=4.65$.

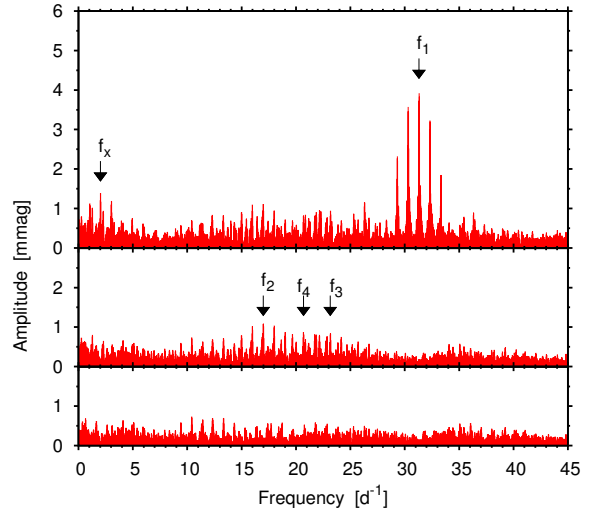


Figure 5. Fourier frequency spectrum of the V -filter data of star 5: original data (top), after removing f_1 and f_x (middle) and after removing f_1 , f_x , f_2 , f_3 and f_4 (bottom).

between 0.5 and 5 d^{-1} and amplitudes of about 0.1 mmag or less. We observed this star, but apparently the amplitudes were below our detection threshold. We did not find any β Cephei or SPB stars in our photometry, but it cannot be excluded that some of early type stars, saturated in our data, pulsate. Two SPB stars discovered by Gruber et al. (2012) were outside our field of view.

Out of 245 variables detected in the observed field, four appear to be δ Scuti stars. The parameters of the sinusoidal terms (frequencies, f_i , amplitudes, A_i , and phases, ϕ_i) for these stars, were derived by fitting the formula

$$\langle m \rangle + \sum_{i=1}^n A_i \sin(2\pi f_i(t - T_0) + \phi_i) \quad (5)$$

to the differential magnitudes. In Eq. (5) $\langle m \rangle$ is the mean differential magnitude, n , the number of fitted terms, t , the time elapsed from the initial epoch $T_0 = \text{HJD } 2455000$. The parameters of the fit are listed in Table 1. Instead of ϕ_i , we provide the time of maximum light, T_{max} .

In order to evaluate signal-to-noise, S/N , corresponding

Table 1. Parameters of the sine-curve fits to the B , V and I_C differential magnitudes of the pulsating stars detected in the observed field. The numbers in parentheses denote the r.m.s. errors of the preceding quantities with the leading zeroes omitted. The σ_{res} is the residual standard deviation, N_{obs} stands for the number of observations, S/N is the signal-to-noise ratio.

star	f_i [d ⁻¹]		Filter	N_{obs}	A_i [mmag]	$T_{\text{max}} - T_0$ [d]	S/N	σ_{res} [mmag]	Spectral type	Other name
5	31.3106(12)	f_1	B	130	5.7(5)	5195.6258(04)	8.8	3.7	A0/A2	W69
			V	1676	4.0(1)	5197.1584(02)	20.8	3.7		
	2.0195(33)	f_x	V		1.5(2)	5197.1268(97)	7.9			
	16.9867(34)	f_2	V		1.4(1)	5197.1210(09)	7.1			
	23.1527(54)	f_3	V		0.9(1)	5197.1634(10)	4.6			
	20.6854(48)	f_4	V		1.0(1)	5197.1412(10)	5.0			
18	8.4058(09)	f_1	V	1664	18.7(5)	5197.1658(04)	32.1	10.1		W1689
	13.1906(15)	f_2	V		11.0(5)	5197.1125(04)	18.9			
	9.1657(22)	f_3	V		10.8(5)	5197.1433(07)	18.4			
	16.0898(24)	f_4	V		14.0(8)	5197.1123(04)	24.0			
	9.6204(18)	f_5	V		10.8(5)	5197.1683(06)	18.5			
	13.6769(21)	f_6	V		7.0(5)	5197.1124(04)	12.0			
	16.3034(28)	f_7	V		5.8(4)	5197.1163(06)	9.9			
	15.0569(52)	f_8	V		5.9(8)	5197.1625(10)	10.1			
	16.8370(23)	f_9	V		7.0(4)	5197.1385(05)	12.0			
	7.0495(33)	f_{10}	V		4.6(4)	5197.1327(20)	8.0			
	10.1020(44)	f_{11}	V		5.1(4)	5197.1656(12)	8.7			
	2.1164(35)	f_x	V		4.1(4)	5197.3522(72)	7.1			
	10.5279(44)	f_{12}	V		4.5(5)	5197.1171(15)	7.8			
	13.8981(41)	f_{13}	V		4.1(4)	5197.1481(11)	7.0			
	16.9900(52)	f_{14}	V		4.3(5)	5197.1508(09)	7.3			
7.2741(44)	f_{15}	V	3.9(5)	5197.2108(25)	6.7					
75	11.5336(13)		B	148	43.6(67)	5196.262(3)	5.4	57.0		
			V	2011	26.4(11)	5198.6010(5)	17.5	31.9		
			I_C	167	15.9(25)	5196.959(2)	5.3	21.7		
92	20.147(4)		V	2033	8.7(11)	5198.555(1)	5.9	35.7		

to the the probability of finding real signal equal to 80%, we used the method described by Baran et al. (2015). First, 1000 files with Gaussian noise for a given standard deviation were generated, and the average noise in the periodogram was calculated. Then, a sinusoidal signal in the form of $A \sin(2\pi ft + \phi)$ was added. In this formula, t represents the time of observation, ϕ is the phase taken as random value in the range $[0, 2\pi]$, and A is amplitude of the signal covered the range of signal-to-noise (S/N) between 1 and 8, with the step of 0.05 mmag. For each amplitude, we generated 1000 time-series datasets for which Fourier periodograms were calculated and the number of files with peak at the added frequency was counted. As can be seen in Fig. 4, the detection threshold with the 80% confidence level corresponding to $S/N=4.64$. For this reason, in Table 1 we show only the frequencies with $S/N \geq 4.6$.

One of δ Scuti candidates is star 5 (GSC 00154-01743). The Fourier frequency spectrum of its V -filter data (Fig. 5) reveals frequency $f_1 = 31.3106 \text{ d}^{-1}$. After prewhitening original data with this frequency, we found the frequency $f_x = 2.0195 \text{ d}^{-1}$ (likely instrumental) and three other significant terms with frequencies $f_2 = 16.9867 \text{ d}^{-1}$, $f_3 = 23.1527 \text{ d}^{-1}$ and $f_4 = 20.6854 \text{ d}^{-1}$, typical for δ Scuti stars. The spec-

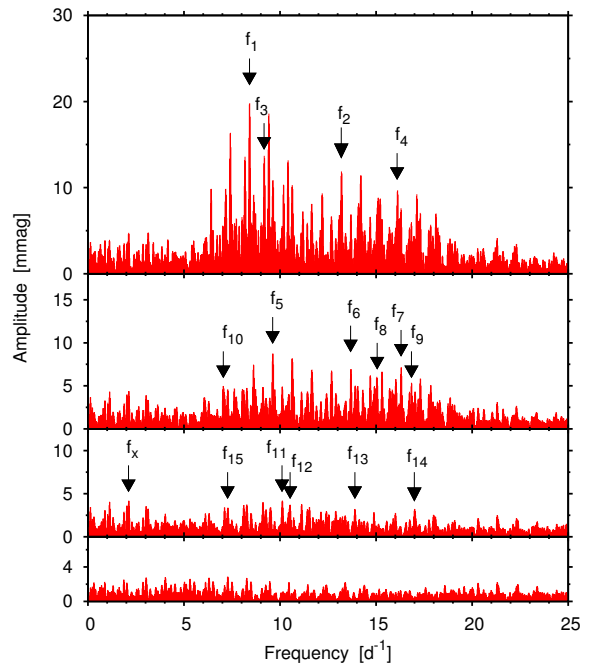


Figure 6. Fourier frequency spectrum of the V -filter data of the δ Scuti candidate, star 18, at four steps of prewhitening.

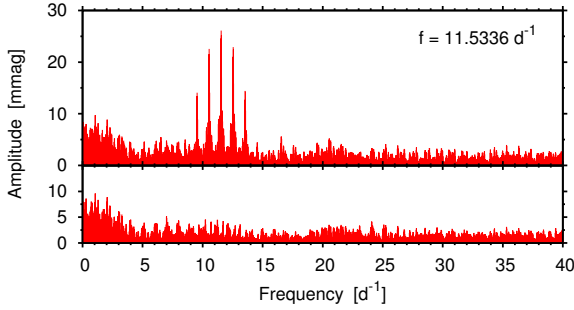


Figure 7. Fourier frequency spectrum of the V -filter data of the δ Scuti candidate, star 75: original data (top), after removing $f = 11.5336 \text{ d}^{-1}$.

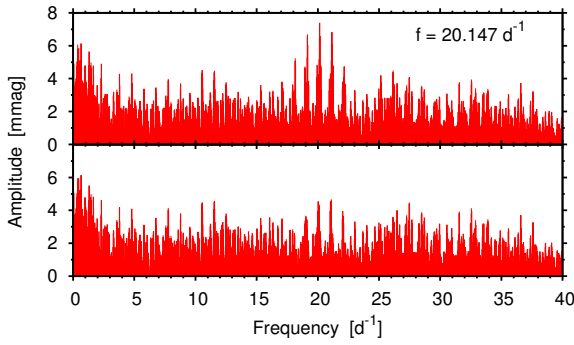


Figure 8. Fourier frequency spectrum of the V -filter data of the δ Scuti candidate, star 92: original data (top), after removing $f = 20.147 \text{ d}^{-1}$.

tral type in WEBDA³ database, reported by Kuznetsov (1986) is A0. In *Simbad* database the spectral type of star 5 is A2. The fitted spectral type, derived from synthetic photometry by Pickles & Depagne (2010), is B8V, however, it appears to be too early for δ Scuti star. The position in $(U - B)$ vs. $(V - I_C)$ colour-colour diagram (Fig. 2) indicates that this star is not a member of NGC 2244. The probability of its membership ranges between 0.16 (Marschall et al. 1982) and 0.88 (Chen et al. 2007). Based on Gaia proper motions we obtained the probability equal to 0.27 (Sect. 4).

For three other δ Scuti candidates the spectral types are not available. Using prewhitening method with the subsequent strongest modes we found fifteen frequencies in Fourier periodogram of star 18 (Fig. 6). The periods, the multiperiodicity and the shape of light curve are typical for a δ Scuti star. In each of two other stars, star 75 and 92, we found only one frequency of variability, characteristic for δ Scuti-type variables: $f = 11.5336 \text{ d}^{-1}$ (Fig. 7) and $f = 20.147 \text{ d}^{-1}$ (Fig. 8), respectively.

Assuming that all four δ Scuti candidates are cluster members, we calculated absolute magnitudes, M_V , and $(B - V)_0$ adopting $A_V = 1.46 \text{ mag}$, $E(B - V) = 0.47 \text{ mag}$ and the distance modulus equal to 11.1 mag found by Park & Sung (2002). These values for two δ Scuti candidates, star 5 and 18, are plotted in colour-magnitude diagram (Fig. 9) together with 18 pulsating PMS stars and candidates from clusters (blue dots) and two pulsating PMS field stars with best

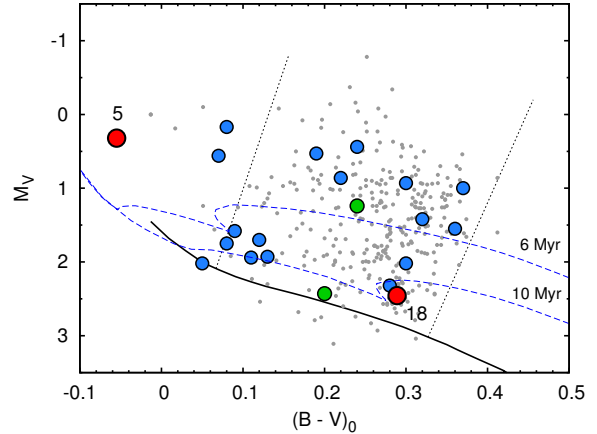


Figure 9. Position of two δ Scuti candidates, star 5 and 18 (red dots) in HR diagram. Additionally, 18 pulsating PMS stars and candidates from clusters (blue dots) and two pulsating PMS field stars (green dots) taken from Zwintz (2008) are plotted. The ZAMS (solid line), the borders of the classical δ Scuti instability strip (dotted lines) and classical δ Scuti stars (grey dots) were transformed from the data of Rodríguez & Breger (2001). The dashed line represents isochrones for 6 and 10 Myr taken from Bressan et al. (2012).

parallaxes (green dots), taken from Table 3 and 4 of Zwintz (2008), respectively. The author notified that PMS pulsators occupy the same instability region in H-R diagram as classical δ Scuti stars, marked with grey dots in Fig. 9. We derived their $(B - V)_0$ from $(b - y)_0$ colours published by Rodríguez & Breger (2001)⁴ using transformation given by Caldwell et al. (1993). The instability strip (dotted line) and ZAMS (solid line) were also transformed from the data of Rodríguez & Breger (2001). As can be seen in this diagram, star 18 is situated inside the instability strip. Its position is quite close to ZAMS and it appears to be older than cluster members. The membership probability determined in Sect. 4 is equal to 62.2%. Furthermore, its position in V vs. $(B - V)$ and V vs. $(V - I_C)$ colour-magnitude diagrams (see Fig. 1) indicates this star is rather old.

Since the $(B - V)_0$ colours of star 75 and star 92 are greater than 0.5 and M_V is close to 5 mag, we did not show them in Fig. 9. If these stars are of δ Scuti-type, they are field stars, located beyond NGC 2244. Their membership probability determined in Sect. 4 is equal to 1.1% and 0% for star 75 and 92, respectively. The star 5 have $(B - V)_0 = -0.05$ and it is outside the instability strip borders. This indicates it is likely a foreground star.

3.2 Binary stars

We identified seven stars (WEBDA numbers: 59, 80, 119, 128, 133, 194, and 201), previously known as single lined spectroscopic binaries (Huang & Gies 2006). All they are not variable in our data. In the observing field there are also two double-lined spectroscopic stars, HD 46149 (Mahy et al. 2009) and HD 46150 (Chini et al. 2012). The primary components of both systems are O-type stars. Unfortunately, they are saturated in our photometry.

NGC 2244 contains a close visual pair, HD 46180 ($V_A =$

³ The WEBDA database is available at <http://www.univie.ac.at/webda/>.

⁴ <http://www.iaa.es/ eloy/dsc00.html>

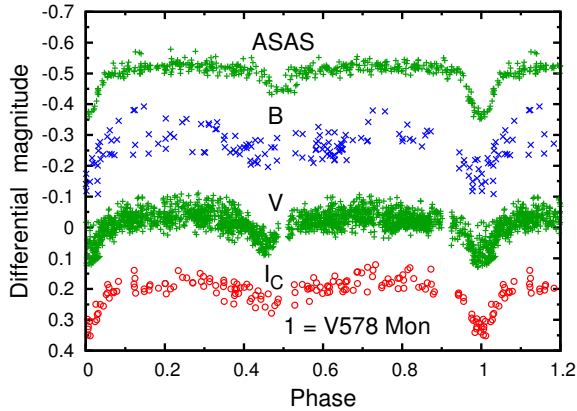


Figure 10. Phase diagrams of the V -filter ASAS observations and our BVI_C observations of eclipsing system V578 Mon. Offsets were applied to separate light curves in different bands.

Table 2. Parameters of eclipsing binary stars found in the observed field. The depths of eclipses are given for the V -filter observations. The numbers in parentheses denote the r.m.s. errors of the preceding quantities with the leading zeroes omitted.

Star	Period [d]	$T_{\min I}$ [d] HJD-2450000	Eclipse depth	
			I [mag]	II [mag]
1	2.411(1)	5203.7289(33)	0.11	0.08
1*	2.408544(1)	3142.0074(04)	0.16	0.07
19	1.7789(17)	5199.4827(49)	0.12	0.12
48	7.3415(86)	5201.146(24)	0.27	0.17
54	0.50241(1)	5197.1875(06)	0.92	–
72	0.72276(10)	5193.07235(6)	0.16	0.04
170	0.58681(11)	5197.9792(22)	0.30	0.15
205	0.26582(2)	5194.2811(03)	0.44	0.38

* for V -filter ASAS data

9.2, $V_B = 10.3$, $\rho = 5.1$ arcsec and $\theta = 82^\circ$; Mason et al. 2001). Based on DDO (David Dunlap Observatory) spectroscopy obtained for MOST variables, Pribulla et al. (2009) discovered that HD 46180 is a quadruple system composed of two binary stars. One pair is an eclipsing system with the orbital period of about 3.09 d and amplitude 0.016 mag (Pribulla et al. 2010). Unfortunately, HD 46180 and the other star are not resolved in our data, and they are saturated. Consequently we are not able to detect any eclipses.

There is also a well-known eclipsing system V578 Mon in the observed field (star 1 in our list of variable stars). According to Hensberge, Pavlovski & Verschueren (2000), this binary has an orbital period equal to 2.40848 d, and consists of two massive ($M_1 = 14.54 \pm 0.08 M_\odot$ and $M_2 = 10.29 \pm 0.06 M_\odot$) early B-type stars (B1V+B2V). The age of the system and the distance derived by these authors are equal to 2.3 ± 0.2 Myr and 1.39 ± 0.1 kpc, respectively. The eccentricity of about 0.077 and apsidal motion equal to $0.071 \text{ deg cycle}^{-1}$ (apsidal period equal to 33.48 yr) were determined by Garcia et al. (2011). The absolute dimensions of V578 Mon were recently determined by Garcia et al. (2014). They found the radii $R_1 = 5.41 \pm 0.04 R_\odot$ and $R_2 = 4.29 \pm 0.05 R_\odot$, and effective temperatures $T_1 = 30000 \pm 500$ K and $T_2 = 25750 \pm 435$ K.

The BVI_C phased diagram of V578 Mon is shown in

Fig. 10. Since this bright system ($V = 8.5$ mag) is partially saturated in our photometry, we were not able to determine the period accurately. For this purpose, we used ASAS data (Pojmański 2003) and we got $P = 2.408544$ d which is consistent with the period of Hensberge, Pavlovski & Verschueren (2000).

V578 Mon was also observed by MOST. Based on this photometry, Pribulla et al. (2010) found the orbital period $P = 2.40860$ d. Adopting mass ratio $q = 0.71$ from spectroscopy, they obtained inclination $i = 73.1^\circ$, the relative radii $r_1 = 0.254$ and $r_2 = 0.178$, the eccentricity $e = 0.066$ and surprisingly low for early B-type stars the effective temperatures, $T_1 = 16980$ K and $T_2 = 13310$ K.

The other eclipsing system found in our data is V552 Mon (star 54 in our list of variable stars). In General Catalog of Variable Stars (GCVS) its type of variability has been assigned as IN:, i.e. probable irregular eruptive star (Samus et al. 2009). There is no information about variability and spectral type of five other eclipsing binaries (19, 48, 72, 170, 205). The periods, the times of minimum, and the eclipse depths for each eclipsing binary are given in Table 2. The phase diagrams are shown in Fig. 11.

The positions of systems 19 and 48 in the $V - (V - I_C)$ colour-magnitude diagram (Fig. 1) indicate that they can be cluster members. Four other binaries (54, 72, 170 and 205) are close to ZAMS in this diagram, so they are probably non-members. It cannot be excluded, however, that the changes in their light curves some of them are caused by cool spots. This type of variability is described in Sect. 3.3.

We found many variables with evident eclipse in their light curve, showing also another type of variability. For this reason we describe them in Sect. 3.4, together with other irregular variables.

3.3 Other periodic variables

In addition to pulsating stars (Sect. 3.1) and eclipsing systems (Sect. 3.2) we found a group of 23 other periodically variable stars. Their periods, times of the maximum and amplitudes are listed in Table 3. The phase diagrams of these stars are available online in electronic version. In colour-magnitude (Fig. 1) and colour-colour (Fig. 2) diagrams these stars are marked as green dots. Almost all these stars appear to be cluster members. The shape of light curves and the position in colour-magnitude diagram indicate that most of these periodic stars may be WTTS stars.

The WTTSs do not have active accretion disks and the changes in their light curves are mainly caused by cool spots (Bouvier et al. 1993, Herbst et al. 1994). As we mentioned in the Introduction, the typical periods of such variability are 0.5–18 d (Semkov 2011). Our observations do not allow to derive the longest periods from this range, so that in Table 3 we list stars only with periods shorter than half of the observing time. We did not find any star with period shorter than one day, although, in other clusters, e.g. NGC 2282, there are up to 50% of such stars (Dutta et al. 2018).

The faster rotation of the stars with decreasing masses is clearly seen in old open clusters (Henderson & Stassun 2012). Some authors, however, show correlation between periods and masses of stars in young open cluster. Lata et al. (2012), who analyzed PMS variable stars of NGC 7380, NGC 1893 and Be59, show that stars with masses greater than $2 M_\odot$ rotate

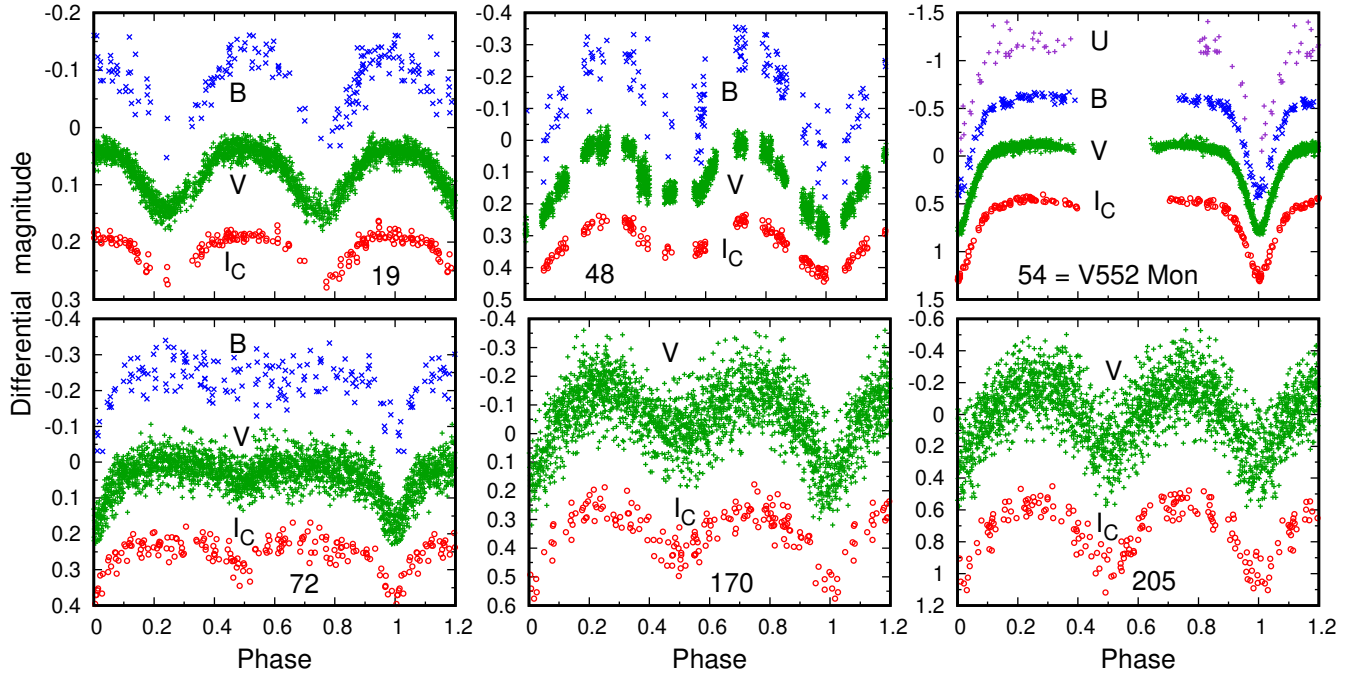


Figure 11. Phase diagrams of six eclipsing systems (star 19, 48, 54, 72, 170 and 205). Offsets were applied to separate light curves in different bands.

Table 3. Parameters of 23 periodic variable stars found in the observed field determined from the V -filter observations ($T_0 = 2450000$). The numbers in parentheses denote the r.m.s. errors of the preceding quantities with the leading zeroes omitted.

Star	Period [d]	$T_{\max} - T_0$ [d]	Amplitude [mmag]
11	1.39484(45)	5198.3285(18)	25.0(02)
20	2.3533(10)	5198.2599(24)	63.5(04)
27	2.9650(30)	5197.988(64)	37.8(61)
43	2.9207(21)	5197.1121(78)	170.3(24)
53	5.715(16)	5196.617(11)	69.7(07)
57	1.73898(41)	5197.36557(91)	361.9(10)
59	1.7338(11)	5199.1084(41)	58.4(09)
62	3.8134(68)	5196.9136(65)	92.5(10)
79	2.2971(17)	5198.6714(39)	100.5(12)
85	4.1615(99)	5200.3439(92)	82.2(12)
90	2.72813(65)	5199.5292(16)	388.3(14)
93	1.58577(91)	5198.5312(26)	132.9(13)
95	1.5282(13)	5198.6391(34)	89.3(12)
100	1.8069(14)	5198.3071(37)	111.1(14)
103	1.6836(16)	5198.3854(59)	58.96(13)
105	5.212(18)	5196.195(13)	86.4(15)
113	1.10223(34)	5198.5434(21)	174.3(19)
135	1.07587(73)	5199.3193(33)	95.9(18)
137	4.4913(51)	5199.7514(99)	231.0(34)
151	2.3023(24)	5196.3062(51)	187.4(24)
166	5.142(17)	5198.089(13)	173.1(27)
182	4.9095(86)	5196.773(14)	257.3(46)
192	6.880(23)	5196.916(20)	176.4(34)

faster. The opposite dependence was found by Lamm et al. (2005) who studied the period distribution of PMS variables in Orion Nebula Cluster and in NGC 2264. They show that low mass stars rotate faster, on average, than high mass stars. In

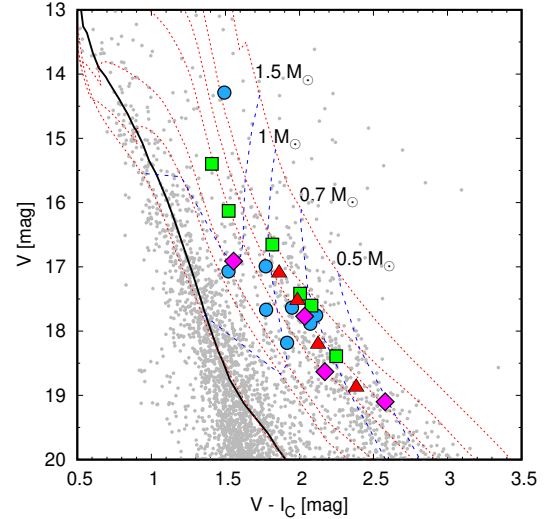


Figure 12. Position of the periodic variables in the colour-magnitude diagram. The ZAMS relation for $Z=0.02$ (thick line) was taken from Pecaut & Mamajek (2013). The symbols represent four ranges of periods: 1–2 days (blue dots), 2–3 days (green squares), 3–5 days (red triangles) and more than 5 days (magenta diamonds). The isochrones (dotted lines) for 0.1, 0.5, 1, 2, 6, 10, and 100 Myr and mass tracks (dashed lines) were taken from Bressan et al. (2012). We adopted here mean values of $E(V - I_C) = 0.6$ mag, $A_V = 1.46$ mag and $(m - M_V)_0 = 11.1$ mag.

order to verify if there is any relation in our sample of periodic variables, we checked their position in the colour-magnitude diagram shown in Fig. 12. The coloured symbols in this diagram represent four ranges of periods: 1–2 days (blue dots), 2–3 days (green squares), 3–5 days (red triangles) and more than 5 days (magenta diamonds). The isochrones and mass

tracks were taken from Bressan et al. (2012). As can be seen in this figure, the stars with different periods are distributed in a wide range of masses. However, we note that in our sample there are no stars with periods of less than 1 day and more than 7 days.

3.4 Irregular variables

The remaining 211 variable stars are classified as irregular. Their light curves are available online in electronic version. As can be seen in these figures, the range of light variation of some stars is greater than 0.5 mag (e.g. stars 149, 186, 216, and 232). Some of them show an increase in the light similar to those observed in FUors (e.g. variable 34 and 131) or EXors (e.g. variable 83, 211) stars, but the time scale of variations is much shorter.

Almost all irregular variables lie between 0.1 and 6 Myr isochrones in the V vs. $(V - I_C)$ colour-magnitude diagram (Fig. 1), in the region of pre-main sequence stars. The variability of these stars can be therefore caused by changes in the accretion disks and hot spots which is typical for CTTSs (Herbst et al. 1994, Kurosawa & Romanova 2013). The eclipses in the light curves which can be seen in some of them (82 and 149) indicate that these stars are obscured by the dust clumps although they can be members of binary or multiple systems.

Five irregular variable (star 2, 3, 9, 50, and 67) have strong $H\alpha$ emission (Park & Sung 2002). Three of them, star 2 (spectral type B4 Ve), star 3 (B7 Ve) and star 9, are marked by these authors as HAeBe candidates. Strong emission in $H\alpha$ line of stars 2, 3 and 6 was notified by Li et al. (2002) who classified star 3 as Herbig Be and star 6 (spectral type F3 Ve) as HAeBe candidate.

In addition to CTTSs and HAeBe, among irregular variables, we can also find WTTS stars. Some more details about classification of PMS variable stars can be found in Sect. 6.3.

4 MEMBERSHIP

An important step in studying a cluster is the determination of the membership in its field. Some non-members can be identified using the colour-magnitude diagram. The $V - (V - I_C)$ colour-magnitude diagram for the observed stars is shown in the left panel of Fig. 13. As we mentioned in Sect. 2, the age of NGC 2244 was estimated at 2–4 Myr so that we considered stars below the 10 Myr isochrone (blue line in Fig. 13) as non-members.

The other way of membership determination is the use of proper motions. A statistical method was proposed by Vasilevskis et al. (1958) who used the distribution functions of proper motions for cluster and field stars to derive membership probability for individual stars. The method was modified over the years (Sanders 1971, Zhao & He 1990). In this paper, we applied the method used by Sariya et al. (2012) who defined the membership probability of the i^{th} star as

$$P_\mu(i) = \frac{n_c \cdot \phi_c^\nu(i)}{n_c \cdot \phi_c^\nu(i) + n_f \cdot \phi_f^\nu(i)}, \quad (6)$$

where n_c and n_f are the normalized numbers of stars for cluster and field ($n_c + n_f = 1$) and ϕ_c^ν and ϕ_f^ν are the frequency distribution functions for the cluster and field stars, defined as:

$$\phi_c^\nu = \frac{1}{2\pi\sqrt{(\sigma_{xc}^2 + \epsilon_{xi}^2)(\sigma_{yc}^2 + \epsilon_{yi}^2)}} \times \exp\left\{-\frac{1}{2}\left[\frac{(\mu_{xi} - \mu_{xc})^2}{\sigma_{xc}^2 + \epsilon_{xi}^2} + \frac{(\mu_{yi} - \mu_{yc})^2}{\sigma_{yc}^2 + \epsilon_{yi}^2}\right]\right\} \quad (7)$$

and

$$\Phi_f^\nu = \frac{1}{2\pi\sqrt{(1-\gamma^2)}\sqrt{(\sigma_{xf}^2 + \epsilon_{xi}^2)(\sigma_{yf}^2 + \epsilon_{yi}^2)}} \times \exp\left\{-\frac{1}{2(1-\gamma^2)}\left[\frac{(\mu_{xi} - \mu_{xf})^2}{\sigma_{xf}^2 + \epsilon_{xi}^2} - \frac{2\gamma(\mu_{xi} - \mu_{xf})(\mu_{yi} - \mu_{yf})}{\sqrt{(\sigma_{xf}^2 + \epsilon_{xi}^2)(\sigma_{yf}^2 + \epsilon_{yi}^2)}} + \frac{(\mu_{yi} - \mu_{yf})^2}{\sigma_{yf}^2 + \epsilon_{yi}^2}\right]\right\}, \quad (8)$$

where μ_{xi} and μ_{yi} are the proper motions of the i^{th} star ($\mu_{xi} = \mu_\alpha \cos \delta$ and $\mu_{yi} = \mu_\delta$ of the i^{th} star) with errors ϵ_{xi} and ϵ_{yi} , respectively. The parameters μ_{xc} and μ_{yc} define the cluster proper motion centre with dispersions σ_{xc} and σ_{yc} , while μ_{xf} and μ_{yf} are the field proper motion centre with dispersions σ_{xf} and σ_{yf} , respectively. The correlation coefficient γ was calculated by

$$\gamma = \frac{(\mu_{xi} - \mu_{xf})(\mu_{yi} - \mu_{yf})}{\sigma_{xf}\sigma_{yf}}, \quad (9)$$

In order to find the membership probability for each star we observed, we used the proper motions from the Gaia DR2 catalogue (Gaia Collaboration et al. 2016, Gaia Collaboration et al. 2018). For about 4000 stars in the observed field, we searched for Gaia counterparts in the search radius of $1''$. Using the sample of about 50 stars with membership probability greater than 70% from the catalogue of Park & Sung (2002), the mean proper motion of the cluster were calculated using 3σ clipping. We obtained $\mu_\alpha \cos \delta = -1.69 \text{ mas yr}^{-1}$ and $\mu_\delta = 0.32 \text{ mas yr}^{-1}$ with standard deviation $\sigma_{\mu_\alpha} = 0.30$ and $\sigma_{\mu_\delta} = 0.35$, respectively. The proper motions from Gaia DR2 catalogue are shown in the right panel of Fig. 13. As we can see, most of our variable stars have proper motions concentrated around the calculated center (black cross). We assumed that cluster stars are within an ellipse with semi-axis equal to $3\sigma_{\mu_\alpha}$ and $3\sigma_{\mu_\delta}$. We find 426 stars within this area, for which V magnitudes and $(V - I_C)$ colours placed them above 10 Myr isochrone in $V - (V - I_C)$ colour-magnitude diagram. For this sample we calculated mean proper motion of the cluster $\mu_{xc} = -1.67$ and $\mu_{yc} = 0.23 \text{ mas yr}^{-1}$ with dispersions $\sigma_{xc} = 0.34$ and $\sigma_{yc} = 0.41 \text{ mas yr}^{-1}$. For the remaining 3546 stars we calculated the mean proper motion of field stars $\mu_{xf} = -0.14$ and $\mu_{yf} = -1.22 \text{ mas yr}^{-1}$ with dispersions $\sigma_{xf} = 3.87$ and $\sigma_{yf} = 4.00 \text{ mas yr}^{-1}$. These values allow to calculate frequency distribution functions ϕ_c^ν and ϕ_f^ν , and then the probability $P_\mu(i)$ for each star. The probabilities for variable stars are shown in Table A1.

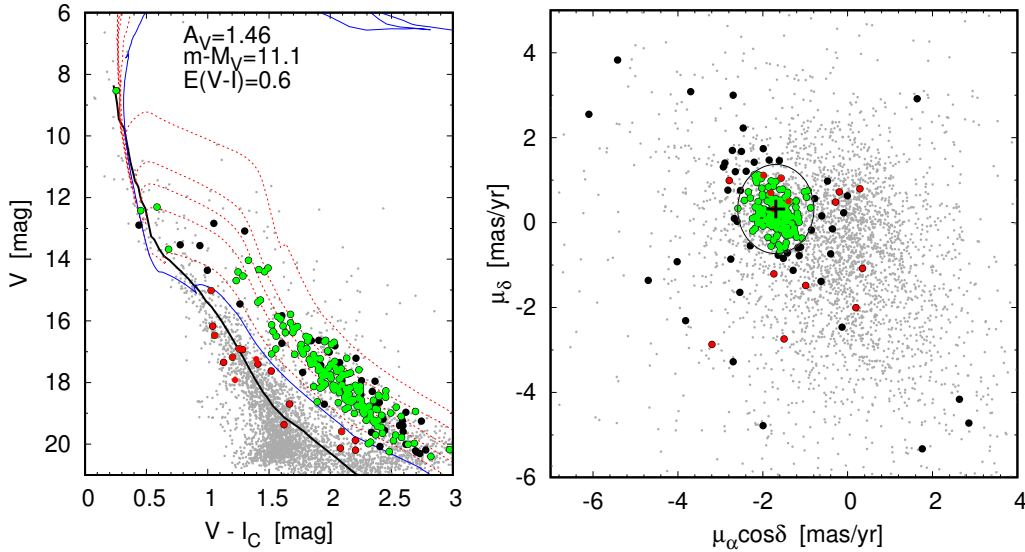


Figure 13. *Left:* Colour-magnitude diagram for about 3600 stars in the observed field. *Right:* Proper motions distribution for about 3600 stars in the observed field. Green circles represent variable stars falling into the oval area around mean proper motion of NGC 2244 (black cross), red circles – variable stars with V and $(V - I_C)$ below isochrone 10 Myr (blue line), black circles – other variable stars.

5 IDENTIFICATION OF YOUNG STELLAR OBJECTS

Before we classify the PMS variable stars, described in Sect. 3.3 and 3.4, first we deal with the classification of young stellar objects (YSOs). The YSOs comprise both protostars and PMS stars. The YSOs are frequently embedded in their parental molecular clouds or have circumstellar disks. The presence of the embedding matter makes classification based on the infrared data quite obvious. In this paper, we use 2MASS, *Spitzer* (IRAC and MIPS), and WISE infrared photometry to identify which stars we detected in NGC 2244 are YSOs.

Lada (1987) divided YSOs into three classes, I, II, and III. Class I sources are objects deeply embedded in the surrounding cloud with emission dominated by the cold dust of their envelopes (protostars). They practically cannot be detected in the visual domain. Class II sources having accretion disks are identified with TTSs and are visible in the optical range although they have infrared excesses. Finally, Class III are post-T Tauri objects with no or little infrared excess. Their photometric properties are similar to the normal main-sequence stars.

Three other classes of YSOs were proposed in the literature. Using observations in the submillimeter domain, Andre et al. (1993) found extremely young object and proposed a fourth class of YSOs, Class 0. The Class 0 source cannot be seen even in near- or mid-infrared. The fifth class, called “flat spectrum” (hereafter FS), was proposed by Greene et al. (1994) based on the slope of SED calculated between 2.2 and 10 μm , defined as $\alpha = d \log(\lambda F_\lambda) / d \log \lambda$, which is between -0.3 and 0.3 for these stars. Class I YSOs have $\alpha > 0.3$, Class II, $-1.6 < \alpha < -0.3$, and Class III, $\alpha < -1.6$. Based on the slope of SED calculated between 3.6 and 8 μm , Lada et al. (2006) found that objects with thick disks have spectral index $\alpha > -1.80$, the objects with “anemic disks” (transition disk objects, objects with thin disks) have $-2.56 < \alpha < -1.8$ and objects without disks $\alpha < -2.56$.

The YSOs of Class I and II can be easily distinguished

using mid-infrared photometry, e.g. from *Spitzer* satellite (Megeath et al. 2004; Allen et al. 2004, 2007). Based on *Spitzer* IRAC (Infrared Array Camera) and MIPS (Multiband Imaging Photometer for *Spitzer*) observations, Balog et al. (2007) found 25 Class I objects and 337 Class II objects in NGC 2244.

For the identification of YSOs among our objects, we used the method described in Appendix A of Gutermuth et al. (2009), developed by Megeath et al. (2012). They utilized *Spitzer* IRAC and MIPS photometry, and 2MASS photometry for selection Class I, Class II and transition disk objects.

5.1 *Spitzer* and 2MASS photometry

The *Spitzer* data were taken from catalogue published by Balog et al. (2007). We found 674 counterparts in this catalogue putting an offset of $2''$ between our and *Spitzer* positions. Almost all of them have photometric uncertainties $\sigma < 0.1$ mag. All of them have photometry in all four IRAC bands ([3.6], [4.5], [5.8] and [8.0] μm) but only 167 stars have MIPS photometry ([24] μm).

At the beginning, according to the criteria of Gutermuth et al. (2009) and Megeath et al. (2009), we identify extragalactic sources that may be misclassified as YSOs. They are marked with white squares in Fig. 14–16. The other symbols shown in Fig. 14–16 denote our final classification of the YSOs, described in Sect. 5. We found only one object that satisfy colour and brightness criteria (marked with dashed line in Fig. 14a) for active galactic nuclei (AGNs). Two objects fall in the region of galaxies with bright PAH (polycyclic aromatic hydrocarbon) emission: one in [4.5]–[5.8] vs. [5.8]–[8.0] colour-colour diagram (Fig. 14b) and one in [3.6]–[5.8] vs. [4.5]–[8.0] colour-colour diagram (Fig. 14c). We did not find any shock emission knots. Five objects, according to criteria of Gutermuth et al. (2009), may be contaminated by saturated PAH emission objects (Fig. 14c). All these objects, are not included in any catalogue of AGNs or galaxies and they

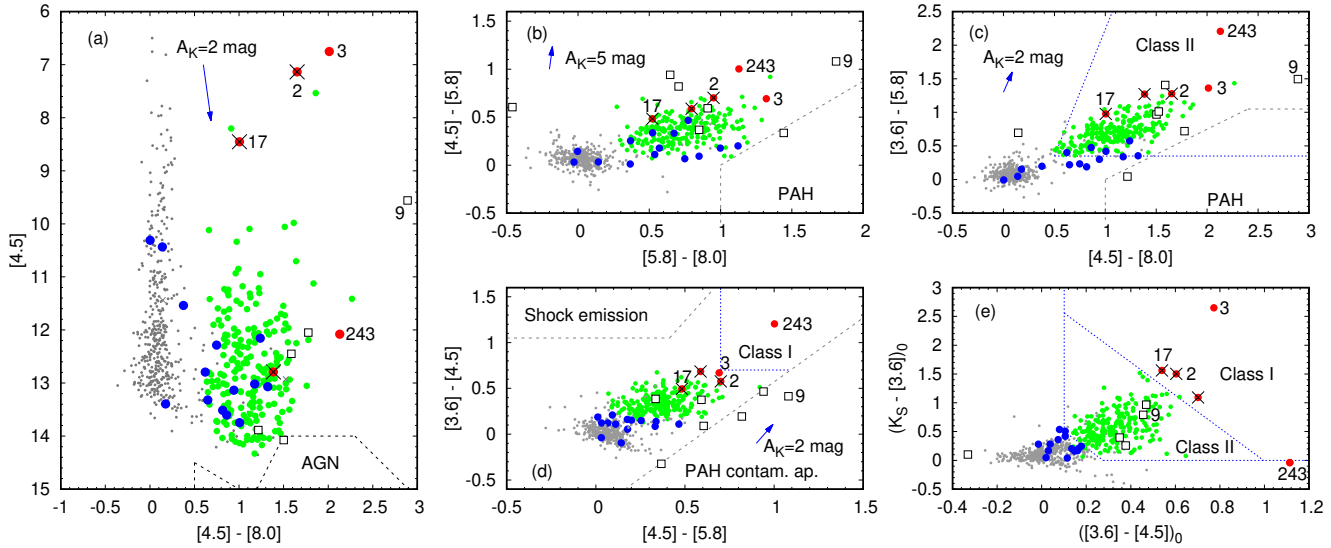


Figure 14. *Spitzer*/IRAC colour-magnitude diagram and colour-colour diagrams used for the selection of Class I (red dots) and Class II (green dots) objects and for the isolation of the extragalactic sources (white squares, see Sect. 5.1 for more details). Dark dots represent Class III objects and/or field stars. Three crossed Class I objects does not fulfil the colour restriction for being a protostar ($[4.5]-[24] > 4.761$). Transition disk objects are marked with blue dots. The arrows show the reddening vectors (Flaherty et al. 2007). Some variables discussed in text are labeled.

are very close to restriction lines in colour-magnitude and colour-colour diagrams, so they are probably not extragalactic sources.

The JHK_S photometry was taken from 2MASS All-Sky Catalog of Point Sources of Cutri et al. (2003). For 3098 our stars we found counterparts among 2MASS sources in the search radius of $2''$, 1517 of them have photometric uncertainty $\sigma < 0.1$ mag in all three bands, and 653 have counterparts in the catalogue of Balog et al. (2007) (605 of them have $\sigma < 0.1$ mag).

The *Spitzer* and 2MASS magnitudes for variable stars are shown in Table A2⁵ in Appendix.

5.1.1 Selection of Class I and Class II objects

After checking for extragalactic objects, we identified Class II objects using restrictions in $[4.5]-[8.0]$ and $[3.6]-[5.8]$ colours (shown in Fig. 14c), and with $[3.6]-[4.5]-\sigma([3.6]-[4.5]) > 0.5$. From this sample, objects with $[4.5]-[5.8]$ and $[3.6]-[4.5]$ colours greater than 0.7 were classified as Class I. We found one such source, variable 243⁶, that fulfil these colour restrictions (Fig. 14d).

Some additional YSOs can be found from the constraints of the dereddened $([3.6]-[4.5])_0$ and $(K_S-[3.6])_0$ colours derived according to procedure described in Appendix A.2. of Gutermuth et al. (2009). Originally, this method was applied to the stars without $[5.8]$ and/or $[8.0]$ μm photometry which have good quality ($\sigma < 0.1$ mag) H , K_S and/or J photometry. Although all our stars with *Spitzer* data have photometry in all four IRAC bands, we apply this method to check if we can find some additional Class I and Class II objects.

This way we found 4 additional Class I candidates

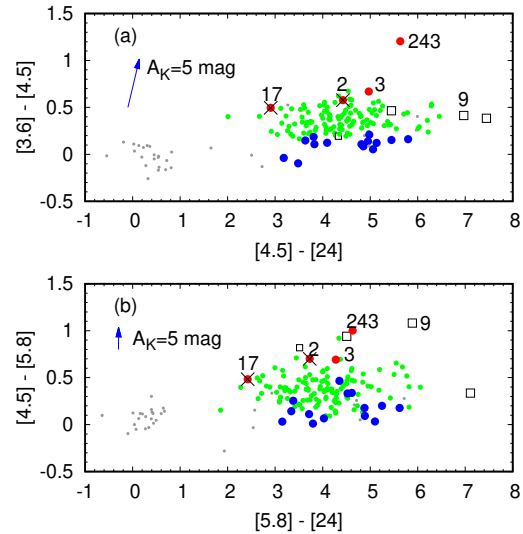


Figure 15. *Spitzer*/IRAC and MIPS colour-colour diagrams used for the selection of transition disk objects (blue circles). The coloured symbols are the same as in Fig. 14. The arrow shows the extinction vector for $A_K = 5$ mag (Flaherty et al. 2007).

(Fig. 14e) and 23 additional Class II candidates. Out of these 23 objects, 12 stars which have $[4.5]-[24] > 2.5$ mag and $[5.8]-[24] > 2.5$ mag (or $[4.5]-[8.0] > 0.5$ mag for objects without $[24]$ μm band photometry), we classified as Class II objects.

All objects selected as protostars must have $[5.8]-[24]$ colour greater than 4 mag. Two objects (variables 2 and 17) found previously as Class I do not meet this condition and for one object there are no $[24]$ -band photometry. They are marked with crosses in Fig. 14–16. Finally, using *Spitzer* and 2MASS photometry, we found two Class I objects (variable 3 and 243) and 227 Class II objects.

⁵ The full version of Table A2 is available in electronic form from the CDS.

⁶ The numbers indicate the variables we found, listed in Table A1

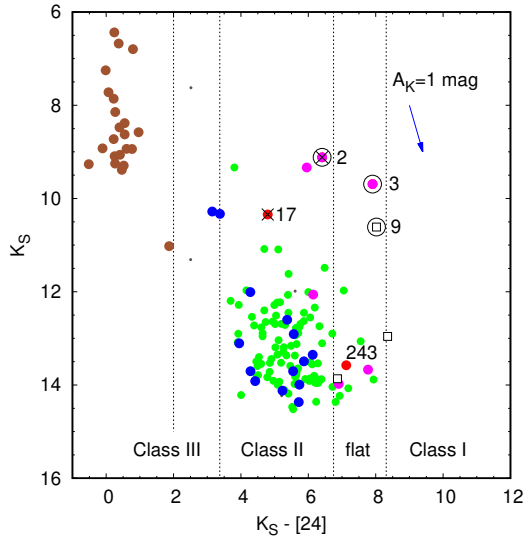


Figure 16. K_S vs. $K_S - [24]$ colour-magnitude diagram for observed stars in NGC 2244. Dotted lines denote the divisions between Class I, flat spectrum, Class II, and Class III objects (Rebull et al. 2007). The arrow shows the extinction vector for $A_K = 1$ mag (Flaherty et al. 2007). Symbols for YSOs are the same as in Fig. 14. Additionally, encircled symbols represent H AeBe stars (Park & Sung 2002), pink dots – flat spectrum object with $-0.3 < \alpha_{\text{IRAC}} < 0.3$, field stars are marked with brown dots.

5.1.2 Selection of transition disk objects

Another class of YSOs are transition disk objects which do not show near- and mid-infrared excess. These sources can be found with the use of $[24] \mu\text{m}$ MIPS photometry. We used the approach of Megeath et al. (2012) who considered objects with $[8] - [24]$ colours greater than 2.5 mag and the dereddened $[3.6] - [4.5]$ colours smaller than 0.2 mag as transition disk object. This way, among 167 objects with MIPS photometry, we found 14 transition disk objects (7 of them are variable). They are marked in blue in Fig. 14–16.

5.1.3 Selection of Class III and flat spectrum objects

Most of the remaining 426 objects which were not classified as Class I, Class II or transition disks are Class III objects (diskless YSOs) and/or field stars (pure photosphere), 84 of them are variable. It is difficult to distinguish between these two groups. One way was presented by Rebull et al. (2007) who used K_S vs. $K_S - [24]$ colour magnitude diagram. The authors established the ranges of $K_S - [24]$ colour for Class I (8.31–14 mag), flat spectrum (6.75–8.31 mag), Class II (3.37–6.75 mag) and Class III (< 3.37 mag) sources. In order to separate Class III objects from foreground/background stars, they set a boundary colour $K_S - [24] = 2$ mag.

The K_S vs. $K_S - [24]$ colour magnitude diagram for stars in the observed field is shown in Fig. 16. In this diagram YSOs found using the selection criteria of Gutermuth et al. (2009) are shown. As can be seen in the figure, none of Class I star have $K_S - [24] > 8.31$ mag. Both Class I objects together with 8 Class II objects have $K_S - [24]$ between 6.75 and 8.31 mag. According to colour criteria of Rebull et al. (2007) they are YSOs with flat spectrum. The encircled symbols in Fig. 16 represent H AeBe stars (Park & Sung 2002). One of them, star

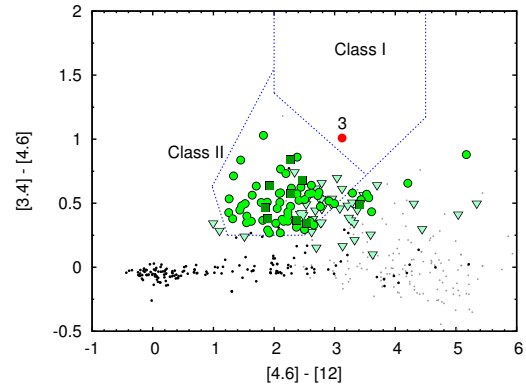


Figure 17. WISE colour-colour diagram used for the selection of Class I and Class II objects base on restrictions of Koenig & Leisawitz (2014). Green symbols represent Class II sources: circles – common from WISE and IRAC, squares – only from WISE, triangles – only from IRAC. Red circle indicate Class I object. Black points are Class III/field stars, grey points – sources that may be extragalactic contaminants.

3, according to criteria of Gutermuth et al. (2009), was classified as Class I object and the other H AeBe star, star 2, was classified as Class II object. Third H AeBe star, star 9, are in the area of sources contaminated by saturated PAH emission objects (Fig. 14d)

For three stars $K_S - [24]$ is between 2 and 3.37 and they are probably diskless YSOs. We found that 22 stars have $K_S - [24] < 2$ mag and 21 of them have $K_S - [24] < 1$ mag.

The position of YSOs in the map of the sky is shown in Fig. 18. The objects of all classes are distributed homogeneously, without any concentration.

5.2 Spectral index α

The classes of YSOs, described in the introduction of this section, were defined based on α spectral index. We computed α indexes, from the slope of the linear fit to the observed fluxes between the IRAC $[3.6] \mu\text{m}$ band and the IRAC $[8.0] \mu\text{m}$ band (α_{IRAC}), as it is quite insensitive to extinction (Muench et al. 2007). The α indexes of the variable stars are given in Table A1 in Appendix.

Since α index of H AeBe star 3, classified in Sect. 5.1.1 as Class I, is less than 0.3, it is rather flat spectrum object. Four other objects which have α between -0.3 and 0.3 , we classified as flat spectrum. They are marked with pink dots in Fig. 16. One object with $\alpha = -0.31$ and $K_S - [24]$ between 6.75 and 8.31 mag we also classified as flat spectrum. For the other Class I object, star 243, the α index is equal to 0.98 confirms its previous classification. Another object, H AeBe star 9, also have α index greater than 0.3, such as Class I objects, but according to colours restrictions of Gutermuth et al. (2009) is classified as object contaminated by PAH emission. The α indexes of almost all Class II YSOs found in Sect. 5.1.1, which are between -1.8 and -0.3 , confirmed their classification.

5.3 WISE photometry

Since not for all our variable stars we found *Spitzer* counterparts, we identify YSOs based on WISE (Wide-field Infrared Survey Explorer, Wright et al. 2010) photometry as well. This photometry was obtained in in four mid-infrared

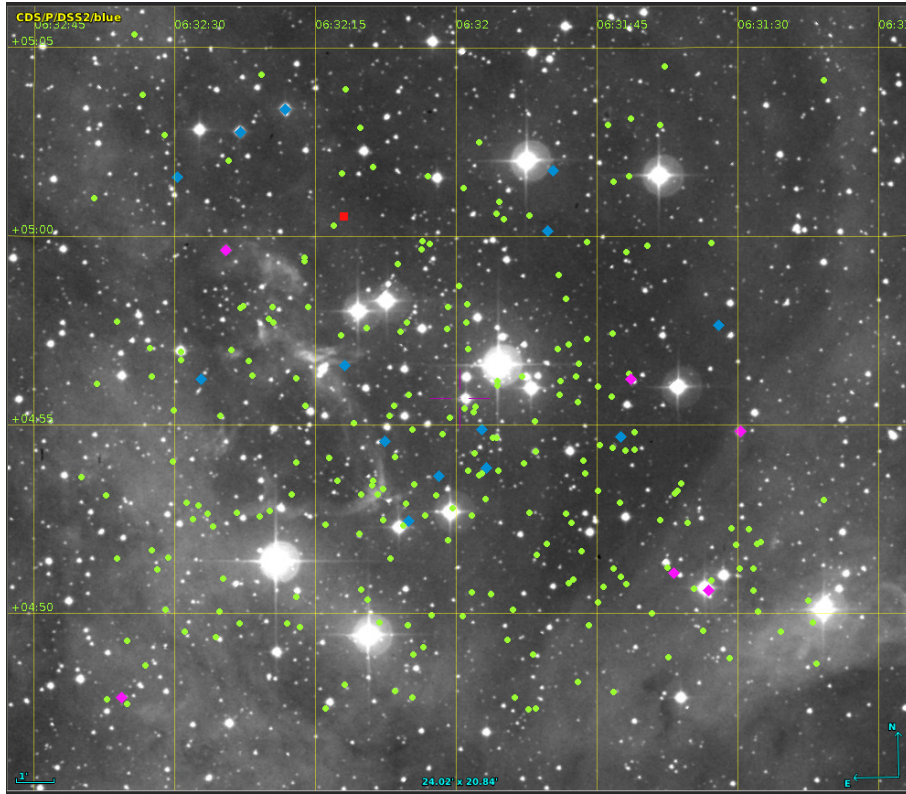


Figure 18. Spatial distribution for Class I object (red square), Class II objects (green circles), flat spectrum objects (magenta rhombus) and transition objects (blue rhombus) found from *Spitzer* and 2MASS photometry (Sect. 5).

Table 4. Number of YSOs found in observed field.

Objects	total	variable
Class I	1	1
Class I/ Flat spectrum	1	1
Flat spectrum ¹	5	3
Flat spectrum ²	10	3
Class II	219	89
Transition disks	14	7
Class III	426	84

¹ objects classified based on α index;

² objects classified based on $K_S - [24]$ colour.

bands: [3.4], [4.6], [12], and [22] μm . Using ALLWISE catalog (Cutri & et al. 2014) we found 1804 counterparts in the search radius of $2''$. In order to find YSOs, to the sources with error less than 0.2 mag in [3.4], [4.6] and [12] μm band, we applied the colour and brightness constraints described in Koenig & Leisawitz (2014). In this way we found only one Class I object (star 3) and 9 additional Class II objects (marked with squares in Fig. 17), 3 of them are variable. From the slope of the linear fit to the observed fluxes in WISE [3.4], [4.6] and [12] μm band, we calculated α indexes (α_{WISE}). The classes of objects and α_{WISE} indexes are written in brackets in Table A1.

The total number of YSOs found in observed field are summarized in Table 4.

6 CHARACTERISTICS OF PMS VARIABLE STARS

The variable PMS stars found in Sect. 3.3 and 3.4 may be WTTs, CTTs or HAeBe stars. Their position in colour-magnitude and colour-colour diagrams, near- and mid-IR excess as well as the properties of $H\alpha$ emission line help to understand the possible origin of their variability. Therefore, additional archival data of the IPHAS (Isaac Newton Telescope Photometric H-Alpha Survey) and UKIDSS (United Kingdom Infrared Deep Sky Survey) surveys were used in our analysis.

6.1 IPHAS photometry

Combination of IPHAS ($r' - i'$) and ($r' - H\alpha$) colour indices allowed to find stars with $H\alpha$ in emission. The method was described by Drew et al. (2005) and Barentsen et al. (2011). The authors provide a grid of colour tracks for stars with different $H\alpha$ emission equivalent widths ($EW_{H\alpha}$), spectral types and reddenings. We found r' , i' and $H\alpha$ -band photometry for about 3700 our objects using IPHAS DR2 catalogue (Barentsen et al. 2014) in the search radius of $1''$.

For 226 variables found in our photometry we identified IPHAS counterparts with photometric errors smaller than 0.1 mag in all three bands. They are shown in the ($r' - H\alpha$) vs. ($r' - i'$) colour-colour and r' vs. ($r' - i'$) colour-magnitude diagrams in Fig. 19 and 20, respectively. In order to find CTTs candidates based on ($r' - i'$) and ($r' - H\alpha$) colours, we used the selection threshold described by Barentsen et al. (2011). For early type stars, this threshold (red line in Fig. 19) is the same as unreddened 10\AA track, but for stars later than M0 the empirical threshold from Barrado y Navascués & Martín

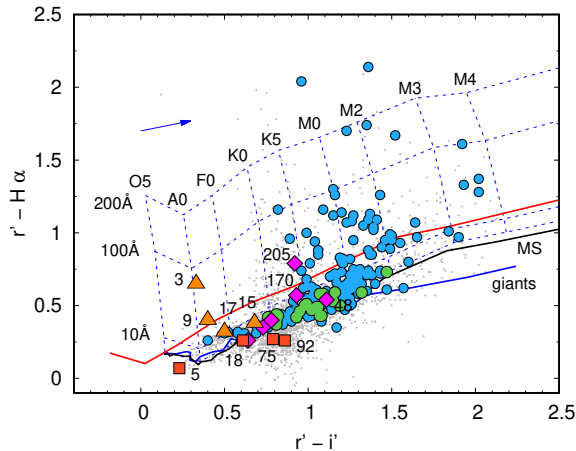


Figure 19. IPHAS ($r' - H\alpha$) vs. ($r' - i'$) colour-colour diagram for the observed field. The symbols indicate variable stars found in this paper: pulsating (red squares), eclipsing (pink diamonds), HAeBe (orange triangles), other periodic (green circles) and irregular (blue circles). Synthetic tracks for MS stars and giants (solid black and blue lines), and for stars with photometric $EW_{H\alpha} = 10, 100$ and 200 \AA for spectral types O5–M6 (dashed blue lines), shifted according to reddening vector for $A_V = 1.46$ mag (blue arrow), were taken from Barentsen et al. (2011). Red line is the selection threshold for CTTS.

(2003) was taken. We found 143 objects above the threshold. Out of them, 30 variable stars lie above the threshold with 3σ confidence level defined by Barentsen et al. (2011). They are notified with the letters "IA" in Table A1 in Appendix. The other stars above the reddened ($E(B - V) = 0.47$ mag) 10 \AA track and the objects lying between 0 and 10 \AA track are marked in Table A1 as "Ia" and "Ib", respectively. As can be seen in Fig. 19, most of the variables with strong $H\alpha$ emission have spectral types later than K0. Only two stars above CTTS threshold with spectral type earlier than K0, star 3 and 9, are HAeBe stars reported by Park & Sung (2002). The IPHAS magnitudes for variable stars are listed in Table A2 in Appendix.

6.2 UKIDSS photometry

The colour-colour diagram of near-infrared JHK photometry is the other useful tool for understanding YSOs. Therefore, we decided to use UKIDSS (United Kingdom Infrared Deep Sky Survey) photometry as it is more accurate than 2MASS photometry. The UKIDSS photometry was obtained with the United Kingdom InfraRed Telescope (UKIRT) during Galactic Plane Survey. Almost for all objects we observed, we found J , H and K photometry in the UKIDSS-DR6 catalogue (Lucas et al. 2008), assuming a search radius of $1''$. The JHK UKIDSS magnitudes for variable stars are shown in Table A2 in the Appendix.

The $(J - H)$ vs. $(H - K)$ diagram for variable stars found in Sect. 3 is shown in Fig. 21. The dashed line represents the locus of CTTSs determined by Meyer et al. (1997). Since this line was derived in the CIT (California Institute of Technology) system, we transformed UKIDSS photometry to 2MASS photometry according to the transformation relations of Hewett et al. (2006) and then to CIT photometry using relations described by Carpenter on "2MASS Color Transforma-

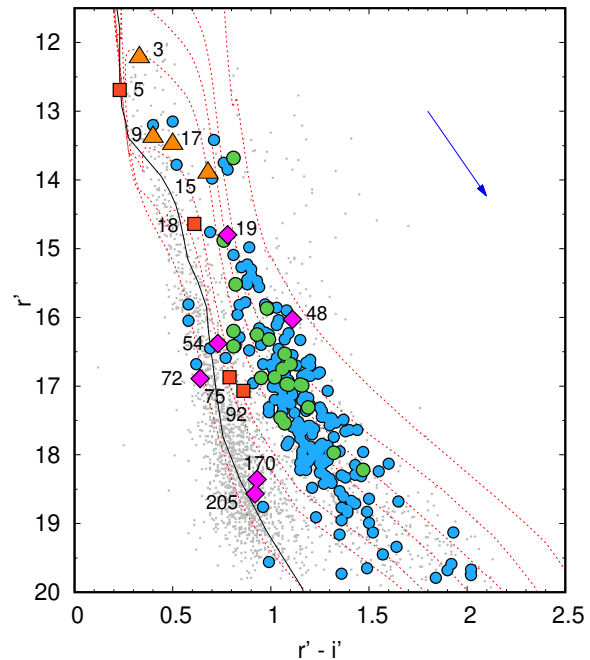


Figure 20. IPHAS r' vs. ($r' - i'$) colour-magnitude diagram for the observed field. The symbols are the same as in Fig. 19. The ZAMS relation for $Z=0.02$ (solid line) was taken from Siess et al. (2000). The isochrones (dotted lines) for 0.1, 0.5, 1, 2, 6, 10, and 100 Myr for adopted $A_V = 1.46$ mag and $(m - M_V)_0 = 11.1$ mag were taken from Bressan et al. (2012).

tions" web page⁷. If the brightness of the star in UKIDSS-DR6 catalogue is flagged as "close to saturated", we show 2MASS colours, transformed to CIT system in Fig. 21.

The solid black line in Fig. 21, taken from Pecaut & Mamajek (2013)⁸, represents the ZAMS and the solid blue line, taken from Bessell & Brett (1988), denote colours for late-type giants. The arrow shows the reddening vector for $A_V = 1.46$ mag. The extinction ratios $A_J/A_V = 0.282$, $A_H/A_V = 0.175$ and $A_K/A_V = 0.112$ we adopted from Rieke & Lebofsky (1985). The blue rectangle is the area of dereddened $(J - H)$ and $(H - K)$ colours for HAeBe stars, defined by Hernández et al. (2005). As can be seen in this figure, five variable stars we found fall into this box. They will be discussed in Sect. 6.3.

We identified 208 stars of Class II lying above CTTS locus, 88 of them are variable. Only 20 of Class II objects lie below CTTS line, four of them (2, 9, 15, 17) are variables in HAeBe box in the $(J - H)$ vs. $(H - K)$ diagram (Fig. 21).

Following Sugitani et al. (2002) we have drawn three lines parallel to the reddening vector: from the tip (spectral type M4) of the giant branch (left line), from the point $(H - K), (J - H) = (0.0, 0.0)$ mag for spectral type A0 of the MS (middle line), and from the tip of the intrinsic CTTS line (right line). The objects lying between left and middle line, marked with "F" in Table A1 in Appendix, are either field stars (main-sequence stars or giants) or Class III/Class II sources with small near-infrared (NIR) excesses (Ojha et al. 2004).

⁷ <http://www.astro.caltech.edu/~jmc/2mass/v3/transformations/>

⁸ New version were used available at http://www.pas.rochester.edu/~emamajek/EEM.dwarf_UBVJHK_colours.Teff.txt

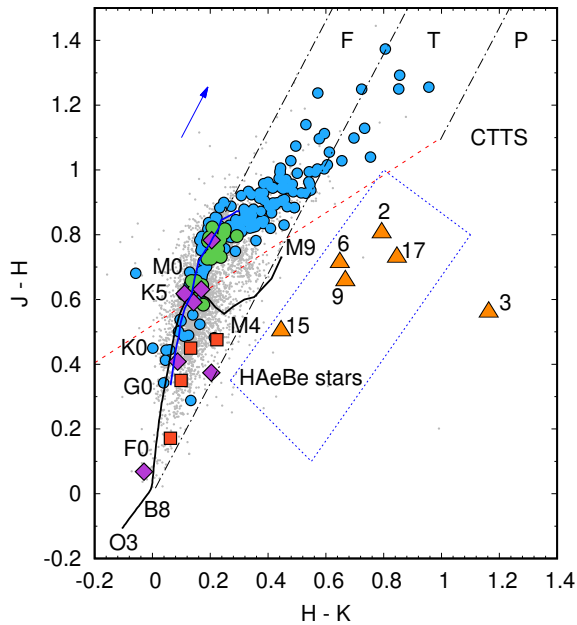


Figure 21. The $(J - H)$ vs. $(H - K)$ UKIDSS colour-colour diagram for the observed field. The symbols are the same as in Fig. 19. The dashed line is the locus of CTTSs (Meyer et al. 1997). Solid black and blue lines denote intrinsic colours for ZAMS and late-type giants, respectively. The arrow shows the reddening vector for $A_V = 1.46$ mag. All the measurements were transformed to the CIT system.

The sources lying between middle and right line, marked with "T" in Table A1 in Appendix, are considered to be Class II sources (mostly CTTSs) with large NIR excesses or Herbig Ae/Be stars with small NIR excess. The sources lying redwards of "T" region are most likely Class I objects (protostars) or Herbig Ae/Be stars.

6.3 Classification of PMS variable stars

The age spread of PMS stars in NGC 2244 estimated by Park & Sung (2002) is between 0.1–0.3 and 5.8–6.4 Myr, depending on the adopted models. Most of our variables lie between 1 and 6 Myr isochrone and plenty of them are PMS stars (HAeBe stars and TTSS). The positions of PMS variable stars in the infrared and optical colour-magnitude and colour-colour diagrams helped us to classify them.

Five variables fall into the HAeBe box in Fig. 21. All of them were classified as Class II objects. Three of these stars, (star 2, 6, and 9) are known HAeBe stars (see Sect.3.4). Fourth known HAeBe, star 3, has strong infrared excess and is placed outside HAeBe box in the $(J - H)$ vs. $(H - K)$ diagram (Fig. 21). We classified this star as HAeBe Class I/flat spectrum object. The other two stars falling into the HAeBe box (Fig. 21) are stars 15 and 17. The photometric $EW_{H\alpha}$ derived from IPHAS photometry of three HAeBe candidates (star 3, 9, and 17) is greater than 10 \AA . For star 15, the photometric $EW_{H\alpha}$ is between 0 and 10 \AA .

A common feature of classical T Tauri stars (CTTSs) is the equivalent width of $H\alpha$ ($EW_{H\alpha}$) emission line greater than 10 \AA . Using IPHAS photometry we have found 68 variables lying above the 10 \AA track ("IA" and "Ia" in Table A1). Most of them, 45 stars, are Class II objects, 43 of them have spectral types, estimated from $(r' - i')$ and $(r' - H\alpha)$ colours

(Fig. 19) later than K0 and lie above CTTS locus in $(J - H)$ vs. $(H - K)$ diagram (Fig. 21). They are the best candidates for CTTS stars and are marked as CTTS in Table A1 in Appendix. Excellent candidates for CTTSs are also four stars with $EW_{H\alpha} < 10 \text{ \AA}$ which large infrared excess placed them in "T" region in Fig. 21 and one Class I object, star 243.

Among 48 Class III/field stars, that lie above the 10 \AA $EW_{H\alpha}$ track in Fig. 19, 36 stars occupy the region of FGK type main sequence stars, with $(J - H) < 0.6$ mag. Seven of them, marked as MS in Table A1, are variable. The remaining twelve stars can be CTTSs as they lie above CTTSs locus in Fig. 21. Nine of them, marked as CTTS* in Table A1, are variable. The position of selected CTTS candidates in r' vs. $(r' - i')$ colour-magnitude diagram (Fig. 20) is typical for PMSs. Only one star, 222, lie in this diagram close to ZAMS and is placed above 200 \AA track in Fig. 19. It may be an active field star, but its position in the V vs. $(V - I_C)$ diagram a little above 10 Myr isochrone and the membership probability, equal to 74.3%, does not exclude it from the members of the cluster.

Our classification of other Class II variables lying above CTTS locus in Fig. 21 with photometric $EW_{H\alpha} < 10$ depends on their spectral index α . Lada et al. (2006) found that objects with thick disks, typical for CTTSs, are characterised by spectral index $\alpha > -1.8$. They also found that large fraction (64%) of WTTSS are diskless stars ($\alpha < -2.56$) and about 22% of WTTSS have thin disks ($-2.56 < \alpha < -1.8$). For this reason, we marked the stars with $\alpha > -1.8$ as CTTS* in Table A1 and stars with $\alpha < -1.8$ as WTTSS. The Class III variables lying above CTTS locus in Fig. 21 and having $EW_{H\alpha}$ between 0 and 10 were also classified as WTTSS. The remaining variable stars lying above CTTS line were classified as WTTSS*. This way, we have found 97 candidates for CTTS stars (49 CTTS and 48 CTTS*), 68 candidates for WTTSS stars (32 WTTSS and 36 WTTSS*) and 6 candidates for HAeBe stars (4 of them were known before).

Common feature of YSOs is emission in X-rays. Using catalogue of X-ray sources from *Chandra* published by Wang et al. (2008), we identified 482 counterparts in the search radius of $1''$, 182 of them are variable stars. They are marked with letters "a", "b" or "c" in Table A1 in Appendix, following the notification used by Wang et al. (2008) indicating variability characterization.

Park & Sung (2002) found ROSAT HRI X-ray counterparts for sixteen stars in NGC 2244. They classified six of them as PMS stars. Four of them (star 10, 13, 14, and 16) are variable in our photometry. The authors denoted two objects as "PMS X-ray binary", one of them is variable star in our data (star 49). Park & Sung (2002) also selected 14 PMS star and seven PMS candidates based on the strength of $H\alpha$ emission line. Since the authors published the positions of stars brighter than 17 mag, we have found only seven counterparts. Six of them, marked with letters "PS" in Table A1, are variable stars.

Berghöfer & Christian (2002) published the results for 138 X-ray sources in NGC 2244 selected from ROSAT PSPC and HRI observations. The majority of them have strong $H\alpha$ emission. Out of them 38 stars are variable in our photometry. They are marked with letters "BC" in Table A1.

On average, the amplitudes of light curve variations of CTTSs are larger than those of WTTSS (Lata et al. 2012). The variability of CTTSs is usually irregular, caused by accretion processes and the changes in their disks. The changes

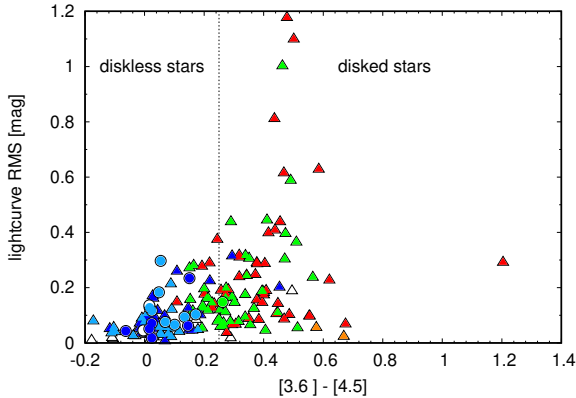


Figure 22. The V-filter light curves RMS (variability amplitude) as a function of *Spitzer* [3.6]–[4.5] colour for periodic (dots) and irregular (triangles) variables. The colours represent variable stars: CTTS (red), CTTS* (green), WTTS (dark blue), and WTTS* (light blue), described in Sect. 6.3. Dashed line is the boundary between diskless and disked stars ([3.6]–[4.5]=0.25 mag), adopted from Dutta et al. (2018).

in light curves of WTTSs are often periodic, caused by cool spots. Dutta et al. (2018) show that variability amplitude of stars with infrared excess is larger for those that have disks. Following the authors, we calculated the observed root mean square ($\text{RMS}=\sigma_{\text{obs}}$) in the light curves, expressed as:

$$\sigma_{\text{obs}}^2 = \frac{n \sum_{i=1}^n w_i (m_i - \bar{m})^2}{(n-1) \sum_{i=1}^n w_i}, \quad (10)$$

where m_i and \bar{m} are respectively individual and average V -filter magnitudes, and $w_i = 1.0/\sigma_i^2$ is the weight assigned to each observation with photometric uncertainties σ_i . The RMS as a function of [3.6]–[4.5] colour is shown in Fig. 22. As can be seen in this figure, most stars classified as CTTS or CTTS* have larger amplitudes than WTTSs. They also have the [3.6]–[4.5] colours greater than 0.25 mag which means, according to Dutta et al. (2018), they are disked stars.

7 SUMMARY

We presented multi-wavelength photometric study of young open cluster NGC 2244. Using $UBVI_C$ photometry we have identified 245 variable stars. The time series photometry of only one of them was published before. Based on near- and mid-infrared excess and photometric equivalent width of $H\alpha$ emission line we classify PMS variables. Among 211 stars irregular stars we have found 96 CTTS candidates, 54 WTTS candidates and 6 HAeBe stars. We have also identified 23 periodic variables with periods greater than one day. Fourteen of them we have classified as WTTS candidates and one star as CTTS* candidate. The relation between mass of the star and its rotational period found in many young open clusters, e.g. NGC 2264, NGC 7380, NGC 1893 and Be 59 is not visible in our sample of periodic variables. We have shown that stars with infrared excess have, on average, higher amplitudes. Similar tendency was found in NGC 2282 (Dutta et al. 2018).

We have found four new δ Scuti stars. All of them are likely non-members. In the observed field there is one star reported in the literature as β Cephei-type star. The small

amplitude of its variability is however below our detection threshold. Unfortunately, the saturation of bright stars makes impossible to verify if in such a young cluster there are any β Cephei or SPB stars.

In addition to the well-known eclipsing binary V578 Mon, we have found six other eclipsing systems. Two of them are probably the cluster members.

Based on *Spitzer*, UKIDSS, 2MASS and WISE photometry we have identified YSOs in our photometry. As a result, one variable was classified as Class I object, one as Class I/flat spectrum object, 91 as Class II objects, 4 as flat spectrum sources and 7 as transition disk objects. In comparison to Balog et al. (2007) we have identified small number of Class I objects. This is due to the fact that we classified only the sources detected from our photometry, while most of these objects are not visible in the optical bands.

Due to the short period of observations, we were not able to find variable PMS stars such as UXors, FUors or EXors, although some candidates were found to have the range of variations greater than 1 mag and the shape of light curves similar to those type of variables. It is not out of the question that some of our HAeBe stars could be classified as UXors, and some of our identified CTTSs as FUors or EXors, in the future.

A large number of identified PMS variable stars (165 TTS and 6 HAeBe stars) can be used to verify models of PMS stars. Since the variability of WTTSs is caused by cool spots, the amplitudes, periods and shape of light curves can change over time (Cohen et al. 2004). It would be interesting to check their variability after several years. Some additional observation can also be useful to check variability among the remaining Class II objects: to find the periods of long period variables and to verify the existence of early-type pulsating stars.

ACKNOWLEDGEMENTS

This paper uses observations made at the Cerro Tololo Inter-American Observatory (CTIO). We thank anonymous referees for comments that have helped us to improve the paper. This work was supported by NCN grant No. 2016/21/B/ST9/01126.

This research has made use of the VizieR catalogue access tool, CDS, Strasbourg, France. The original description of the VizieR service was published in A&AS 143, 23.

This research has made use of the WEBDA database, operated at the Department of Theoretical Physics and Astrophysics of the Masaryk University.

This paper makes use of data obtained as part of the INT Photometric H-alpha Survey of the Northern Galactic Plane (IPHAS, www.iphas.org) carried out at the Isaac Newton Telescope (INT). The INT is operated on the island of La Palma by the Isaac Newton Group in the Spanish Observatorio del Roque de los Muchachos of the Instituto de Astrofísica de Canarias. All IPHAS data are processed by the Cambridge Astronomical Survey Unit, at the Institute of Astronomy in Cambridge. The bandmerged DR2 catalogue was assembled at the Centre for Astrophysics Research, University of Hertfordshire, supported by STFC grant ST/J001333/1.

This work is based in part on data obtained as part of the UKIRT Infrared Deep Sky Survey.

This publication makes use of data products from the Wide-field Infrared Survey Explorer, which is a joint project of

the University of California, Los Angeles, and the Jet Propulsion Laboratory/California Institute of Technology, funded by the National Aeronautics and Space Administration.

This publication makes use of data products from the Two Micron All Sky Survey, which is a joint project of the University of Massachusetts and the Infrared Processing and Analysis Center/California Institute of Technology, funded by the National Aeronautics and Space Administration and the National Science Foundation.

This publication makes use of data products from the Wide-field Infrared Survey Explorer, which is a joint project of the University of California, Los Angeles, and the Jet Propulsion Laboratory/California Institute of Technology, funded by the National Aeronautics and Space Administration.

This research has also made use of IRAF. IRAF is distributed by the National Optical Astronomy Observatory, which is operated by the Association of Universities for Research in Astronomy, Inc., under cooperative agreement with the National Science Foundation.

This work has made use of data from the European Space Agency (ESA) mission *Gaia* (<https://www.cosmos.esa.int/gaia>), processed by the *Gaia* Data Processing and Analysis Consortium (DPAC, <https://www.cosmos.esa.int/web/gaia/dpac/consortium>).

Funding for the DPAC has been provided by national institutions, in particular the institutions participating in the *Gaia* Multilateral Agreement.

We are indebted to Prof. Andrzej Pigulski and Przemysław Mikoajczyk for his comments made upon reading the manuscript. We thank Ewa Niemczura, Stefan Meingast and Ivanka Stateva who helped to carry out some additional observations which were, however, not included to the analysis.

REFERENCES

- Allen L., Megeath S. T., Gutermuth R., Myers P. C., Wolk S., Adams F. C., Muzerolle J., Young E., Pipher J. L., 2007, *Protostars and Planets V*, pp 361–376
- Allen L. E., Calvet N., D’Alessio P., Merin B., Hartmann L., Megeath S. T., Gutermuth R. A., Muzerolle J., Pipher J. L., Myers P. C., Fazio G. G., 2004, *ApJS*, 154, 363
- Andre P., Ward-Thompson D., Barsony M., 1993, *ApJ*, 406, 122
- Artemenko S. A., Grankin K. N., Petrov P. P., 2010, *Astronomy Reports*, 54, 163
- Bagnulo S., Hensberge H., Landstreet J. D., Szeifert T., Wade G. A., 2004, *A&A*, 416, 1149
- Balog Z., Muzerolle J., Rieke G. H., Su K. Y. L., Young E. T., Megeath S. T., 2007, *ApJ*, 660, 1532
- Baran A. S., Koen C., Pokrzywka B., 2015, *MNRAS*, 448, L16
- Barentsen G., Farnhill H. J., Drew J. E., González-Solares E. A., Greimel R., Irwin M. J., Miszalski B., Ruhland C., Groot P., Mampaso A., Sale S. E., Henden A. A., Aungwerojwit A., Barlow M. J., Carter P. J., Corradi R. L. M., et al. 2014, *MNRAS*, 444, 3230
- Barentsen G., Vink J. S., Drew J. E., Greimel R., Wright N. J., Drake J. J., Martin E. L., Valdivielso L., Corradi R. L. M., 2011, *MNRAS*, 415, 103
- Barrado y Navascués D., Martín E. L., 2003, *AJ*, 126, 2997
- Bell C. P. M., Naylor T., Mayne N. J., Jeffries R. D., Littlefair S. P., 2013, *MNRAS*, 434, 806
- Berghöfer T. W., Christian D. J., 2002, *A&A*, 384, 890
- Bessell M. S., Brett J. M., 1988, *PASP*, 100, 1134
- Bonatto C., Bica E., 2009, *MNRAS*, 394, 2127
- Bouvier J., Cabrit S., Fernandez M., Martin E. L., Matthews J. M., 1993, *A&A*, 272, 176
- Bressan A., Marigo P., Girardi L., Salasnich B., Dal Cero C., Rubele S., Nanni A., 2012, *MNRAS*, 427, 127
- Briquet M., Aerts C., Baglin A., Nieva M. F., Degroote P., Przybilla N., Noels A., Schiller F., Vučković M., Oreiro R., Smolders K., Auvergne M., Baudin F., Catala C., Michel E., Samadi R., 2011, *A&A*, 527, A112
- Caldwell J. A. R., Cousins A. W. J., Ahlers C. C., van Wamelen P., Maritz E. J., 1993, *South African Astronomical Observatory Circular*, 15, 1
- Chen L., de Grijs R., Zhao J. L., 2007, *AJ*, 134, 1368
- Chini R., Hoffmeister V. H., Nasserri A., Stahl O., Zinnecker H., 2012, *MNRAS*, 424, 1925
- Cohen R. E., Herbst W., Williams E. C., 2004, *AJ*, 127, 1602
- Cutri R. M., et al. 2014, *VizieR Online Data Catalog*, 2328
- Cutri R. M., Skrutskie M. F., van Dyk S., Beichman C. A., Carpenter J. M., Chester T., Cambresy L., Evans T., Fowler J., Gizis J., Howard E., Huchra J., Jarrett T., Kopan E. L., Kirkpatrick J. D., Light R. M., Marsh K. A. e. a., 2003, *VizieR Online Data Catalog*, 2246, 0
- Díaz-Fraile D., Rodríguez E., Amado P. J., 2014, *A&A*, 568, A32
- Drew J. E., Greimel R., Irwin M. J., Aungwerojwit A., Barlow M. J., Corradi R. L. M., Drake J. J., Gänsicke B. T., Groot P., Hales A., Hopewell E. C., Irwin J., Knigge C., Leisy P., 2005, *MNRAS*, 362, 753
- Dutta S., Mondal S., Joshi S., Jose J., Das R., Ghosh S., 2018, *MNRAS*, 476, 2813
- Flaherty K. M., Pipher J. L., Megeath S. T., Winston E. M., Gutermuth R. A., Muzerolle J., Allen L. E., Fazio G. G., 2007, *ApJ*, 663, 1069
- Gaia* Collaboration Brown A. G. A., Vallenari A., Prusti T., de Bruijne J. H. J., Babusiaux C., Bailer-Jones C. A. L., 2018, *ArXiv e-prints*
- Gaia* Collaboration Prusti T., de Bruijne J. H. J., Brown A. G. A., Vallenari A., Babusiaux C., Bailer-Jones C. A. L., Bastian U., Biermann M., Evans D. W., et al. 2016, *A&A*, 595, A1
- García E. V., Stassun K. G., Hebb L., Gómez Maqueo Chew Y., Heiser A., 2011, *AJ*, 142, 27
- García E. V., Stassun K. G., Pavlovski K., Hensberge H., Gómez Maqueo Chew Y., Claret A., 2014, *AJ*, 148, 39
- Greene T. P., Wilking B. A., Andre P., Young E. T., Lada C. J., 1994, *ApJ*, 434, 614
- Gruber D., Saio H., Kuschnig R., Fossati L., Handler G., Zwintz K., Weiss W. W., Matthews J. M., Guenther D. B., Moffat A. F. J., Rucinski S. M., Sasselov D., 2012, *MNRAS*, 420, 291
- Gutermuth R. A., Megeath S. T., Myers P. C., Allen L. E., Pipher J. L., Fazio G. G., 2009, *ApJS*, 184, 18
- Henderson C. B., Stassun K. G., 2012, *ApJ*, 747, 51
- Hensberge H., Pavlovski K., Verschueren W., 2000, *A&A*, 358, 553
- Herbig G. H., 1960, *ApJS*, 4, 337
- Herbig G. H., 1977, *ApJ*, 217, 693
- Herbig G. H., 1989, in Reipurth B., ed., *European Southern Observatory Conference and Workshop Proceedings Vol. 33 of European Southern Observatory Conference and Work-*

- shop Proceedings, FU Orionis eruptions.. pp 233–246
- Herbst W., Herbst D. K., Grossman E. J., Weinstein D., 1994, *AJ*, 108, 1906
- Herbst W., Maley J. A., Williams E. C., 2000, *AJ*, 120, 349
- Hernández J., Calvet N., Hartmann L., Briceño C., Sicilia-Aguilar A., Berlind P., 2005, *AJ*, 129, 856
- Hewett P. C., Warren S. J., Leggett S. K., Hodgkin S. T., 2006, *MNRAS*, 367, 454
- Huang W., Gies D. R., 2006, *ApJ*, 648, 580
- Koenig X. P., Leisawitz D. T., 2014, *ApJ*, 791, 131
- Kurosawa R., Romanova M. M., 2013, *MNRAS*, 431, 2673
- Kuznetsov V. I., 1986, *Kinematika i Fizika Nebesnykh Tel*, 2, 45
- Lada C. J., 1987, in Peimbert M., Jugaku J., eds, *Star Forming Regions Vol. 115 of IAU Symposium, Star formation - From OB associations to protostars*. pp 1–17
- Lada C. J., Muench A. A., Luhman K. L., Allen L., Hartmann L., Megeath T., Myers P., Fazio G., Wood K., Muzerolle J., Rieke G., Siegler N., Young E., 2006, *AJ*, 131, 1574
- Lamm M. H., Mundt R., Bailer-Jones C. A. L., Herbst W., 2005, *A&A*, 430, 1005
- Lata S., Pandey A. K., Chen W. P., Maheswar G., Chauhan N., 2012, *MNRAS*, 427, 1449
- Li J. Z., Wu C. H., Chen W. P., Rector T., Chu Y. H., Ip W. H., 2002, *AJ*, 123, 2590
- Lucas P. W., Hoare M. G., Longmore A., Schröder A. C., Davis C. J., Adamson A., Bandyopadhyay R. M., de Grijs R., Smith M., Gosling A., Mitchison S., Gáspár A., Coe M., Tamura M., Parker Q. e. a., 2008, *MNRAS*, 391, 136
- Mahy L., Nazé Y., Rauw G., Gosset E., De Becker M., Sana H., Eenens P., 2009, *A&A*, 502, 937
- Marschall L. A., van Altena W. F., Chiu L.-T. G., 1982, *AJ*, 87, 1497
- Mason B. D., Wycoff G. L., Hartkopf W. I., Douglass G. G., Worley C. E., 2001, *AJ*, 122, 3466
- Massey P., Johnson K. E., Degioia-Eastwood K., 1995, *ApJ*, 454, 151
- Megeath S. T., Allen L. E., Gutermuth R. A., Pipher J. L., Myers P. C., Calvet N., Hartmann L., Muzerolle J., Fazio G. G., 2004, *ApJS*, 154, 367
- Megeath S. T., Allgaier E., Young E., Allen T., Pipher J. L., Wilson T. L., 2009, *AJ*, 137, 4072
- Megeath S. T., Gutermuth R., Muzerolle J., Kryukova E., Flaherty K., Hora J. L., Allen L. E., Hartmann L., Myers P. C., Pipher J. L., Stauffer J., Young E. T., Fazio G. G., 2012, *AJ*, 144, 192
- Meyer M. R., Calvet N., Hillenbrand L. A., 1997, *AJ*, 114, 288
- Michalska G., 2014, in Guzik J. A., Chaplin W. J., Handler G., Pigulski A., eds, *Precision Asteroseismology Vol. 301 of IAU Symposium, Variable stars in the young open cluster NGC 2244*. pp 453–454
- Muench A. A., Lada C. J., Luhman K. L., Muzerolle J., Young E., 2007, *AJ*, 134, 411
- Ogura K., Ishida K., 1981, *PASJ*, 33, 149
- Ojha D. K., Tamura M., Nakajima Y., Fukagawa M., Sugitani K., Nagashima C., Nagayama T., Nagata T., Sato S., Vig S., Ghosh S. K., Pickles A. J., Momose M., Ogura K., 2004, *ApJ*, 616, 1042
- Park B.-G., Sung H., 2002, *AJ*, 123, 892
- Pecaut M. J., Mamajek E. E., 2013, *ApJS*, 208, 9
- Pickles A., Depagne É., 2010, *PASP*, 122, 1437
- Pojmański G., 2003, *Acta Astronomica*, 53, 341
- Pribulla T., Rucinski S. M., Kuschnig R., Ogoza W., Pilecki B., 2009, *MNRAS*, 392, 847
- Pribulla T., Rucinski S. M., Latham D. W., Quinn S. N., Siwak M., Matthews J. M., Kuschnig R., Rowe J. F., Guenther D. B., Moffat A. F. J., Sasselov D., Walker G. A. H., Weiss W. W., 2010, *Astronomische Nachrichten*, 331, 397
- Rebull L. M., Stapelfeldt K. R., Evans II N. J., Jørgensen J. K., Harvey P. M., Brooke T. Y., Bourke T. L., Padgett D. L., Chapman N. L., Lai S.-P., Spiesman W. J., Noriega-Crespo A., Merín B., Huard T., Allen L. E., Blake G. A. e. a., 2007, *ApJS*, 171, 447
- Rieke G. H., Lebofsky M. J., 1985, *ApJ*, 288, 618
- Ripepi V., Cusano F., di Criscienzo M., Catanzaro G., Palla F., Marconi M., Ventura P., Neiner C., Catala C., Bernabei S., 2011, *MNRAS*, 416, 1535
- Rodríguez E., Breger M., 2001, *A&A*, 366, 178
- Samus N. N., Durlevich O. V., et al. 2009, *VizieR Online Data Catalog*, 1, 2025
- Sanders W. L., 1971, *A&A*, 14, 226
- Sariya D. P., Yadav R. K. S., Bellini A., 2012, *A&A*, 543, A87
- Semkov E. H., 2011, *Bulgarian Astronomical Journal*, 15, 65
- Siess L., Dufour E., Forestini M., 2000, *A&A*, 358, 593
- Stetson P. B., 1987, *PASP*, 99, 191
- Stetson P. B., 1992, in Worrall D. M., Biemesderfer C., Barnes J., eds, *Astronomical Data Analysis Software and Systems I Vol. 25 of Astronomical Society of the Pacific Conference Series, More Experiments with DAOPHOT II and WF/PC Images*. p. 297
- Sugitani K., Tamura M., Nakajima Y., Nagashima C., Nagayama T., Nakaya H., Pickles A. J., Nagata T., Sato S., Fukuda N., Ogura K., 2002, *ApJ*, 565, L25
- Vasilevskis S., Klemola A., Preston G., 1958, *AJ*, 63, 387
- Wang J., Townsley L. K., Feigelson E. D., Broos P. S., Getman K. V., Román-Zúñiga C. G., Lada E., 2008, *ApJ*, 675, 464
- Zacharias N., Finch C. T., Girard T. M., Henden A., Bartlett J. L., Monet D. G., Zacharias M. I., 2013, *AJ*, 145, 44
- Zhao J. L., He Y. P., 1990, *A&A*, 237, 54
- Zwintz K., 2008, *ApJ*, 673, 1088
- Zwintz K., Fossati L., Ryabchikova T., Kaiser A., Gruberbauer M., Barnes T. G., Baglin A., Chaintreuil S., 2013, *A&A*, 550, A121

This paper has been typeset from a $\text{\TeX}/\text{\LaTeX}$ file prepared by the author.

APPENDIX A:

In Table A1 we present $UBVI_C$ photometry and coordinates of variable stars found in NGC 2244 together with some important information about these stars. In Table A2 we present 2MASS, UKIDSS, Spitzer and IPHAS infrared photometry of variable stars.

Phase diagrams of other periodic variables described in Sect.3.3 are shown in Appendix A1 and the light curves of irregular variables variables described in Sect. 3.4. are shown in Appendix A2.

Table A1. $UBVI_C$ photometry and coordinates of variable stars found in NGC 2244 together with some important information about these stars.

Star	R.Asc. (2000.0)	Dec. (2000.0)	V mag	$V-I_C$ mag	$B-V$ mag	$U-B$ mag	$\chi^{(1)}$	$H\alpha^{(2)}$	Cl. ⁽³⁾	$\alpha^{(4)}$	Var. ⁽⁵⁾ type	NIR ⁽⁶⁾ reg.	Prob. ⁽⁷⁾ [%]	Other ⁽⁸⁾ name	Notes ⁽⁹⁾
1	6:32:00.61	4:52:40.9	8.530	0.254	0.156	-0.746	a	-	III	-2.61	ECL	-	48.6	V578 Mon	B0V+B1V
2	6:31:33.11	4:50:35.5	12.304	0.587	0.344	-0.177	-	BC PS	FS	-0.25	HAeBe	-	87.5	HD 259012B	B4/A1Ve
3	6:31:29.76	4:54:49.2	12.421	0.453	0.328	-0.256	a	BC PS IA	I/FS	0.24	HAeBe	-	84.7	W74	B7Ve
4	6:31:25.39	5:02:08.8	12.836	1.051	0.747	-0.189	-	-	-	-	-	-	0.0	W62	B3
5	6:31:30.88	4:58:12.4	12.892	0.439	0.415	0.296	-	-	III	-2.93	DSCT	-	27.1	W69	A2
6	6:31:40.02	5:05:56.8	13.084	1.302	0.987	0.115	-	BC	(II)	(-0.48)	HAeBe	-	0.0	W106	F3Ve
7	6:32:35.43	4:51:58.7	13.535	0.776	0.700	0.181	-	Ia	III	-2.61	MS	-	0.0	W264	G2
8	6:32:30.90	4:47:53.8	13.556	0.937	0.924	0.543	a	BC Ia	III	-2.84	MS	-	0.0	W761	
9	6:31:51.57	4:54:17.5	13.677	0.681	0.519	0.340	-	PS IA	-	1.06	HAeBe	-	92.1	W131	
10	6:31:41.12	4:56:07.7	14.037	1.332	1.105	0.479	b	BC Ib	III	-2.78	-	-	89.7	W126	
11	6:32:15.85	4:54:30.1	14.287	1.493	1.253	0.665	c	BC Ib	III	-2.56	WTTS	-	41.7	W257	
12	6:32:19.94	4:48:19.2	14.335	1.418	1.183	0.571	a	BC	III	-2.61	-	-	85.6	W272	
13	6:32:24.84	4:57:46.4	14.361	0.997	0.896	0.417	a	BC Ia	III	-2.74	MS	-	0.0	W250	
14	6:32:07.09	4:56:29.9	14.406	1.464	1.255	0.687	c	BC Ib	III	-2.47	WTTS	-	91.9	W187	
15	6:32:31.01	4:50:05.9	14.410	1.247	1.019	0.468	-	BC Ib	II	-0.78	HAeBe*	-	89.3	W269	
16	6:32:28.08	4:54:03.8	14.544	1.287	1.070	0.449	c	BC Ib	III	-2.77	-	-	90.2	W1406	
17	6:32:06.52	4:47:55.4	14.690	1.233	1.082	0.751	-	Ia	II	-1.11	HAeBe*	P	91.4	V551 Mon	
18	6:32:06.37	5:02:36.9	15.021	1.027	0.759	0.360	-	-	III	-2.84	DSCT	-	62.2	W1689	nm
19	6:32:24.42	4:52:22.6	15.325	1.431	1.183	0.609	a	BC Ib	III	-2.71	ECL	-	80.6	W2400	
20	6:32:09.98	4:54:23.2	15.396	1.409	1.215	0.604	a	BC Ib	III	-2.73	-	-	91.2	W2301	
21	6:32:04.35	4:57:58.2	15.453	1.263	1.038	0.266	b	Ib	III	-2.87	-	-	0.0	W1505	
22	6:32:05.41	4:56:59.4	15.788	1.675	1.404	0.908	a	BC Ib	III	-2.70	WTTS	F	90.8	W2258	
23	6:32:11.62	4:53:57.0	15.834	1.605	1.338	0.830	a	-	III	-2.73	WTTS*	F	17.2	W2308	
24	6:31:47.39	4:53:20.3	15.863	1.572	1.311	0.818	a	-	III	-2.97	-	-	91.7	W2121	
25	6:32:02.10	4:48:55.5	15.936	1.595	1.340	0.808	a	BC	III	-2.79	WTTS*	F	90.7	W2236	
26	6:32:21.47	4:50:27.4	16.064	1.676	1.336	0.922	a	-	III	-2.78	WTTS*	F	91.9	W2379	
27	6:31:57.48	4:55:04.5	16.130	1.522	1.307	0.821	-	Ib	III	-2.54	WTTS	F	91.5	W2203	
28	6:31:59.94	4:51:10.0	16.168	1.614	1.369	0.875	c	-	III	-2.58	WTTS*	F	91.8	W2220	
29	6:31:30.58	4:58:35.8	16.173	1.040	0.916	0.331	a	Ib	-	-	-	-	0.0	W2030	nm
30	6:31:51.41	4:57:28.6	16.183	1.734	1.387	0.982	a	BC Ib	III	-2.61	WTTS	F	91.5	W2149	
31	6:31:48.13	4:53:37.9	16.218	1.695	1.421	0.993	a	-	III	-2.64	WTTS*	F	91.7	W2124	
32	6:32:00.31	5:00:42.0	16.231	1.716	1.439	0.979	-	BC	III	-2.77	WTTS*	F	90.2	W2222	
33	6:32:11.64	4:50:27.1	16.343	1.533	1.259	0.676	a	-	III	-2.63	WTTS*	F	91.5	W2309	
34	6:32:03.37	4:52:35.9	16.374	1.695	1.540	1.029	a	-	II	-1.33	CTTS*	F	51.6	W2245	
35	6:32:04.72	4:49:14.8	16.384	1.634	1.390	0.925	b	BC	III	-2.56	WTTS*	F	90.0	W2256	
36	6:31:33.44	4:58:26.0	16.475	1.057	0.891	0.233	a	Ib	-	-	-	-	85.0	W2042	nm
37	6:31:28.44	4:54:50.4	16.498	1.559	1.288	0.874	a	-	-	-	-	F	88.6	W2019	
38	6:32:06.03	4:50:31.2	16.503	1.802	1.497	1.163	b	-	III	-2.71	WTTS*	F	90.5	W2267	
39	6:31:56.30	4:54:16.2	16.539	1.827	1.487	1.124	-	Ib	III	-2.74	WTTS	F	90.7	W2194	
40	6:32:05.90	4:57:05.4	16.629	1.906	1.527	1.062	b	Ib	III	-2.70	WTTS	F	0.4	W2264	
41	6:31:50.56	4:55:53.1	16.630	1.962	1.565	0.890	-	Ib	III	-2.72	WTTS	F	89.2	W2141	
42	6:32:00.94	4:51:55.9	16.647	1.846	1.526	1.344	a	-	II	0.42	CTTS*	F	1.5	V549 Mon	
43	6:32:02.10	4:56:47.2	16.653	1.817	1.421	0.959	a	BC	III	-2.64	WTTS*	F	91.3	W2235	
44	6:31:57.30	4:54:51.5	16.674	1.953	1.495	1.016	-	BC Ib	TD	-2.24	WTTS	F	88.4	W2200	
45	6:31:43.86	5:02:57.5	16.697	2.032	1.664	0.962	a	BC Ia	FS*	-0.43	CTTS	F	91.4	W725	
46	6:32:30.92	4:50:07.3	16.727	1.605	1.329	0.948	-	Ib	-	(-0.82)	-	-	0.0	W2457	
47	6:32:15.02	4:52:35.4	16.764	1.762	1.393	0.957	-	Ia	III	-2.11	WTTS	F	69.7	W2324	
48	6:31:51.63	4:51:24.0	16.765	2.009	1.554	1.128	a	BC	III	-2.57	ECL	F	83.1	W2152	
49	6:31:48.30	4:58:19.8	16.809	2.038	1.395	0.267	b	BC	II	-1.72	CTTS*	F	0.0	W2125	
50	6:32:04.54	4:53:25.0	16.892	1.809	1.340	0.796	c	PS Ib	II	-1.53	CTTS*	F	78.3	W2254	
51	6:32:13.83	4:49:36.5	16.898	1.759	1.519	1.171	a	-	III	-2.82	WTTS*	F	91.3	-	
52	6:32:05.22	4:48:27.9	16.908	1.255	1.044	0.380	-	BC	-	-	-	-	85.1	W745	nm
53	6:32:21.40	4:54:04.0	16.912	1.555	1.343	0.858	c	-	-	-	-	F	88.0	W2378	
54	6:32:07.71	5:05:24.3	16.928	1.285	0.993	0.255	-	-	-	-	ECL	-	0.0	V552 Mon	nm
55	6:31:25.81	4:58:14.1	16.932	1.816	1.421	0.916	-	Ib	III	-2.86	WTTS	F	-	W2010	
56	6:32:31.59	4:55:25.1	16.974	1.979	1.612	1.083	-	BC	III	-2.43	WTTS*	F	82.7	W2469	
57	6:32:23.18	5:00:57.2	16.990	1.772	1.538	0.757	a	-	III	-2.66	WTTS*	F	81.7	W2392	
58	6:32:06.70	4:55:30.6	17.011	1.992	1.572	0.870	-	BC	II	-0.71	CTTS*	F	21.5	W746	
59	6:31:32.02	5:05:16.1	17.069	1.521	1.315	0.793	-	-	-	-	-	F	88.3	-	
60	6:31:49.26	4:57:01.0	17.074	1.779	1.528	0.571	b	BC Ia	II	-1.20	CTTS	F	90.2	W730	
61	6:31:41.98	4:54:18.2	17.087	1.709	1.379	0.698	b	IA	II	-1.39	CTTS	F	89.0	-	
62	6:31:50.78	4:54:34.7	17.100	1.863	1.462	0.991	a	BC Ib	III	-2.88	WTTS	F	91.1	W732	
63	6:31:40.87	4:59:01.1	17.182	1.203	1.014	0.376	a	Ib	-	-	-	-	50.0	-	nm
64	6:32:18.03	4:49:02.0	17.211	1.878	1.535	1.033	a	-	III	-2.60	WTTS*	F	89.3	-	
65	6:32:16.13	4:55:30.0	17.214	2.209	0.937	0.461	-	Ia	II	-0.45	CTTS	T	0.0	V555 Mon	
66	6:31:59.26	5:01:17.2	17.215	2.134	1.646	0.944	c	-	II	-1.58	CTTS*	F	89.2	-	
67	6:31:28.84	4:52:13.3	17.234	1.918	1.488	0.691	a	PS IA	II	-1.26	CTTS	F	77.7	W2021	
68	6:31:59.33	5:05:59.9	17.244	1.396	1.184	0.554	-	Ib	-	-	-	-	-	-	nm
69	6:32:17.58	4:53:08.3	17.250	1.830	1.525	0.914	b	-	II	-1.47	CTTS*	F	89.7	-	
70	6:32:20.83	5:04:16.5	17.281	1.834	1.632	0.880	-	-	II	-1.13	CTTS*	F	82.6	-	

Table A1 – continued

Star	R.Asc. (2000.0)	Dec. (2000.0)	V mag	V-I _C mag	B-V mag	U-B mag	X ⁽¹⁾	H α ⁽²⁾	Cl. ⁽³⁾	α ⁽⁴⁾	Var. ⁽⁵⁾ type	NIR ⁽⁶⁾ reg.	Prob. ⁽⁷⁾ [%]	Other ⁽⁸⁾ name	Notes ⁽⁹⁾
71	6:32:14.74	4:50:23.7	17.314	2.036	1.677	—	a	—	III	-2.73	WTTS*	F	88.5	—	
72	6:31:34.31	5:04:16.0	17.349	1.131	0.854	0.267	-	—	—	—	ECL	-	0.0	—	nm
73	6:32:05.93	4:57:27.7	17.350	2.077	1.493	0.686	a	Ia	II	-0.73	CTTS	F	29.1	—	
74	6:31:57.34	4:53:42.3	17.383	1.874	1.465	—	a	—	II	-1.85	—	F	89.7	—	
75	6:31:43.92	5:02:38.9	17.404	1.410	1.056	0.454	-	—	—	—	DSCT	-	1.1	—	nm
76	6:32:07.82	4:52:28.5	17.407	1.843	1.439	0.565	c	IA	II	-1.16	CTTS	F	88.9	—	
77	6:31:51.48	4:51:32.0	17.408	2.216	1.727	0.724	a	Ib	II	-1.78	CTTS*	F	—	—	
78	6:32:20.34	4:58:41.8	17.413	2.016	1.617	0.639	a	Ib	III	-2.79	WTTS	F	91.0	—	
79	6:32:08.02	4:50:33.6	17.418	2.005	1.574	0.734	a	—	III	-2.67	WTTS*	F	89.6	—	
80	6:32:04.69	4:47:45.6	17.442	1.922	1.563	0.710	-	Ib	II	-1.25	CTTS*	F	48.4	—	
81	6:31:57.19	4:50:12.0	17.458	2.125	1.636	0.391	a	—	III	-2.77	WTTS*	F	—	—	
82	6:31:51.64	4:55:05.3	17.460	1.902	1.610	0.749	-	Ib	II	-1.62	CTTS*	F	88.7	V547 Mon	
83	6:31:27.85	4:50:03.0	17.515	1.909	0.998	—	-	IA	II	-1.04	CTTS	T	36.8	V544 Mon	
84	6:32:16.67	4:49:38.2	17.523	1.912	1.564	0.843	c	—	FS*	-0.61	CTTS*	F	87.5	—	
85	6:32:20.25	4:57:55.8	17.527	1.987	1.496	0.952	c	—	III	-2.31	WTTS*	F	80.0	—	
86	6:32:05.44	4:57:30.1	17.532	2.045	1.658	—	b	—	III	-2.91	—	F	90.8	—	
87	6:31:59.12	4:55:26.0	17.552	2.090	1.213	—	-	Ib	II	-1.80	CTTS*	F	89.4	—	
88	6:31:41.02	4:54:47.9	17.567	1.919	1.451	0.559	b	BC IA	II	-1.15	CTTS	F	86.1	W724	
89	6:32:23.11	4:49:43.2	17.585	2.233	1.873	—	a	BC	II	-1.42	CTTS*	F	90.6	W756	
90	6:31:50.44	4:56:38.4	17.603	2.081	1.425	0.563	c	Ib	III	-2.12	WTTS	F	0.4	—	
91	6:32:22.77	5:00:31.9	17.609	1.903	1.591	0.690	b	—	III	-2.73	WTTS*	F	86.3	—	
92	6:31:30.03	5:00:45.6	17.625	1.519	1.116	0.731	-	—	—	—	DSCT	-	0.0	—	nm
93	6:32:10.65	4:51:32.7	17.634	1.949	1.593	—	a	—	III	-2.78	WTTS*	F	88.8	—	
94	6:31:21.43	4:54:05.8	17.637	2.055	1.602	—	-	—	—	—	—	F	85.0	—	
95	6:31:43.89	5:03:56.5	17.669	1.775	1.437	0.733	c	BC	—	—	—	F	15.3	W726	
96	6:32:23.41	4:52:39.2	17.690	2.164	1.596	0.527	-	Ib	II	-1.66	CTTS*	F	85.5	—	
97	6:31:44.47	5:03:42.2	17.693	1.962	1.508	0.700	a	Ib	III	-2.63	WTTS	F	57.3	—	
98	6:31:36.42	4:53:13.9	17.713	2.147	1.497	0.291	a	BC Ia	II	-0.87	CTTS	F	53.3	W721	
99	6:32:04.66	4:54:51.5	17.727	2.134	1.692	—	c	Ia	II	-1.71	CTTS	F	80.2	—	
100	6:31:46.07	4:54:30.8	17.744	2.098	1.559	0.859	b	—	III	-2.68	WTTS*	F	83.3	—	
101	6:31:50.26	5:00:07.8	17.749	1.999	1.597	0.710	c	—	TD	-1.94	WTTS	F	78.5	—	
102	6:31:20.86	5:04:08.7	17.752	1.989	1.548	—	-	Ib	II	-1.52	CTTS*	F	0.1	—	
103	6:31:38.78	4:55:24.9	17.755	2.113	1.658	—	a	Ib	III	-2.60	WTTS	F	86.0	—	
104	6:31:50.43	4:51:50.1	17.765	1.930	1.362	—	a	IA	II	-1.96	CTTS	F	73.9	—	
105	6:32:20.79	4:52:58.2	17.770	2.035	1.605	—	b	BC Ib	III	-2.72	WTTS	F	—	W754	
106	6:32:01.17	4:55:27.3	17.775	1.951	1.613	—	-	Ib	III	-2.09	WTTS	F	84.5	—	
107	6:32:14.81	4:48:55.4	17.788	1.951	1.499	—	b	—	III	-2.73	WTTS*	F	90.3	—	
108	6:31:47.56	4:49:07.7	17.795	2.003	1.586	—	a	BC	III	-2.93	WTTS*	F	85.3	W729	
109	6:31:55.25	4:53:29.9	17.805	1.997	1.544	0.688	-	—	III	-2.99	WTTS*	F	78.4	W735	
110	6:32:10.89	4:57:06.2	17.854	1.914	1.663	—	c	Ib	III	-2.62	WTTS	F	—	—	
111	6:31:55.82	4:51:27.3	17.858	2.084	1.601	—	c	—	—	—	—	F	77.6	—	
112	6:31:55.60	4:55:17.3	17.868	2.006	1.419	—	b	Ib	III	-1.85	WTTS	F	87.2	—	
113	6:31:45.38	4:59:02.4	17.885	2.073	1.609	—	a	—	III	-2.55	WTTS*	F	69.9	—	
114	6:32:23.85	5:06:13.5	17.918	1.224	1.325	0.522	-	—	—	—	—	-	—	—	nm
115	6:31:57.61	5:02:29.1	17.938	2.095	1.570	—	b	Ib	II	-1.41	CTTS*	F	42.4	—	
116	6:31:36.87	4:51:04.3	17.942	2.255	1.620	—	b	—	FS	-0.18	CTTS	F	0.0	W2062	
117	6:32:29.24	5:05:15.9	17.945	1.924	1.584	—	-	Ia	—	—	—	F	90.2	—	
118	6:31:27.66	4:54:02.8	17.957	2.365	1.681	—	a	—	III	-2.47	WTTS*	F	8.0	—	
119	6:32:00.54	5:05:33.5	18.032	1.943	1.563	—	-	—	—	—	—	-	71.7	W2225	
120	6:32:25.13	4:55:14.4	18.046	1.960	1.574	—	a	—	II	-1.58	CTTS*	F	88.0	—	
121	6:31:55.52	4:53:46.9	18.072	2.096	1.619	—	-	Ib	II	-1.05	CTTS*	F	89.2	—	
122	6:31:48.72	4:55:21.0	18.087	2.024	1.678	—	-	—	—	—	—	F	86.8	—	
123	6:32:00.48	4:59:46.9	18.088	2.018	1.594	—	a	—	III	-2.50	WTTS*	F	—	—	
124	6:31:55.03	4:53:20.8	18.094	2.205	1.709	—	-	—	III	-2.62	WTTS*	F	87.6	—	
125	6:32:09.92	4:50:15.0	18.110	2.039	1.677	—	c	—	—	—	—	F	83.9	—	
126	6:32:07.55	4:56:15.3	18.119	2.244	1.691	—	a	—	III	-2.68	WTTS*	F	57.4	—	
127	6:32:10.92	4:55:02.6	18.127	1.940	1.579	—	-	Ia	II	-1.28	CTTS	F	84.7	—	
128	6:32:27.18	4:52:41.9	18.127	1.864	1.493	—	-	—	—	—	—	F	85.0	—	
129	6:31:47.44	4:53:31.5	18.133	2.244	1.699	—	a	—	—	—	—	F	0.0	—	
130	6:31:47.70	4:56:49.8	18.141	2.219	1.686	—	a	BC	III	-2.77	WTTS*	F	90.3	W728	
131	6:32:05.08	4:55:46.9	18.160	1.927	1.478	—	c	Ib	II	-0.94	CTTS	T	89.0	—	
132	6:31:56.93	4:53:02.0	18.168	2.066	1.691	—	b	—	II	-1.49	CTTS*	F	80.9	—	
133	6:32:01.84	4:53:38.6	18.179	2.024	1.472	—	a	BC IA	TD	-1.24	CTTS	F	78.8	W740	
134	6:31:36.77	4:53:10.0	18.182	2.156	1.593	—	a	—	II	-0.82	CTTS*	F	76.6	—	
135	6:31:54.60	4:59:41.7	18.182	1.916	1.491	—	a	—	—	—	—	F	89.2	—	
136	6:31:57.09	4:54:36.4	18.184	2.161	1.650	—	-	—	III	-2.72	WTTS*	F	82.4	—	
137	6:32:08.29	4:50:56.5	18.209	2.126	1.756	—	a	—	—	—	—	F	81.1	—	
138	6:32:02.93	4:58:54.0	18.226	2.218	1.617	—	a	Ib	III	-2.75	WTTS	F	88.3	—	
139	6:31:52.01	4:54:08.4	18.237	2.032	1.660	—	a	BC Ib	—	—	—	F	88.1	W734	
140	6:32:07.67	4:54:33.7	18.251	2.132	1.606	—	b	—	TD	-1.17	CTTS*	F	67.7	—	

Table A1 – continued

Star	R.Asc. (2000.0)	Dec. (2000.0)	V mag	V-I _C mag	B-V mag	U-B mag	X ⁽¹⁾	H α ⁽²⁾	Cl. ⁽³⁾	α ⁽⁴⁾	Var. ⁽⁵⁾ type	NIR ⁽⁶⁾ reg.	Prob. ⁽⁷⁾ [%]	Other ⁽⁸⁾ name	Notes ⁽⁹⁾
141	6:31:59.63	4:52:16.8	18.264	2.245	—	—	a	lb	III	-2.51	WTTS	F	88.3	—	
142	6:31:39.62	4:59:45.1	18.270	2.454	1.640	—	a	la	II	-1.53	CTTS	F	74.9	—	
143	6:31:49.81	4:49:06.8	18.277	2.268	1.611	—	-	lb	III	-2.71	WTTS	F	—	—	
144	6:31:59.70	4:55:36.0	18.280	2.225	—	—	-	-	III	-2.66	WTTS*	F	89.1	—	
145	6:31:48.05	4:50:48.3	18.287	2.343	1.389	—	-	IA	II	-0.54	CTTS	F	0.0	—	
146	6:31:43.57	4:59:49.1	18.310	2.238	1.632	—	b	-	-	—	—	F	57.7	—	
147	6:31:30.24	4:51:48.5	18.318	2.141	1.506	—	-	la	II	-1.50	CTTS	F	88.7	—	
148	6:31:37.22	4:56:57.3	18.329	2.075	1.620	—	-	-	-	—	—	F	87.8	—	
149	6:32:01.02	4:57:31.8	18.379	2.153	1.457	—	a	la	II	-1.22	CTTS	F	89.0	—	
150	6:31:47.45	4:58:32.9	18.387	2.133	—	—	a	-	III	-2.58	WTTS*	F	89.1	—	
151	6:32:15.12	4:59:57.5	18.390	2.248	1.586	—	-	-	III	-2.44	—	F	42.2	—	
152	6:31:47.59	4:50:52.9	18.408	2.393	1.545	—	c	lb	II	-1.19	CTTS*	F	81.7	—	
153	6:32:25.76	4:58:23.3	18.443	2.448	—	—	-	-	-	—	—	F	89.7	—	
154	6:32:22.27	4:47:14.1	18.449	2.399	1.015	—	-	la	III	-2.77	WTTS	F	85.7	—	
155	6:31:39.56	4:53:38.6	18.462	2.120	1.331	—	c	IA	III	-1.22	CTTS*	F	78.9	—	
156	6:32:09.33	4:52:41.4	18.481	2.451	—	—	c	IA	III	-2.85	WTTS	F	79.2	—	
157	6:31:52.56	4:58:17.4	18.498	2.231	—	—	a	lb	III	-2.70	WTTS	F	88.0	—	
158	6:31:56.79	4:53:51.1	18.498	2.126	—	—	-	-	TD	-1.33	CTTS*	F	80.7	—	
159	6:31:46.10	4:57:50.8	18.540	2.122	—	—	a	-	-	—	—	F	89.8	—	
160	6:31:32.09	4:57:38.8	18.555	2.172	—	—	a	lb	TD	-1.57	CTTS*	F	83.6	—	
161	6:31:45.11	4:51:26.2	18.562	2.190	—	—	-	BC	-	—	—	F	65.7	W727	
162	6:31:58.14	4:48:29.9	18.574	2.255	—	—	a	-	-	—	—	F	74.5	—	
163	6:31:30.95	4:48:48.4	18.579	2.353	—	—	-	lb	II	-0.88	CTTS*	F	86.7	—	
164	6:32:12.21	4:56:32.8	18.602	2.140	—	—	-	-	-	—	—	F	77.4	—	
165	6:31:39.18	4:49:59.5	18.628	1.894	1.038	—	b	IA	II	-1.06	CTTS	F	84.8	—	
166	6:31:48.89	4:56:09.3	18.631	2.171	—	—	-	lb	II	-1.12	CTTS*	F	88.0	—	
167	6:31:39.31	4:54:01.0	18.648	2.401	—	—	a	-	-	—	—	F	3.1	—	
168	6:32:30.05	4:57:26.4	18.651	2.065	—	—	-	la	-	—	—	F	48.5	—	
169	6:31:41.98	4:54:16.3	18.676	2.255	—	—	a	IA	-	—	—	F	74.2	—	
170	6:31:24.42	4:53:05.5	18.695	1.667	1.188	—	-	lb	-	—	ECL	F	0.0	—	nm
171	6:31:49.53	4:52:00.0	18.707	1.951	—	—	a	-	-	—	—	F	42.3	—	
172	6:31:48.31	4:52:38.8	18.760	2.219	—	—	-	lb	II	-1.48	CTTS*	F	85.8	—	
173	6:31:56.53	4:54:28.4	18.771	2.317	—	—	-	-	III	-2.49	WTTS*	F	86.9	—	
174	6:31:41.13	4:55:51.5	18.777	2.242	—	—	a	-	-	—	—	F	83.3	—	
175	6:32:01.50	4:54:45.1	18.779	2.274	—	—	a	lb	II	-0.86	CTTS*	F	86.3	—	
176	6:32:01.11	4:54:49.8	18.797	2.538	—	—	a	-	-	—	—	F	86.1	—	
177	6:32:06.49	4:48:46.6	18.803	2.367	—	—	a	-	III	-2.37	WTTS*	F	40.0	—	
178	6:31:41.58	4:59:40.5	18.814	2.146	—	—	a	-	-	—	—	F	79.6	—	
179	6:32:12.34	4:57:21.9	18.853	2.368	—	—	a	lb	II	-1.30	CTTS*	F	84.3	—	
180	6:32:26.57	4:52:38.3	18.865	2.122	—	—	-	IA	II	-0.92	CTTS	F	82.1	—	
181	6:31:41.90	4:50:46.1	18.868	2.288	—	—	c	la	II	-1.93	CTTS	F	83.3	—	
182	6:32:12.86	4:58:38.1	18.875	2.384	—	—	a	-	III	-2.60	WTTS*	F	70.0	—	
183	6:31:43.35	4:57:24.9	18.934	2.264	—	—	a	lb	II	-1.68	CTTS*	F	80.4	—	
184	6:31:53.78	4:48:47.1	18.941	2.696	—	—	-	lb	III	-2.78	WTTS	F	60.0	—	
185	6:32:12.18	5:01:39.8	18.953	2.028	—	—	a	-	II	-1.34	CTTS*	F	—	—	
186	6:31:44.92	4:56:00.2	18.963	2.617	—	—	-	la	II	-1.34	CTTS	F	0.0	—	
187	6:31:47.79	4:52:23.9	18.973	2.326	—	—	-	la	II	-0.61	CTTS	F	66.8	—	
188	6:31:50.35	4:57:39.0	18.994	2.493	—	—	a	lb	-	—	—	F	80.5	—	
189	6:31:18.44	4:54:40.2	19.002	2.196	—	—	-	la	-	—	—	F	85.8	—	
190	6:32:04.47	4:58:26.2	19.014	2.276	—	—	c	la	III	-1.96	WTTS	F	86.1	—	
191	6:32:16.16	4:59:20.1	19.060	2.420	—	—	-	c	II	-1.06	CTTS*	F	87.1	—	
192	6:31:56.87	4:55:14.7	19.100	2.579	—	—	-	lb	-	—	—	F	83.9	—	
193	6:31:54.93	4:51:36.1	19.121	2.327	—	—	-	IA	-	—	—	F	80.2	—	
194	6:32:30.12	4:55:22.2	19.187	2.431	—	—	-	IA	II	-1.65	CTTS	F	0.3	—	
195	6:31:59.30	4:51:37.6	19.202	2.354	—	—	a	-	-	—	—	F	—	—	
196	6:31:39.88	4:56:39.2	19.224	2.363	—	—	-	IA	III	-2.32	WTTS	F	53.3	—	
197	6:32:03.08	5:01:34.9	19.225	2.293	—	—	a	IA	II	-0.98	CTTS	F	63.2	—	
198	6:32:06.99	4:48:03.8	19.227	2.390	—	—	b	lb	-	—	—	F	82.0	—	
199	6:31:19.48	4:53:09.7	19.242	2.588	—	—	-	lb	-	—	—	F	52.1	—	
200	6:31:58.92	4:57:43.2	19.242	2.351	—	—	-	lb	II	-1.28	CTTS*	F	82.5	—	
201	6:32:01.51	4:55:02.2	19.251	2.359	—	—	b	lb	-	—	—	F	86.1	—	
202	6:31:42.59	4:52:56.2	19.256	2.743	—	—	a	la	II	-0.81	CTTS	F	58.1	—	
203	6:32:27.50	4:52:51.3	19.272	2.489	—	—	c	IA	II	-1.42	CTTS	F	—	—	
204	6:31:58.89	4:58:11.1	19.299	2.360	—	—	-	IA	II	-0.60	CTTS	F	78.2	—	
205	6:32:20.34	4:53:20.7	19.368	1.623	—	—	-	la	-	—	ECL	F	33.6	—	nm
206	6:32:05.07	4:52:26.7	19.391	2.566	—	—	b	la	TD	-1.99	WTTS	F	44.7	—	
207	6:32:35.69	4:47:46.0	19.402	2.592	—	—	-	-	FS	-0.31	CTTS*	F	0.7	—	
208	6:31:30.72	4:52:15.0	19.418	2.384	—	—	c	-	II	-1.24	CTTS*	F	87.6	—	
209	6:31:51.56	4:47:28.0	19.453	2.416	—	—	-	IA	II	-0.52	CTTS	F	78.5	—	
210	6:31:52.21	4:52:40.0	19.553	2.443	—	—	a	la	II	-1.10	CTTS	F	22.4	—	

Table A1 – continued

Star	R.Asc. (2000.0)	Dec. (2000.0)	<i>V</i> mag	<i>V</i> – <i>I</i> _C mag	<i>B</i> – <i>V</i> mag	<i>U</i> – <i>B</i> mag	X ⁽¹⁾	H α ⁽²⁾	Cl. ⁽³⁾	α ⁽⁴⁾	Var. ⁽⁵⁾ type	NIR ⁽⁶⁾ reg.	Prob. ⁽⁷⁾ [%]	Other ⁽⁸⁾ name	Notes ⁽⁹⁾
211	6:31:32.87	4:59:49.5	19.590	2.092	—	—	a	—	II	-1.33	CTTS	T	86.9	—	nm
212	6:32:24.01	4:56:59.3	19.593	2.594	—	—	c	IA	II	-1.31	CTTS	F	56.8	—	
213	6:32:31.92	4:51:09.0	19.615	2.336	—	—	—	la	II	-1.60	CTTS	F	12.7	—	
214	6:32:22.70	4:58:08.4	19.617	2.586	—	—	a	IA	II	-1.28	CTTS	F	—	—	
215	6:31:29.84	4:51:10.7	19.645	2.604	—	—	a	IA	II	-1.04	CTTS	T	—	—	
216	6:31:25.46	4:49:31.0	19.648	2.426	—	—	c	la	II	-1.19	CTTS	F	67.8	—	
217	6:31:47.36	4:49:43.6	19.699	2.370	—	—	—	lb	—	—	—	F	60.3	—	
218	6:32:10.37	4:52:05.9	19.703	2.534	—	—	—	la	II	-1.19	CTTS	F	65.4	—	
219	6:31:59.36	4:49:55.0	19.784	2.581	—	—	b	la	II	-1.34	CTTS	F	72.2	—	
220	6:31:58.73	4:53:46.9	19.880	2.205	—	—	—	la	II	-1.84	CTTS	F	20.8	—	nm
221	6:31:29.41	4:50:34.9	19.881	2.516	—	—	a	—	—	—	—	F	75.0	—	
222	6:32:31.50	4:54:53.3	19.932	2.330	—	—	—	IA	III	-2.03	WTTS	T	74.3	—	
223	6:32:32.66	4:57:01.1	19.976	2.685	—	—	—	la	II	-1.28	CTTS	F	75.7	—	
224	6:31:36.59	5:05:15.2	19.984	3.013	—	—	—	IA	(II)	(-0.54)	CTTS	F	71.6	—	
225	6:32:08.95	5:01:51.3	19.984	2.311	—	—	—	—	—	(-1.49)	—	F	69.3	—	
226	6:31:57.58	4:53:39.0	20.002	2.617	—	—	a	lb	II	-0.82	CTTS*	F	25.9	—	
227	6:31:56.58	4:59:51.6	20.007	2.635	—	—	b	—	—	—	—	F	57.8	—	
228	6:32:23.92	4:54:21.0	20.077	2.405	—	—	—	IA	III	-1.26	CTTS*	F	7.4	—	
229	6:31:43.36	4:54:23.0	20.131	2.083	—	—	—	la	II	-1.74	CTTS	F	35.8	—	nm
230	6:31:32.48	5:06:05.5	20.178	2.972	—	—	—	IA	(II)	(-0.93)	CTTS	F	75.0	—	
231	6:31:41.05	4:54:19.9	20.193	2.779	—	—	b	lb	II	-0.94	CTTS	T	0.0	—	
232	6:31:58.10	4:54:15.0	20.199	2.206	—	—	—	—	II	-1.00	CTTS*	F	0.0	—	nm
233	6:31:48.54	5:04:07.2	20.212	2.696	—	—	—	la	III	-1.55	CTTS*	F	53.7	—	
234	6:31:55.47	5:00:54.2	20.242	2.480	—	—	—	IA	II	-1.47	CTTS	—	75.3	—	
235	6:31:59.69	5:06:27.2	20.252	2.705	—	—	—	lb	—	—	—	F	46.4	—	
236	6:32:30.20	4:54:01.3	20.297	2.306	—	—	—	—	II	-1.19	CTTS*	T	19.0	—	
237	6:31:49.00	4:55:47.0	20.302	2.731	—	—	a	—	II	-1.29	CTTS*	F	55.7	—	
238	6:32:03.65	4:59:52.2	20.396	2.589	—	—	a	—	II	-1.32	CTTS*	F	43.9	—	
239	6:31:38.34	5:02:56.6	20.399	2.821	—	—	—	la	II	-1.22	CTTS	F	63.4	—	
240	6:32:19.28	4:56:29.6	20.422	2.157	—	—	—	IA	—	—	—	F	35.3	—	
241	6:32:07.17	4:55:14.5	20.472	2.486	—	—	—	—	II	-0.95	CTTS*	F	39.5	—	
242	6:31:28.41	4:50:35.2	20.495	2.475	—	—	—	—	II	-0.83	CTTS*	T	—	—	
243	6:32:11.98	5:00:31.1	20.496	2.166	—	—	a	la	I	0.98	CTTS	F	43.9	—	
244	6:32:19.98	4:57:48.5	20.630	2.393	—	—	—	—	II	-1.65	CTTS*	F	—	—	
245	6:32:28.81	4:52:56.1	20.751	2.090	—	—	—	—	II	-1.63	CTTS*	F	—	—	

(1) a, b, c – X-ray variability from Wang et al. (2008):

- a = no evidence for variability;
- b = possibly variable;
- c = definitely variable.

(2) H α emission:

- IA – stars with H α emission above the empirical threshold in IPHAS ($r' - H\alpha$) vs. ($r' - i'$) colour-colour diagram (see Sect. 6.1);
- Ia – stars with photometric EW_{H α} > 10 Å based on IPHAS photometry (see Sect. 6.1);
- Ib – stars with photometric EW_{H α} between 0 and 10 Å based on IPHAS photometry (see Sect. 6.1);
- BC – stars with H α excess from Berghöfer & Christian (2002);
- PS – stars with H α excess from Park & Sung (2002).

(3) Classification based on *Spitzer* photometry (see Sect. 5):

- I – Class I objects;
- II – Class II objects;
- TD – transition disks objects;
- FS – flat spectrum objects with α index between -0.3 and 0.3;
- FS* – flat spectrum objects with ($K - [24]$) colour between 6.75 and 8.31 (Sect. 5.1.3);
- III – field stars and/or diskless YSOs (Class III);
- (II) – Class II objects found based on WISE photometry in case of lack *Spitzer* photometry (see Sect. 5.3).

(4) Spectral index $\alpha = d \log(\lambda F_\lambda) / d \log(\lambda)$ calculated from the slope of the linear fit to the fluxes between the K band and the IRAC [8] μ m band (Lada et al. 2006):

- $\alpha > 0.3$: Class I YSOs;
- $-0.3 < \alpha < 0.3$: flat spectrum objects;
- $-1.8 < \alpha < -0.3$: Class II YSOs;
- $\alpha < -1.8$: Class III objects.
- α in brackets – spectral index found based on WISE photometry in case of lack *Spitzer* photometry (see Sect. 5.3).

(5) Variability type:

- CTTS – the best candidates for CTTSs: Class II stars with photometric EW_{H α} > 10 Å lying above CTTS line in ($J - H$) vs. ($H - K$) colour-colour diagram (Fig. 21);
- CTTS* – additional candidates for CTTSs: objects lying above CTTS line in ($J - H$) vs. ($H - K$) colour-colour diagram and having spectra index $\alpha > -1.8$ (Class III stars with photometric EW_{H α} > 10 Å and Class II objects with photometric EW_{H α} < 10 Å or without EW_{H α});
- WTTS – candidates for WTTSs: objects lying above CTTS line with spectral index $\alpha < -1.8$ (Class II with photometric EW_{H α} < 10 Å or Class III objects with photometric 0 < EW_{H α} < 10 Å);
- WTTS* – remaining objects lying above CTTS line.

(6) The area in ($J - H$) vs. ($H - K$) colour-colour diagram in Fig. 21.

(7) Membership probability determined in Sect. 4.

(8) Other name:

- the other name of the star (from GCVS, HD catalogues or WEBDA number). The names from UKIDSS-DR6 catalogue (Lucas et al. 2008) are shown in Table A2

(9) Notes:

- nm – non-member – the membership determined from V vs. ($V - I_C$) colour-magnitude diagram.

Table A2. 2MASS, UKIDSS, Spitzer and IPHAS infrared photometry of variable stars.

Star	Name	<i>J</i> mag	<i>H</i> mag	<i>K_S</i> mag	<i>J</i> mag	<i>H</i> mag	<i>K</i> mag	[3.6] mag	[4.5] mag	[5.8] mag	[8.0] mag	[24] mag	<i>r</i> mag	<i>i</i> mag	<i>H_α</i> mag
1	J063200.60+045240.9	8.152	8.125	8.120	10.825	11.668	9.523	8.376	8.311	8.197	8.184	—	—	—	—
2	J063133.11+045035.4	10.770	9.942	9.115	10.715	10.823	9.641	7.713	7.136	6.435	5.484	2.707	—	—	—
3	J063129.76+045449.1	11.449	10.887	9.690	11.371	11.148	9.843	7.422	6.753	6.061	4.740	1.783	12.22	11.89	11.57
4	J063125.42+050209.3	10.977	10.711	10.544	10.913	11.005	10.560	—	—	—	—	—	—	—	—
5	J063130.87+045812.3	12.047	11.908	11.812	12.020	11.926	11.879	11.862	11.859	11.963	11.912	—	12.69	12.46	12.62
6	J063140.00+050556.4	9.684	8.956	8.274	10.209	11.272	9.477	—	—	—	—	—	—	—	—
7	J063235.43+045158.6	12.227	11.902	11.829	12.244	11.928	11.864	11.837	12.015	11.794	11.698	—	13.20	12.80	12.94
8	J063230.89+044753.7	11.972	11.530	11.495	11.983	11.592	11.474	11.427	11.408	11.518	11.399	—	13.15	12.65	12.84
9	J063151.57+045417.5	11.981	11.314	10.613	12.057	11.611	10.828	9.974	9.560	8.479	6.669	2.591	13.38	12.98	12.98
10	J063141.12+045607.6	11.634	11.096	10.966	11.608	11.349	10.981	10.870	10.885	10.796	10.836	—	13.42	12.71	13.06
11	J063215.84+045430.0	11.583	10.947	10.769	11.652	11.148	10.825	10.705	10.681	10.622	10.458	—	13.68	12.87	13.24
12	J063219.94+044819.1	11.842	11.320	11.122	11.816	11.371	11.133	11.051	10.988	10.933	10.849	—	13.75	12.99	13.40
13	J063224.84+045746.2	12.613	12.175	12.075	12.597	12.189	12.079	12.023	12.132	11.956	11.985	—	13.78	13.26	13.46
14	J063207.08+045629.8	11.783	11.162	11.022	11.778	11.290	10.992	10.869	10.801	11.082	10.455	9.152	13.85	13.07	13.44
15	J063231.01+045005.9	12.070	11.571	11.092	12.120	11.572	11.041	10.345	10.056	9.674	8.544	5.986	13.90	13.22	13.52
16	J063228.07+045037.7	12.327	11.794	11.661	12.254	11.808	11.618	11.541	11.647	11.499	11.524	—	13.98	13.28	13.63
17	J063206.51+044755.3	11.970	11.224	10.344	12.593	11.567	10.329	8.949	8.454	7.971	7.449	5.548	13.48	12.98	13.16
18	J063206.36+050236.8	13.118	12.808	12.644	13.123	12.814	12.659	12.552	12.563	12.529	12.561	—	14.64	14.03	14.38
19	J063224.41+045222.6	12.872	12.225	12.074	12.771	12.219	12.014	11.895	11.899	11.838	11.791	—	14.80	14.02	14.40
20	J063209.97+045423.1	12.893	12.305	12.095	12.847	12.307	12.100	12.049	12.053	11.991	11.962	—	14.88	14.12	14.46
21	J063204.35+045758.1	12.954	12.477	12.369	13.026	12.577	12.391	12.252	12.275	12.213	12.296	—	14.76	14.07	14.40
22	J063205.41+045659.2	12.608	11.940	11.764	12.675	12.039	11.792	11.684	11.700	11.569	11.586	—	14.98	14.09	14.52
23	J063211.61+045357.0	12.967	12.270	12.107	12.914	12.288	12.056	12.072	11.983	12.044	11.942	—	15.23	14.35	14.82
24	J063147.38+045320.3	13.064	12.414	12.106	13.037	12.468	12.240	12.054	12.085	12.064	12.178	—	15.09	14.28	14.71
25	J063202.09+044855.4	13.116	12.488	12.210	13.087	12.482	12.258	12.142	12.180	12.136	12.108	—	15.27	14.42	14.90
26	J063221.47+045027.4	13.134	12.409	12.181	13.055	12.406	12.168	12.061	12.072	12.073	12.004	—	15.39	14.49	15.00
27	J063157.47+045504.4	13.438	12.789	12.590	13.397	12.780	12.564	12.535	12.598	12.427	12.308	—	15.52	14.70	15.09
28	J063159.93+045109.9	13.266	12.580	12.348	13.290	12.654	12.412	12.312	12.196	12.071	12.092	—	15.52	14.64	15.09
29	J063130.58+045835.7	14.405	13.965	13.841	14.361	13.953	13.858	—	—	—	—	—	15.81	15.23	15.49
30	J063151.41+045728.4	13.097	12.306	12.088	12.948	12.301	12.054	11.957	11.923	11.880	11.755	—	15.47	14.54	14.99
31	J063148.13+045337.9	13.124	12.418	12.218	13.101	12.476	12.236	12.220	12.163	12.089	12.050	—	15.45	14.57	15.03
32	J063200.30+050041.9	13.178	12.421	12.203	13.158	12.480	12.235	12.015	12.114	12.029	11.976	—	15.56	14.62	15.11
33	J063211.64+045027.0	13.646	12.988	12.821	13.646	13.034	12.810	12.736	12.657	12.668	12.528	—	15.82	14.98	15.41
34	J063203.37+045235.9	13.132	12.345	11.971	13.725	12.963	12.447	11.478	11.313	10.911	10.193	7.806	15.30	14.40	14.87
35	J063204.72+044914.8	13.524	12.848	12.622	13.480	12.852	12.635	12.669	12.617	12.598	12.412	—	15.78	14.91	15.37
36	J063133.43+045825.9	14.638	14.283	14.008	14.615	14.238	14.146	—	—	—	—	—	16.05	15.47	15.74
37	J063128.44+045450.3	13.753	13.089	12.884	13.736	13.129	12.941	—	—	—	—	—	15.96	15.13	15.57
38	J063206.02+045031.2	13.298	12.570	12.374	13.319	12.610	12.357	12.260	12.371	12.235	12.182	—	15.81	14.84	15.36
39	J063156.29+045416.1	13.261	12.473	12.252	13.214	12.523	12.258	12.160	12.277	12.125	12.113	—	15.88	14.89	15.36
40	J063205.89+045705.3	13.177	12.399	12.192	13.174	12.469	12.199	11.993	12.003	11.930	11.878	—	15.86	14.83	15.33
41	J063150.55+045553.0	13.199	12.365	12.136	13.139	12.413	12.131	11.996	11.996	11.841	11.924	—	15.90	14.82	15.35
42	J063200.93+045155.9	13.413	12.632	12.340	13.314	12.599	12.275	11.927	11.413	10.494	9.146	6.151	15.85	14.86	15.38
43	J063202.10+045647.1	13.327	12.597	12.334	13.295	12.611	12.350	12.169	12.145	12.097	11.997	—	15.87	14.89	15.37
44	J063157.30+045451.4	13.117	12.299	12.008	13.123	12.412	12.093	11.726	11.539	11.528	11.162	7.731	16.04	15.00	15.44
45	J063143.85+050257.4	13.273	12.379	11.973	13.154	12.365	11.990	11.146	10.703	10.117	9.063	4.920	16.62	15.42	15.89
46	J063230.92+045007.2	—	—	—	—	13.064	12.841	—	—	—	—	—	16.29	15.45	15.85
47	J063215.02+045235.4	13.345	12.503	11.985	13.738	12.808	12.137	11.508	11.214	11.164	10.827	6.375	16.22	15.25	15.60
48	J063151.63+045124.0	13.155	12.365	12.125	13.166	12.425	12.147	11.978	11.941	11.851	11.752	—	16.03	14.92	15.49
49	J063148.30+045820.2	12.428	11.573	11.084	12.538	11.724	11.429	10.457	10.119	9.908	9.456	6.390	—	—	—
50	J063204.53+045325.0	13.589	12.705	12.226	13.541	12.770	12.324	11.513	11.241	10.996	10.362	7.069	16.16	15.22	15.59
51	J063213.83+044936.5	13.851	13.074	12.811	13.753	13.041	12.806	12.712	12.816	12.624	12.745	—	16.29	15.33	15.83
52	J063205.21+044827.8	14.779	14.314	14.073	14.752	14.304	14.138	—	—	—	—	—	16.45	15.76	16.14
53	J063221.40+045403.9	14.130	13.450	13.291	14.134	13.516	13.319	—	—	—	—	—	16.20	15.39	15.80
54	J063207.71+050524.3	14.474	14.017	13.756	14.942	14.572	14.431	—	—	—	—	—	16.38	15.65	16.03
55	J063125.81+045814.0	13.637	12.941	12.612	13.702	13.043	12.785	12.516	12.510	12.435	12.545	—	16.25	15.26	15.70
56	J063231.59+045525.0	13.434	12.688	12.399	13.401	12.662	12.405	12.299	12.265	12.184	11.940	—	16.23	15.14	15.70
57	J063223.18+050057.1	13.670	12.902	12.703	13.777	13.081	12.804	12.593	12.539	12.596	12.405	—	16.25	15.32	15.83
58	J063206.69+045530.5	13.570	12.725	12.449	13.433	12.689	12.331	11.902	11.547	11.077	10.050	7.040	16.32	15.25	15.79
59	J063132.01+050516.1	14.289	13.607	13.418	14.280	13.676	13.437	—	—	—	—	—	16.42	15.61	16.05
60	J063149.25+045700.8	13.700	12.847	12.269	13.788	12.966	12.354	11.572	11.177	10.791	10.137	—	16.29	15.30	15.61
61	J063141.98+045418.2	13.887	13.175	12.896	13.937	13.237	12.863	12.465	12.189	12.003	11.171	6.183	16.48	15.59	15.52
62	J063150.78+045434.7	13.825	13.006	12.787	13.660	12.970	12.684	12.561	12.537	12.495	12.604	—	16.32	15.33	15.81
63	J063140.86+045901.0	15.052	14.592	14.322	15.081	14.617	14.472	—	—	—	—	—	16.68	16.06	16.37
64	J063218.03+044902.0	13.914	13.103	12.828	13.833	13.101	12.849	12.927	12.748	12.770	12.681	—	16.59	15.56	16.10
65	J063216.13+045529.9	13.075	12.171	11.487	13.421	12.370	11.475	10.461	9.983	9.513	8.369	5.002	17.58	16.39	16.75
66	J063159.25+050117.1	13.488	12.645	12.233	13.402	12.584	12.107	11.485	11.230	10.922	10.395	7.157	16.33	15.18	15.76
67	J063128.83+045213.1	13.621	12.770	12.400	13.573	12.844	12.388	11.341	10.933	10.522	9.971	7.706	16.46	15.42	15.52
68	J063159.33+050559.9	14.796	14.189	14.015	14.744	14.232	14.029	—	—	—	—	—	16.59	15.82	16.17
69</															

Star	Name	<i>J</i> mag	<i>H</i> mag	<i>K_S</i> mag	<i>J</i> mag	<i>H</i> mag	<i>K</i> mag	[3.6] mag	[4.5] mag	[5.8] mag	[8.0] mag	[24] mag	<i>r</i> mag	<i>i</i> mag	<i>H_α</i> mag
71	J063214.74+045023.6	13.794	12.906	12.676	13.780	12.999	12.723	12.728	12.581	12.604	12.609	—	16.55	15.44	16.01
72	J063134.30+050416.0	—	—	—	15.138	14.812	14.535	—	—	—	—	—	16.89	16.25	16.63
73	J063205.92+045727.6	13.449	12.502	12.068	13.622	12.735	12.176	11.887	11.212	10.869	9.991	6.671	16.70	15.50	15.90
74	J063157.34+045342.3	13.958	13.091	12.824	13.934	13.208	12.910	12.233	12.060	11.874	11.360	—	16.40	15.45	15.96
75	J063143.91+050238.9	14.923	14.384	14.376	14.858	14.449	14.256	—	—	—	—	—	16.87	16.08	16.60
76	J063207.82+045228.4	14.030	13.208	12.764	14.067	13.225	12.683	11.990	11.504	11.249	10.485	8.159	16.74	15.73	15.95
77	J063151.48+045132.0	13.398	12.573	12.195	13.665	12.805	12.334	11.663	11.418	11.142	10.747	8.500	16.82	15.58	16.16
78	J063220.34+045841.7	13.860	13.065	12.780	13.810	13.053	12.775	12.719	12.652	12.639	12.668	—	16.85	15.69	16.25
79	J063208.01+045033.5	13.933	13.088	12.806	13.856	13.116	12.802	12.583	12.514	12.496	12.426	—	16.53	15.46	16.10
80	J063204.68+044745.5	13.726	12.849	12.282	13.873	13.039	12.506	11.861	11.608	11.086	10.519	8.347	16.70	15.67	16.12
81	J063157.18+045011.9	13.749	12.854	12.625	13.700	12.957	12.644	12.560	12.467	12.571	12.460	—	16.66	15.48	16.08
82	J063151.64+045505.2	13.908	13.013	12.452	13.915	13.127	12.637	11.932	11.593	11.422	10.831	6.583	16.85	15.80	16.24
83	J063127.84+045002.9	13.792	12.802	12.006	13.491	12.531	11.613	10.551	10.096	9.658	8.979	6.007	16.42	15.60	16.26
84	J063216.67+044938.2	14.231	13.414	13.063	14.118	13.395	13.137	12.369	11.963	11.565	10.409	5.509	16.80	15.78	16.30
85	J063220.25+045755.6	14.063	13.193	12.940	14.033	13.295	13.031	12.658	12.557	12.358	12.211	—	16.75	15.69	16.26
86	J063205.44+045729.9	13.888	13.066	12.788	13.902	13.142	12.878	12.693	12.706	12.651	12.766	—	16.72	15.58	16.16
87	J063159.12+045525.9	13.733	12.866	12.561	13.702	12.942	12.596	12.096	11.901	11.674	11.188	—	16.82	15.64	16.21
88	J063141.02+045447.8	14.178	13.363	12.954	14.118	13.345	12.890	12.273	11.967	11.601	10.800	8.314	16.68	15.72	15.94
89	J063223.11+044943.2	13.649	12.700	12.286	13.643	12.768	12.279	11.715	11.450	11.120	10.478	7.296	16.80	15.55	16.27
90	J063150.44+045638.2	13.111	13.038	12.783	13.802	13.116	12.801	12.308	12.157	11.927	11.696	—	16.68	15.58	16.12
91	J063222.77+050031.8	14.259	13.513	13.303	14.215	13.471	13.240	13.130	13.119	12.943	13.065	—	16.96	15.94	16.53
92	J063130.02+050045.6	14.824	14.327	14.028	14.815	14.387	14.087	—	—	—	—	—	17.07	16.21	16.81
93	J063210.65+045132.7	14.200	13.407	13.137	14.138	13.409	13.131	13.120	12.948	12.942	13.047	—	16.97	15.89	16.54
94	J063121.42+045405.7	14.060	13.249	12.998	13.982	13.278	13.007	—	—	—	—	—	16.78	15.71	16.29
95	J063143.88+050356.5	14.366	13.620	13.379	14.450	13.767	13.491	—	—	—	—	—	16.88	15.93	16.42
96	J063223.41+045239.1	13.879	13.012	12.692	13.872	13.089	12.740	12.360	12.167	11.917	11.335	7.676	16.85	15.65	16.22
97	J063144.47+050342.2	14.179	13.379	13.138	14.140	13.436	13.152	13.037	13.011	13.028	12.838	—	16.84	15.77	16.28
98	J063136.42+045313.8	13.843	12.930	12.511	13.832	13.021	12.501	12.062	11.507	11.130	10.316	7.467	17.15	15.98	16.44
99	J063204.66+045451.5	13.801	12.920	12.538	13.732	12.959	12.568	12.040	11.813	11.624	11.042	8.214	16.70	15.57	16.00
100	J063146.07+045430.7	14.001	13.176	12.874	13.982	13.269	12.965	12.917	12.783	12.817	12.749	—	16.98	15.83	16.45
101	J063150.25+050007.6	14.214	13.473	13.107	14.211	13.451	13.162	12.942	12.793	12.539	12.171	9.160	16.92	15.83	16.38
102	J063120.86+050408.5	14.068	13.227	12.711	14.357	13.464	12.947	12.188	11.974	11.745	11.030	7.401	16.91	15.85	16.35
103	J063138.78+045524.8	14.035	13.258	12.975	14.058	13.319	13.055	12.816	12.800	12.758	12.605	—	16.99	15.83	16.40
104	J063150.43+045150.1	14.224	13.339	12.796	14.298	13.412	12.836	12.244	11.963	11.805	11.460	7.143	17.20	16.14	16.35
105	J063220.79+045258.2	14.216	13.411	13.274	14.225	13.475	13.206	13.040	12.894	12.953	12.898	—	16.98	15.89	16.40
106	J063201.15+045527.3	14.148	13.344	13.143	14.205	13.467	13.206	12.904	12.744	12.644	12.230	—	16.82	15.75	16.28
107	J063214.81+044855.3	14.372	13.577	13.343	14.414	13.661	13.386	13.223	13.207	13.190	13.118	—	17.06	16.00	16.57
108	J063147.56+044907.7	14.301	13.588	13.256	14.266	13.545	13.266	13.054	13.053	12.933	13.158	—	17.13	16.02	16.62
109	J063155.25+045329.9	14.096	13.316	13.111	14.165	13.483	13.192	13.007	13.008	12.832	13.181	—	17.04	15.93	16.53
110	J063210.88+045706.1	14.403	13.620	13.388	14.370	13.632	13.381	13.272	13.228	13.069	13.100	—	17.01	16.00	16.48
111	J063155.81+045127.3	14.243	13.424	13.170	14.190	13.453	13.153	—	—	—	—	—	17.21	16.05	16.67
112	J063155.60+045517.2	—	—	—	14.432	13.608	13.198	12.722	12.632	12.374	11.877	7.660	17.02	15.98	16.42
113	J063145.37+045902.3	14.241	13.401	13.149	14.128	13.376	13.095	12.914	12.897	12.850	12.654	—	16.87	15.85	16.40
114	J063223.83+050613.6	—	—	—	15.675	15.018	15.046	—	—	—	—	—	—	—	—
115	J063157.60+050229.1	14.410	13.496	13.204	14.215	13.463	13.101	12.672	12.407	12.087	11.425	—	17.18	16.01	16.52
116	J063136.86+045104.3	13.634	12.650	12.059	13.423	12.552	11.873	11.592	11.124	10.527	9.288	5.913	16.11	15.08	15.63
117	J063229.24+050515.8	14.617	13.824	13.611	14.612	13.860	13.623	—	—	—	—	—	17.20	16.18	16.57
118	J063127.65+045402.7	13.936	13.154	12.815	13.941	13.204	12.901	12.751	12.682	12.573	12.435	—	17.07	15.78	16.45
119	J063200.57+050533.4	14.095	13.397	13.318	14.317	13.882	13.593	—	—	—	—	—	—	—	—
120	J063225.12+045514.3	14.380	13.563	13.084	14.572	13.780	13.338	12.442	12.229	11.896	11.361	9.181	17.37	16.31	16.91
121	J063155.51+045346.8	—	—	—	14.179	13.432	13.086	12.464	12.118	11.761	10.899	8.346	17.29	16.11	16.69
122	J063148.72+045520.9	14.588	13.742	13.412	14.496	13.758	13.472	—	—	—	—	—	17.18	16.11	16.65
123	J063200.47+045946.8	14.520	13.680	13.470	14.402	13.684	13.391	13.241	13.240	13.104	12.966	—	17.39	16.27	16.84
124	J063155.02+045320.8	14.212	13.328	13.102	14.208	13.457	13.121	12.971	12.931	12.809	12.797	—	17.17	15.98	16.59
125	J063209.91+045015.0	14.583	13.701	13.460	14.577	13.806	13.532	—	—	—	—	—	17.27	16.21	16.80
126	J063207.55+045615.2	14.122	13.328	13.088	14.132	13.388	13.076	12.919	13.091	12.725	12.872	—	17.31	16.06	16.70
127	J063210.91+045502.4	14.637	13.789	13.420	14.617	13.828	13.408	12.922	12.628	12.225	11.577	—	17.38	16.39	16.75
128	J063227.18+045241.8	14.786	14.079	13.887	14.876	14.131	13.884	—	—	—	—	—	17.31	16.32	16.87
129	J063147.43+045331.5	14.264	13.465	13.188	14.320	13.546	13.243	—	—	—	—	—	17.28	16.08	16.72
130	J063147.69+045649.7	14.228	13.387	13.127	14.235	13.486	13.183	12.958	12.886	12.768	12.915	—	17.36	16.10	16.74
131	J063205.07+045546.8	14.684	13.457	12.551	14.164	13.141	12.289	11.386	10.950	10.583	9.712	6.496	16.96	16.05	16.43
132	J063156.92+045302.0	14.515	13.563	13.179	14.369	13.481	12.957	12.400	12.098	11.742	11.229	—	17.26	16.16	16.73
133	J063201.83+045338.6	14.262	13.320	12.906	14.212	13.425	12.950	12.264	12.155	11.689	10.916	7.338	17.16	16.10	16.28
134	J063136.76+045309.9	14.746	13.675	13.160	14.802	13.929	13.490	12.853	12.515	12.105	11.087	7.671	17.70	16.49	17.14
135	J063154.59+045941.5	14.816	14.003	13.698	14.788	14.082	13.793	—	—	—	—	—	17.46	16.41	16.97
136	J063157.08+045436.4	14.388	13.529	13.363	14.381	13.618	13.323	13.186	13.140	13.159	13.063	—	17.36	16.18	16.78
137	J063208.28+045056.4	14.461	13.603	13.344	14.299	13.550	13.270	—	—	—	—	—	17.31	16.12	16.81
138	J063202.92+045853.9	14.372	13.588	13.341	14.457	13.694	13.417	13.148	13.165	12.972	13.113	—	17.45	16.19	16.82
139	J063152.00+045408.														

Star	Name	<i>J</i> mag	<i>H</i> mag	<i>K_S</i> mag	<i>J</i> mag	<i>H</i> mag	<i>K</i> mag	[3.6] mag	[4.5] mag	[5.8] mag	[8.0] mag	[24] mag	<i>r</i> mag	<i>i</i> mag	<i>H_α</i> mag
141	J063159.62+045216.8	14.161	13.353	13.160	14.168	13.439	13.127	12.868	12.845	12.745	12.589	—	16.95	15.86	16.39
142	J063139.61+045945.0	14.117	13.132	12.650	14.099	13.192	12.627	12.005	11.655	11.484	10.823	7.916	17.64	16.20	16.74
143	J063149.80+044906.8	14.372	13.501	13.216	14.389	13.630	13.303	13.024	12.993	13.035	12.890	—	17.47	16.18	16.81
144	J063159.69+045535.9	14.320	13.471	13.292	14.352	13.574	13.277	13.151	13.063	13.135	12.960	—	17.57	16.27	16.99
145	J063148.05+045048.3	14.152	13.253	12.763	14.311	13.427	12.843	12.194	11.725	11.129	10.210	7.033	17.53	16.20	16.48
146	J063143.56+045949.0	14.450	13.652	13.360	14.478	13.720	13.427	—	—	—	—	—	17.58	16.38	16.99
147	J063130.24+045148.3	14.612	13.623	13.190	14.649	13.799	13.227	12.300	11.916	11.651	11.116	7.916	17.94	16.73	17.15
148	J063137.21+045657.2	14.715	13.917	13.716	14.753	13.997	13.759	—	—	—	—	—	17.45	16.36	16.95
149	J063201.02+045731.7	14.608	13.633	13.142	14.863	13.929	13.374	12.493	12.220	11.762	11.106	—	17.57	16.42	16.86
150	J063147.45+045832.7	14.658	13.874	13.566	14.547	13.767	13.474	13.286	13.278	13.205	13.063	—	17.66	16.52	17.17
151	J063215.12+045957.4	14.490	13.672	13.364	14.397	13.616	13.336	13.158	13.142	13.115	12.801	—	—	—	—
152	J063147.58+045052.9	14.205	13.137	12.630	14.195	13.309	12.741	11.702	11.386	11.057	10.259	6.765	17.47	16.16	16.74
153	J063225.76+045823.1	14.358	13.491	13.229	14.260	13.493	13.209	—	—	—	—	—	17.64	16.24	16.99
154	J063222.26+044714.0	14.430	13.504	13.310	14.727	13.871	13.543	13.058	13.029	12.918	13.018	—	17.66	16.28	16.81
155	J063139.55+045338.5	14.619	13.622	13.050	14.648	13.782	13.142	12.363	12.351	11.923	10.994	—	17.81	16.72	16.65
156	J063209.32+045241.4	14.295	13.455	13.221	14.332	13.568	13.271	13.098	13.022	13.019	13.098	—	17.49	16.12	16.64
157	J063152.55+045817.2	14.522	13.732	13.447	14.563	13.818	13.511	13.249	13.224	13.000	13.174	—	17.61	16.41	17.01
158	J063156.78+045351.0	14.699	13.873	13.352	14.737	13.974	13.622	13.182	13.020	12.843	11.845	7.222	17.66	16.50	17.09
159	J063146.10+045750.7	14.687	13.913	13.679	14.697	13.968	13.676	—	—	—	—	—	17.67	16.53	17.13
160	J063132.09+045738.7	14.852	13.978	13.704	14.776	14.016	13.732	13.345	13.136	13.043	12.194	8.156	17.76	16.61	17.17
161	J063145.11+045126.2	14.905	14.127	13.837	14.823	14.070	13.788	—	—	—	—	—	17.93	16.68	17.38
162	J063158.14+044829.8	14.723	13.890	13.651	14.754	13.968	13.660	—	—	—	—	—	17.98	16.75	17.40
163	J063130.95+044848.3	14.606	13.687	13.194	14.638	13.811	13.364	12.800	12.529	12.239	11.073	8.170	17.95	16.60	17.24
164	J063212.21+045632.7	14.833	14.054	13.721	14.855	14.058	13.793	—	—	—	—	—	17.84	16.67	17.49
165	J063139.17+044959.4	14.824	13.662	12.933	14.950	13.964	13.211	12.508	12.107	11.811	10.929	7.308	18.06	16.86	16.92
166	J063148.89+045609.2	14.807	14.002	13.566	14.837	14.090	13.710	13.186	12.924	12.451	11.715	—	17.54	16.47	16.96
167	J063139.30+045400.9	14.418	13.613	13.346	14.512	13.755	13.446	—	—	—	—	—	17.74	16.42	17.09
168	J063230.05+045726.2	14.989	14.153	14.014	15.004	14.227	13.964	—	—	—	—	—	17.95	16.79	17.23
169	J063141.97+045416.2	—	—	—	14.713	13.988	13.676	—	—	—	—	—	18.06	16.79	17.11
170	J063124.42+045305.4	—	—	—	15.758	15.168	14.932	—	—	—	—	—	18.36	17.43	17.79
171	J063149.52+045200.0	15.281	14.458	14.273	15.150	14.414	14.144	—	—	—	—	—	17.86	16.78	17.47
172	J063148.31+045238.8	14.179	13.935	13.364	14.730	13.840	13.314	12.764	12.537	12.163	11.601	8.017	17.87	16.58	17.18
173	J063156.53+045428.3	14.811	13.949	13.687	14.755	13.979	13.680	13.509	13.518	13.381	13.221	—	17.97	16.67	17.37
174	J063141.13+045551.4	14.880	14.021	13.727	14.841	14.053	13.775	—	—	—	—	—	17.88	16.68	17.38
175	J063201.49+045445.0	14.569	13.656	13.124	14.485	13.643	13.118	12.249	11.855	11.504	10.507	7.474	17.62	16.40	16.98
176	J063201.10+045449.7	14.400	13.692	13.388	14.380	13.669	13.337	—	—	—	—	—	17.96	16.49	17.35
177	J063206.48+044846.5	14.792	13.873	13.565	14.652	13.842	13.547	13.494	13.403	13.308	13.082	—	17.84	16.58	17.33
178	J063141.57+045940.4	15.094	14.276	14.069	15.033	14.269	13.999	—	—	—	—	—	18.10	16.91	17.52
179	J063212.33+045721.7	15.176	14.072	13.443	14.837	13.953	13.527	12.504	12.107	11.746	11.155	8.541	18.08	16.79	17.37
180	J063226.57+045238.3	14.901	13.914	13.589	14.965	14.157	13.714	12.848	12.447	12.067	11.162	8.126	18.02	16.86	16.76
181	J063141.90+045046.1	15.021	14.184	13.789	14.874	14.093	13.646	13.350	13.116	12.986	12.530	8.148	18.26	17.01	17.44
182	J063212.85+045837.9	14.546	13.777	13.575	14.662	13.902	13.573	13.274	13.226	13.262	13.041	—	17.97	16.65	17.38
183	J063143.35+045724.8	15.181	14.273	13.911	15.249	14.376	13.979	13.313	13.063	12.816	12.298	—	18.06	16.81	17.35
184	J063153.77+044847.0	14.535	13.608	13.298	14.550	13.741	13.441	13.160	13.133	13.088	13.110	—	18.13	16.53	17.33
185	J063212.18+050139.8	15.252	14.317	13.934	15.196	14.436	14.036	13.635	13.188	12.821	12.319	—	18.22	17.04	17.68
186	J063144.91+045600.1	14.117	13.192	12.625	14.281	13.354	12.658	12.047	11.609	11.289	10.720	—	18.68	17.03	17.71
187	J063147.79+045223.9	15.149	14.101	13.367	14.877	13.949	13.325	12.580	12.027	11.495	10.633	7.767	18.41	17.10	17.66
188	J063150.35+045738.9	14.754	13.925	13.633	14.779	14.011	13.690	—	—	—	—	—	18.15	16.72	17.43
189	J063118.43+045440.1	14.932	14.086	13.652	14.942	14.113	13.704	—	—	—	—	—	18.48	17.27	17.66
190	J063204.46+045826.1	14.885	13.959	13.706	14.894	14.126	13.790	13.337	13.190	13.087	12.550	—	18.12	16.85	17.37
191	J063216.16+045920.0	14.761	13.856	13.535	14.685	13.862	13.446	13.077	12.803	12.436	11.524	7.253	17.87	16.62	17.37
192	J063156.86+045514.7	14.639	13.802	13.509	14.645	13.873	13.541	—	—	—	—	—	18.22	16.75	17.49
193	J063154.92+045136.1	15.152	14.241	14.037	15.166	14.324	13.967	—	—	—	—	—	18.26	17.00	17.18
194	J063230.12+045522.1	15.221	14.120	13.594	15.342	14.297	13.563	12.666	12.473	12.129	11.649	9.101	18.61	17.24	17.48
195	J063159.29+045137.5	15.057	14.254	14.002	15.104	14.344	14.016	—	—	—	—	—	17.97	16.75	17.50
196	J063139.87+045639.1	15.053	14.099	13.615	15.086	14.182	13.693	12.894	12.675	12.557	12.431	—	18.12	16.97	17.00
197	J063203.08+050134.8	—	—	—	15.115	14.204	13.626	13.038	12.731	12.296	11.431	7.793	18.42	17.15	17.30
198	J063206.98+044803.7	15.148	14.327	14.068	15.198	14.386	14.094	—	—	—	—	—	18.35	17.05	17.66
199	J063119.47+045309.6	14.828	13.963	13.574	14.851	14.011	13.699	—	—	—	—	—	18.29	16.86	17.55
200	J063158.91+045743.0	15.307	14.407	13.995	15.176	14.380	13.983	13.565	13.369	12.975	12.229	—	18.31	17.03	17.65
201	J063201.50+045502.2	15.170	14.232	13.953	15.187	14.417	14.109	—	—	—	—	—	18.13	16.88	17.46
202	J063142.58+045256.1	14.717	13.801	13.523	14.684	13.915	13.482	12.477	12.029	11.510	10.717	8.332	18.24	16.69	17.31
203	J063227.50+045251.3	14.791	13.810	13.291	14.810	13.927	13.361	12.506	12.305	11.828	11.318	8.036	17.95	16.72	16.88
204	J063158.89+045811.0	15.092	14.188	13.741	15.016	14.181	13.673	12.995	12.618	12.015	11.079	—	18.22	17.07	16.92
205	J063220.33+045320.7	—	—	—	16.371	15.790	15.621	—	—	—	—	—	18.57	17.65	17.78
206	J063205.07+045226.7	14.898	14.070	13.917	14.880	14.110	13.711	13.429	13.320	13.209	12.671	9.495	18.31	16.85	17.36
207	J063235.67+044745.8	16.015	14.689	13.978	15.453	14.280	13.573	12.815	12.250	11.677	10.606	7.075	—	—	—
208	J063130.72+045214.9	15.295	14.317	13.909	15.249	14.484	14.120	13.476	13.182	13.092	12.017	8.947	18.53	17.18	17.93
209	J063151.55+044727.9	15.185	14.235	13.511	15.253	14.222	13.510	12.406	11.785	11.306	10.358	7.449	18.71	17.2	

Star	Name	<i>J</i> mag	<i>H</i> mag	<i>K_S</i> mag	<i>J</i> mag	<i>H</i> mag	<i>K</i> mag	[3.6] mag	[4.5] mag	[5.8] mag	[8.0] mag	[24] mag	<i>r</i> mag	<i>i</i> mag	<i>H_α</i> mag
211	J063132.86+045949.4	14.692	13.605	12.884	14.831	13.623	12.586	11.782	11.281	11.074	10.411	7.183	17.53	16.46	17.04
212	J063224.01+045659.1	14.971	14.072	13.710	14.895	14.096	13.721	13.190	12.786	12.508	11.833	—	18.30	16.94	17.21
213	J063231.91+045109.0	15.632	14.511	13.928	15.446	14.433	13.815	13.146	12.828	12.641	12.037	8.787	18.80	17.41	17.78
214	J063222.70+045808.2	15.048	14.198	13.645	15.040	14.213	13.630	12.673	12.296	12.020	11.294	7.954	18.67	17.26	17.58
215	J063129.84+045110.6	15.015	13.671	12.738	14.962	13.799	12.645	11.434	10.849	10.390	9.858	6.408	19.13	17.61	17.46
216	J063125.45+044930.9	15.345	14.550	14.154	15.206	14.393	13.981	13.424	13.167	12.756	12.007	—	18.84	17.45	17.80
217	J063147.36+044943.6	—	—	—	15.631	14.849	14.562	—	—	—	—	—	18.95	17.59	18.21
218	J063210.36+045205.8	15.246	14.210	13.833	15.127	14.188	13.635	12.966	12.623	12.234	11.533	9.052	18.64	17.14	17.66
219	J063159.35+044954.9	15.098	14.160	13.819	15.317	14.441	13.968	13.398	13.154	12.654	12.137	—	18.77	17.41	17.89
220	J063158.73+045346.8	15.676	14.596	14.014	15.615	14.666	14.110	13.389	13.171	12.940	12.520	—	18.99	17.49	18.04
221	J063129.40+045034.8	15.592	14.708	14.524	15.642	14.889	14.560	—	—	—	—	—	19.45	17.88	18.83
222	J063231.50+045453.2	15.803	14.754	14.115	15.686	14.751	14.018	13.059	12.606	12.599	12.284	—	18.76	17.80	16.72
223	J063232.66+045701.0	15.437	14.670	14.346	15.452	14.702	14.341	14.166	13.750	13.465	12.783	—	19.67	17.65	18.39
224	J063136.58+050515.3	14.963	13.909	13.352	14.874	14.010	13.352	—	—	—	—	—	19.13	17.20	17.80
225	J063208.95+050151.3	—	—	—	15.208	14.300	13.794	—	—	—	—	—	—	—	—
226	J063157.57+045339.0	15.458	14.236	13.682	15.555	14.477	13.819	12.786	12.435	12.041	11.019	—	18.33	16.95	17.62
227	J063156.58+045951.4	—	—	—	15.546	14.771	14.449	—	—	—	—	—	—	—	—
228	J063223.92+045420.9	15.729	14.817	14.505	15.820	14.977	14.412	13.802	13.651	13.269	12.451	—	19.16	17.81	17.42
229	J063143.35+045422.9	15.681	14.541	14.115	15.881	14.983	14.313	13.340	12.973	12.878	12.333	8.816	19.65	18.16	18.66
230	J063132.47+050605.6	15.521	14.313	13.610	15.017	14.195	13.583	—	—	—	—	—	19.59	17.67	17.98
231	J063141.05+045419.8	15.119	14.184	13.765	15.715	14.768	14.024	12.998	12.679	12.330	11.334	—	19.79	17.95	18.78
232	J063158.09+045414.9	16.183	14.676	13.719	15.981	14.687	13.707	12.477	11.986	11.488	10.882	8.869	—	—	—
233	J063148.53+050407.2	15.631	14.840	14.229	15.956	15.110	14.548	14.097	13.897	13.686	12.956	9.021	19.34	17.70	18.27
234	J063155.47+050054.1	15.802	14.731	14.218	17.567	15.391	14.548	13.238	12.860	12.560	12.031	—	18.91	17.68	17.21
235	J063159.68+050627.2	15.255	14.223	13.831	15.335	14.418	13.868	—	—	—	—	—	19.68	17.78	18.71
236	J063230.20+045401.2	15.550	14.586	13.858	16.199	15.033	14.001	12.760	12.289	11.905	11.308	7.806	—	—	—
237	J063149.00+045547.0	15.626	14.726	14.111	15.598	14.818	14.333	13.808	13.465	13.183	12.442	—	—	—	—
238	J063203.65+045952.1	—	—	—	15.650	14.755	14.151	13.639	13.176	12.822	12.300	—	—	—	—
239	J063138.33+050256.5	15.284	14.229	13.665	15.281	14.345	13.640	12.861	12.543	12.154	11.459	—	19.75	17.73	18.38
240	J063219.28+045629.4	—	—	—	16.325	15.495	14.984	—	—	—	—	—	19.73	18.37	17.59
241	J063207.16+045514.4	—	—	—	16.120	15.231	14.658	14.444	14.033	13.752	12.758	9.224	—	—	—
242	J063128.39+045035.1	16.038	15.049	14.361	16.009	15.053	14.250	13.198	12.688	12.127	11.468	8.130	—	—	—
243	J063211.98+050030.9	—	—	—	15.460	14.286	13.403	13.285	12.081	11.079	9.951	6.449	19.56	18.57	18.56
244	J063219.98+045748.3	—	—	—	16.182	15.293	14.618	13.802	13.329	13.099	12.733	—	—	—	—
245	J063228.81+045255.9	—	—	—	16.086	15.234	14.743	14.195	13.905	13.566	13.154	—	—	—	—

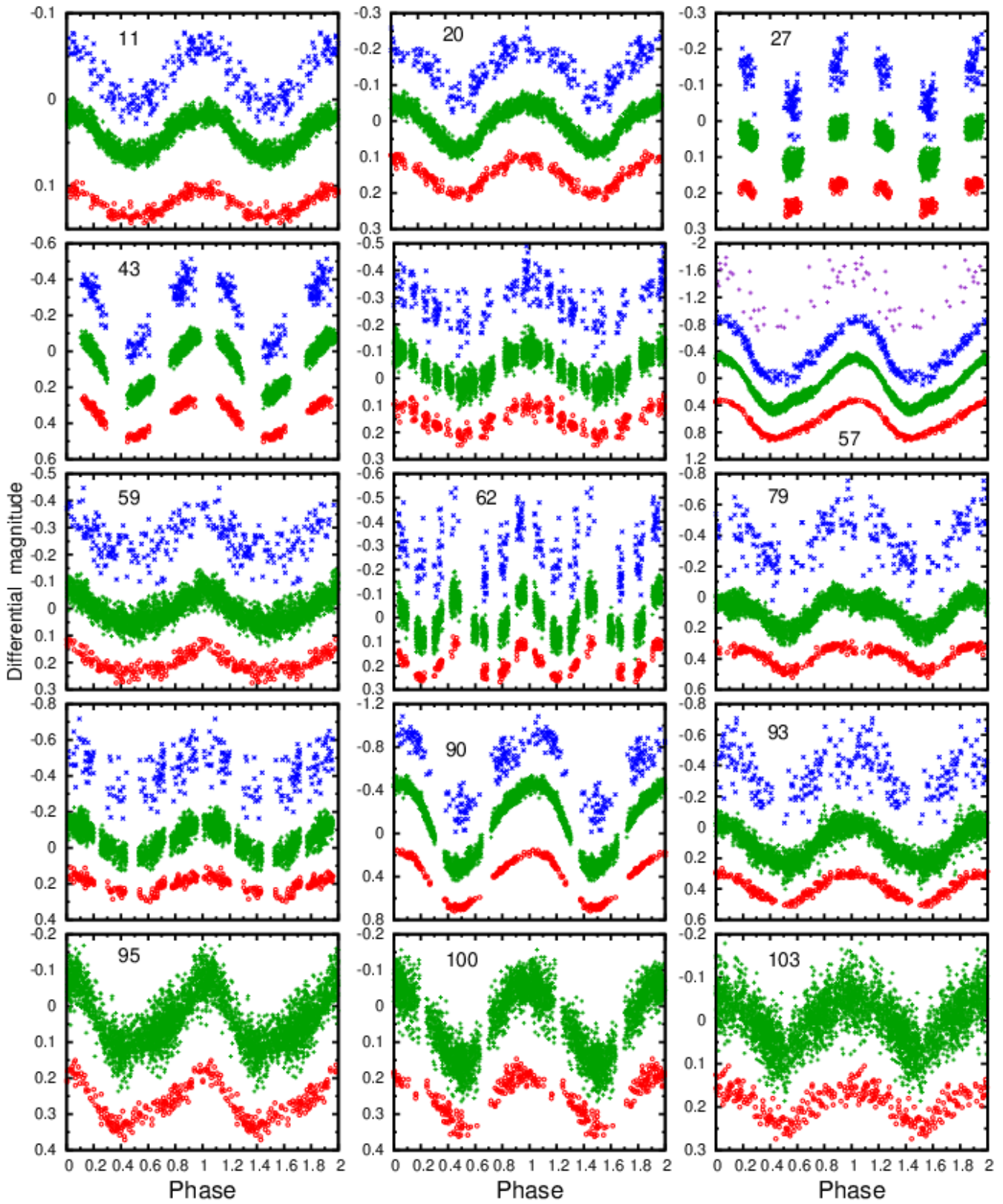


Figure A1. Phase diagrams of *B* (blue), *V* (green) and *I* (red) observations of other periodic variables found in observed field of NGC 2244 (see Sect. 3.3).

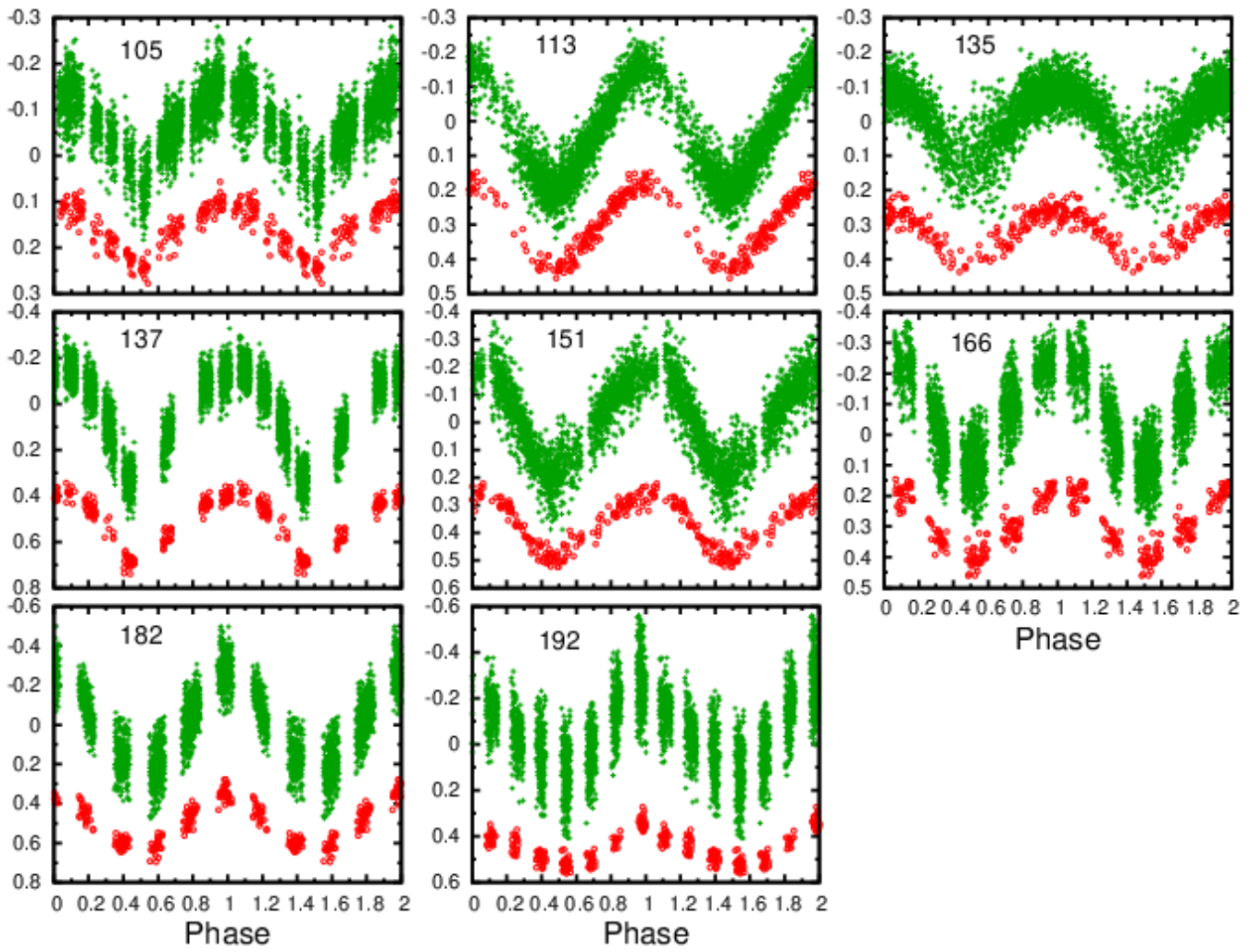


Figure A1 – continued

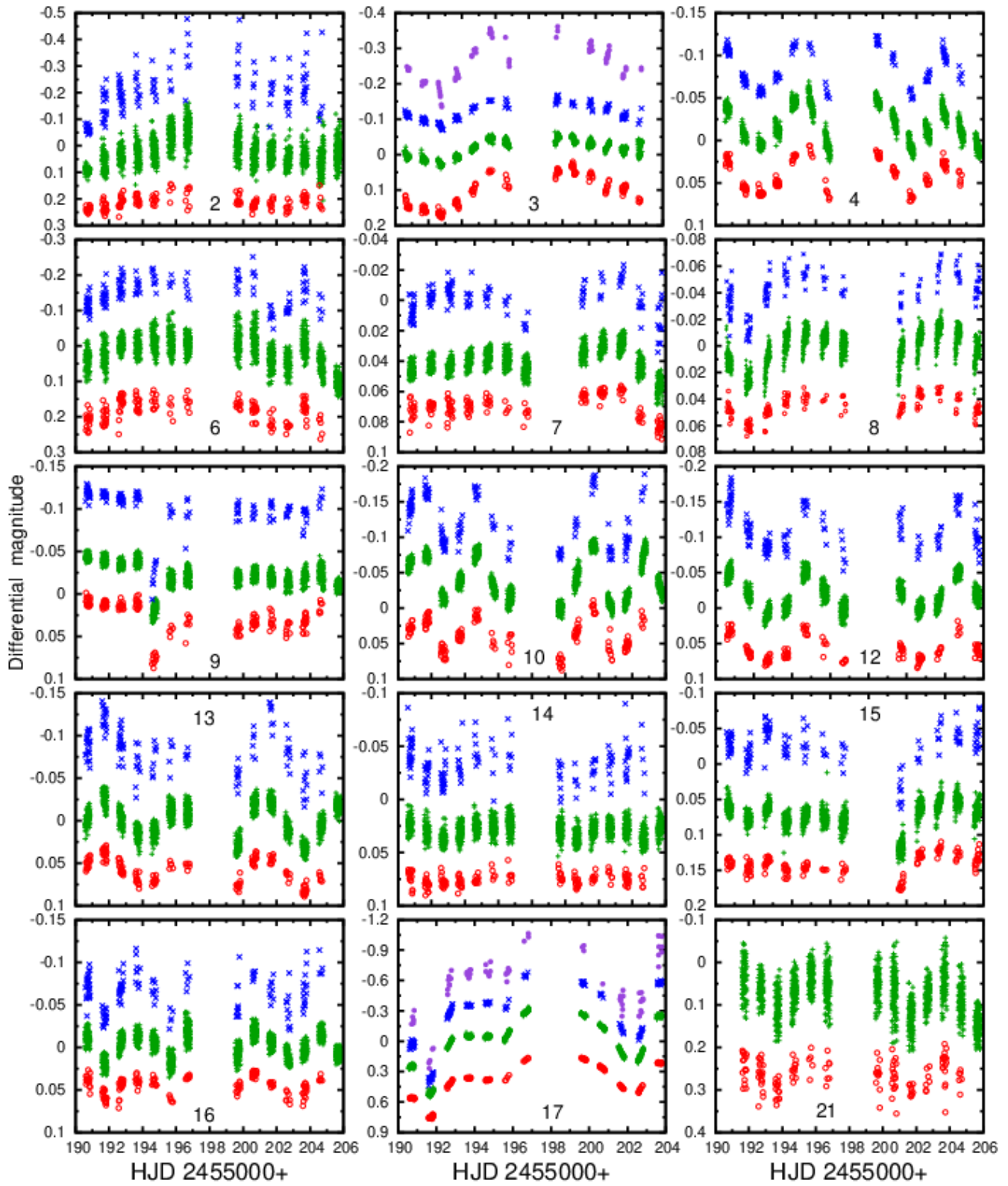


Figure A2. Light curves of *B* (blue), *V* (green) and *I* (red) observations of irregular variables found in observed field of NGC 2244 (see Sect. 3.4).

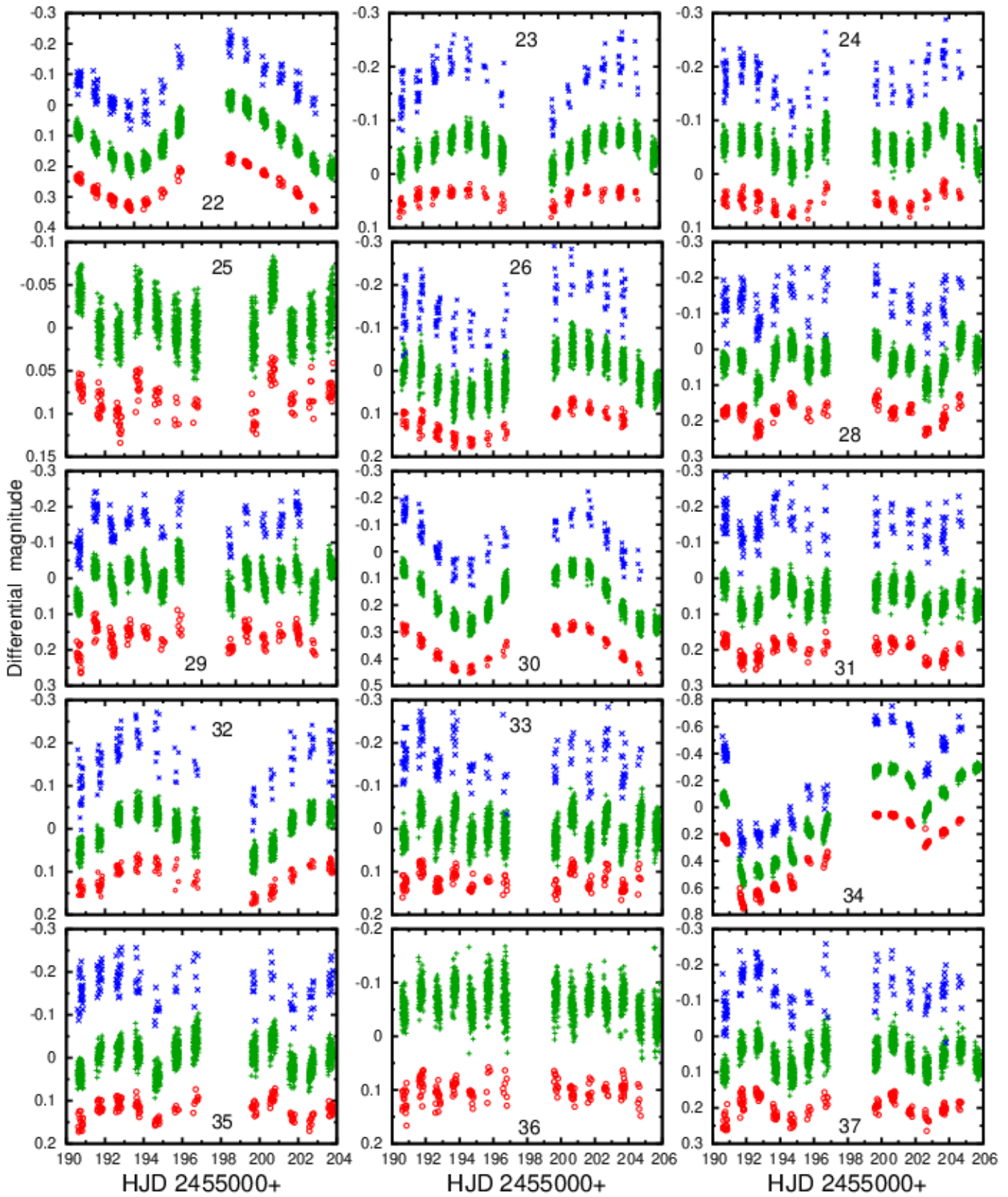


Figure A2 – *continued*

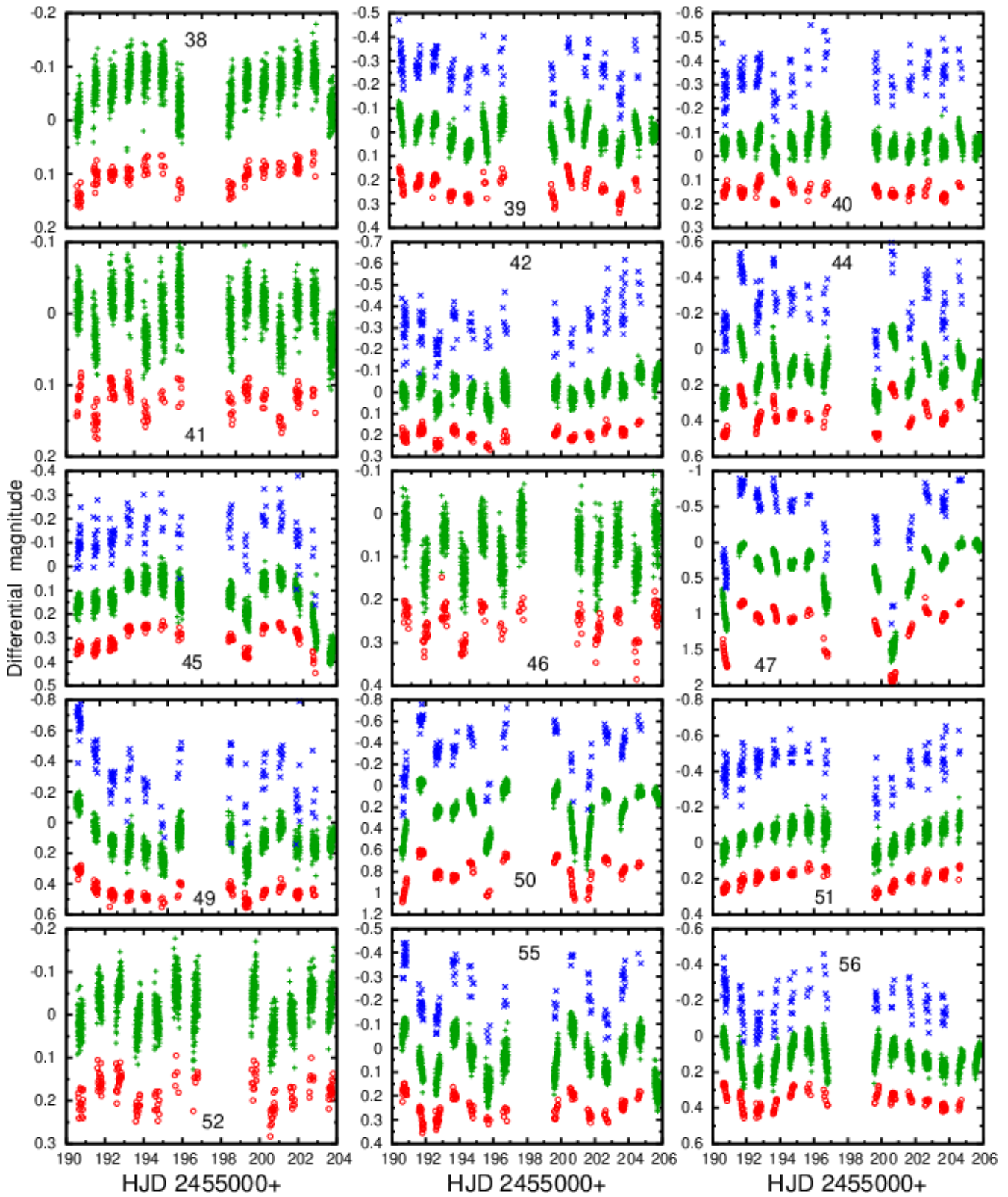


Figure A2 – continued

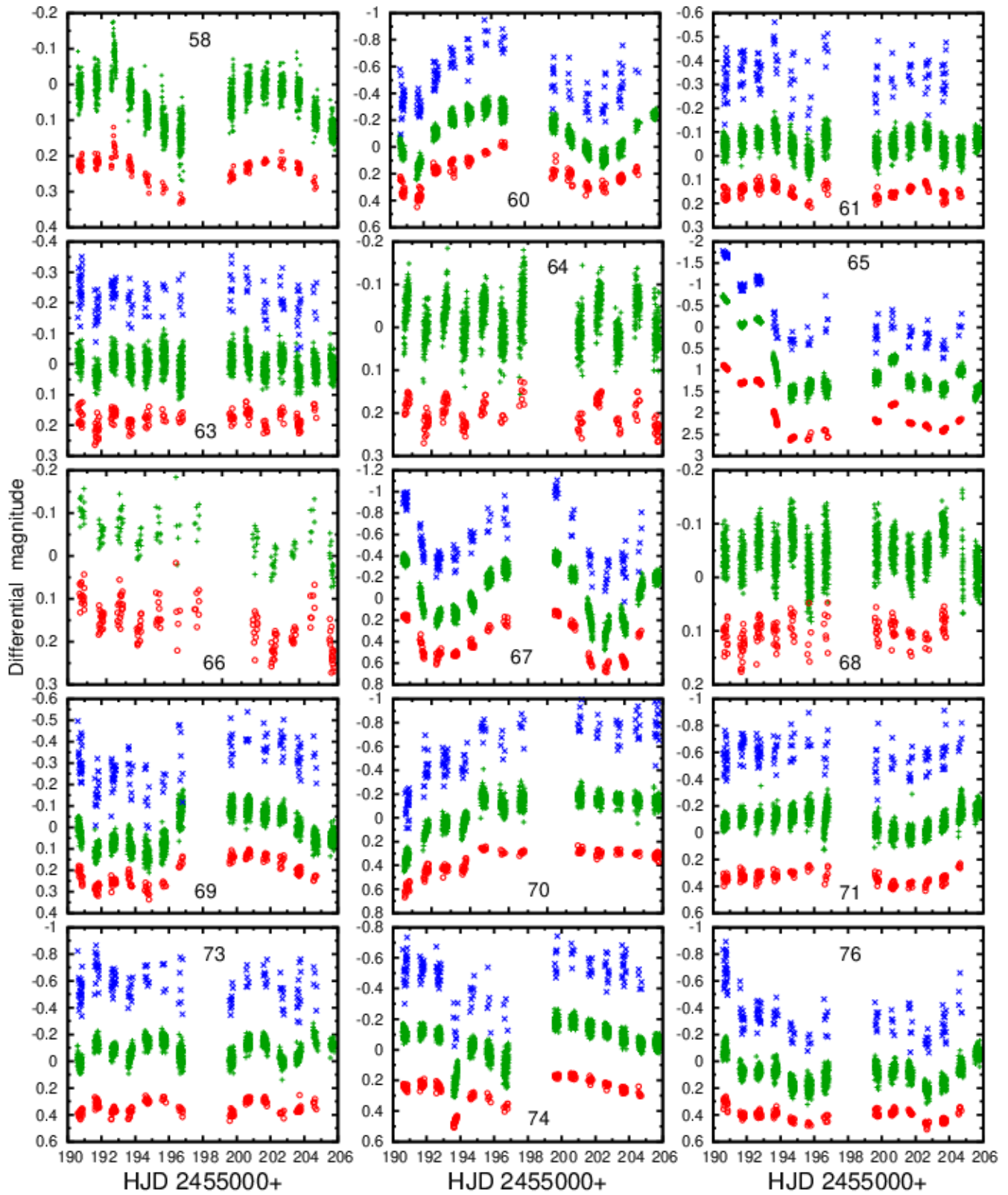


Figure A2 – continued

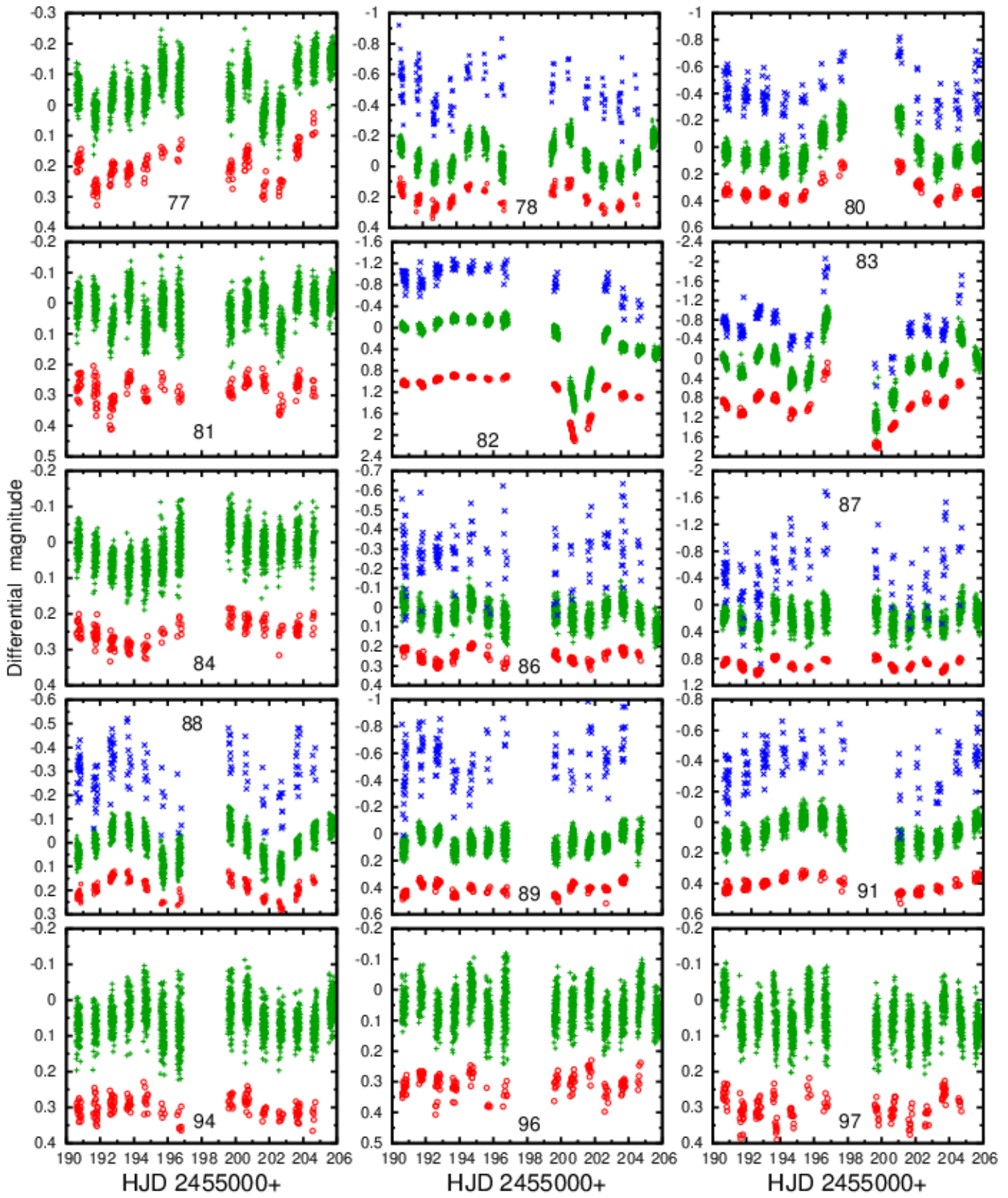


Figure A2 – continued

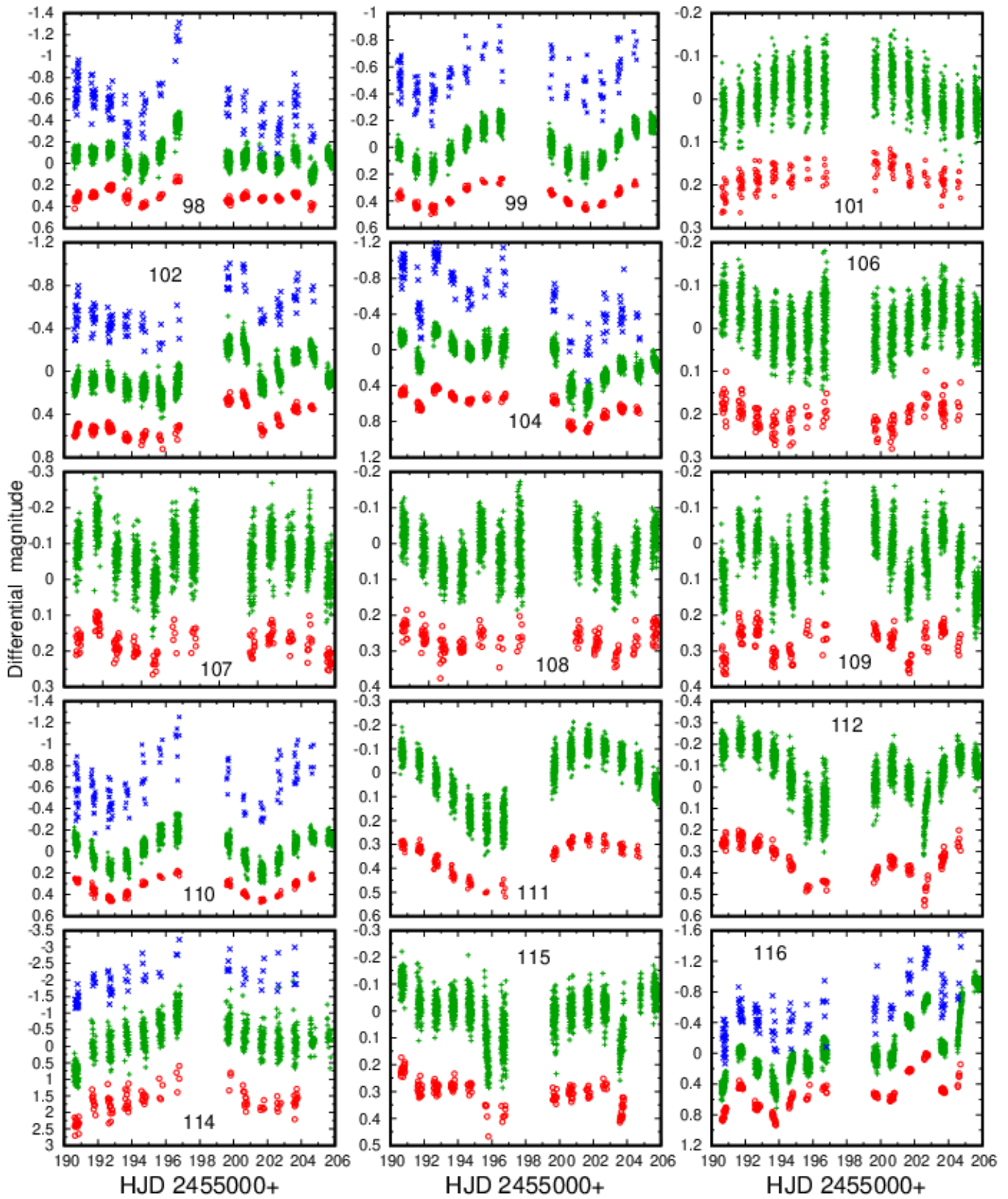


Figure A2 – *continued*

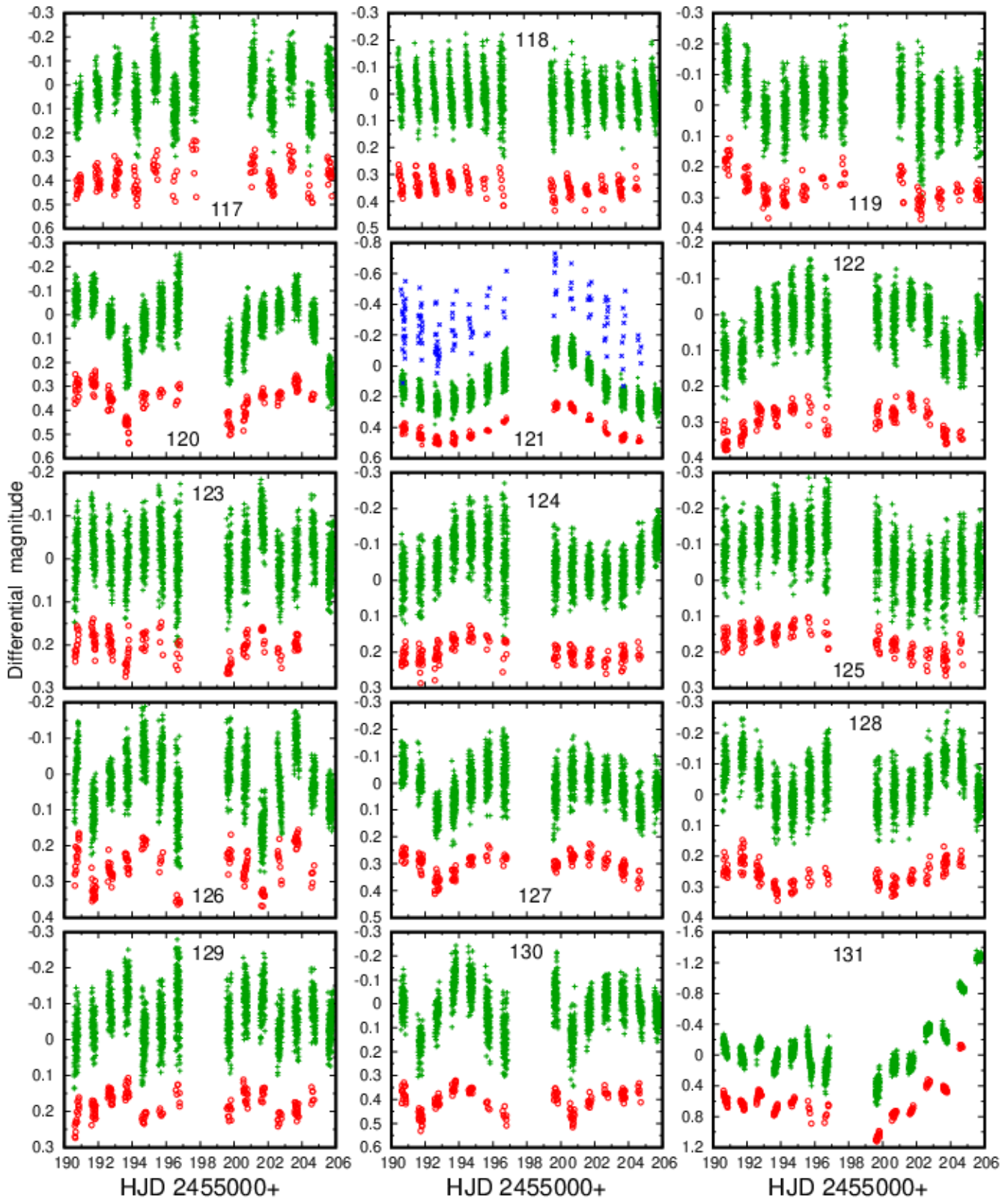


Figure A2 – continued

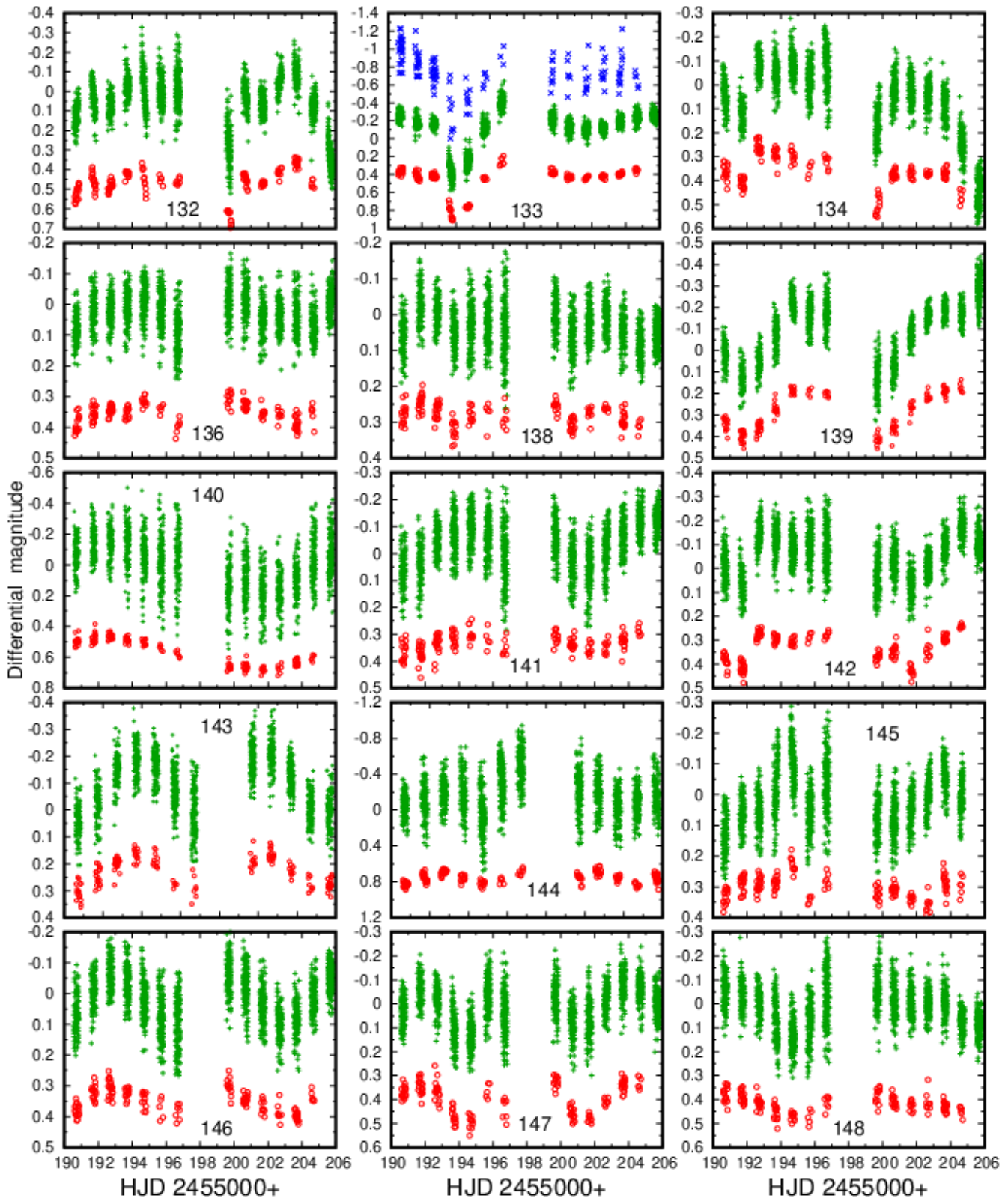


Figure A2 – *continued*

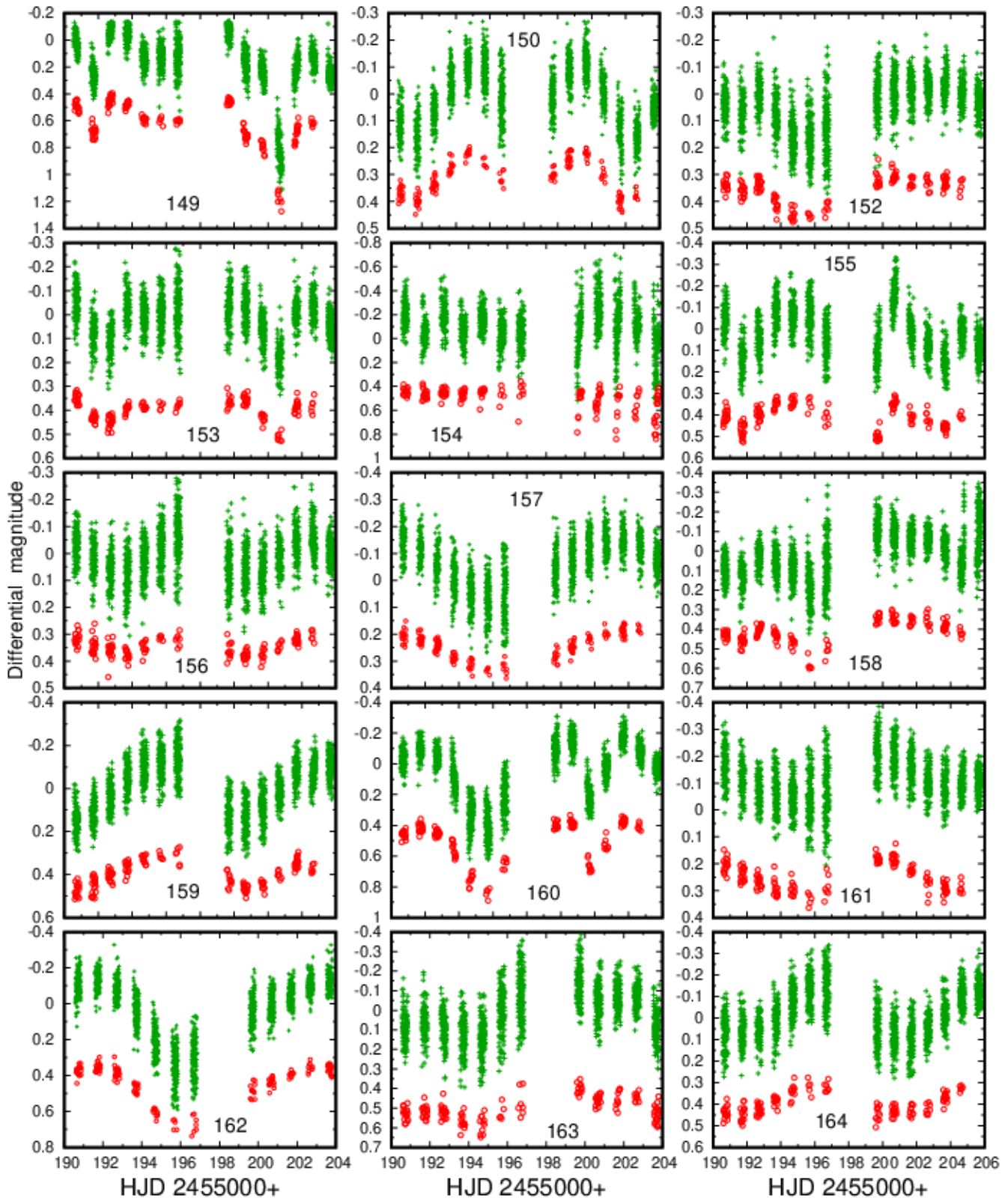


Figure A2 – continued

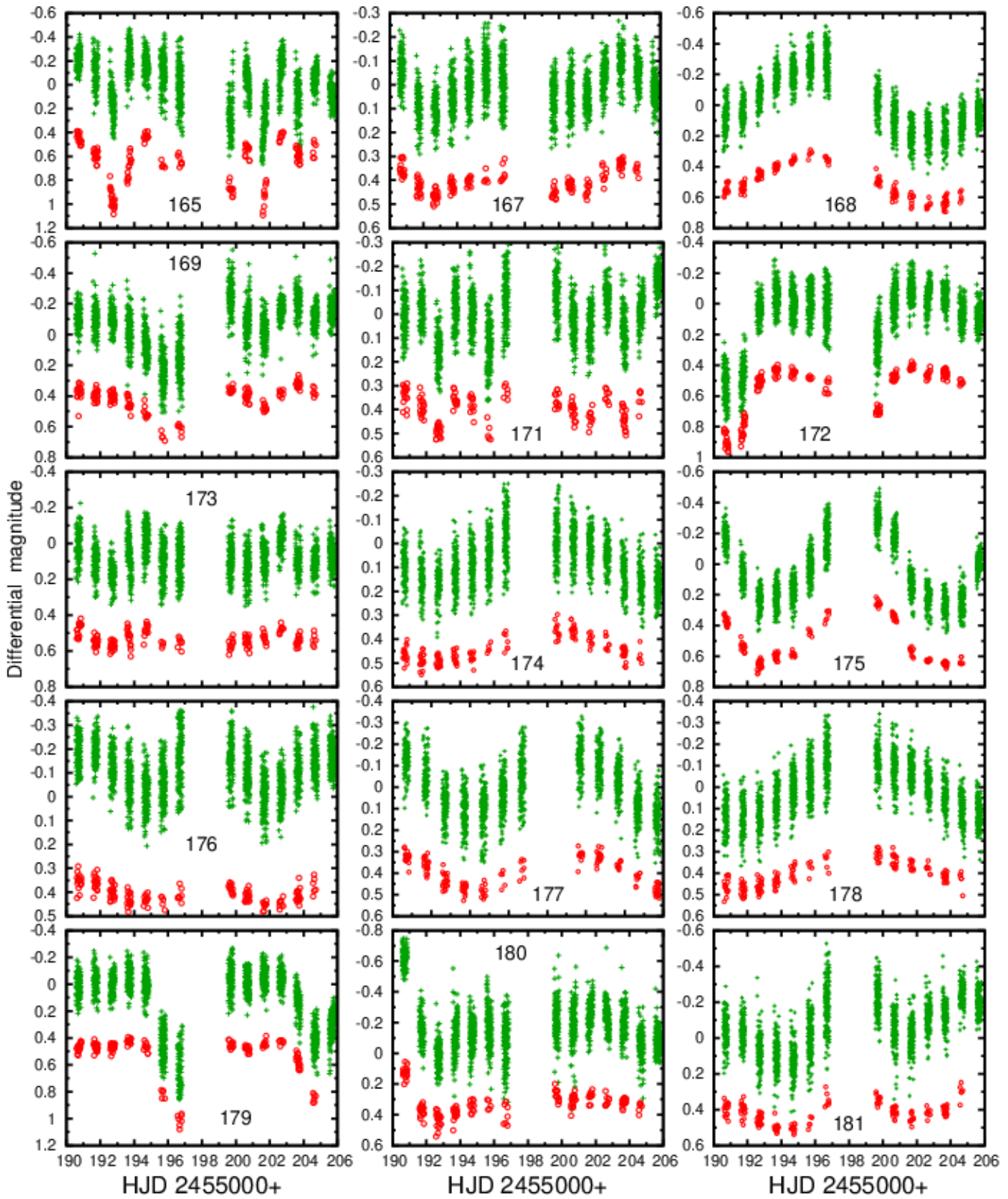


Figure A2 – *continued*

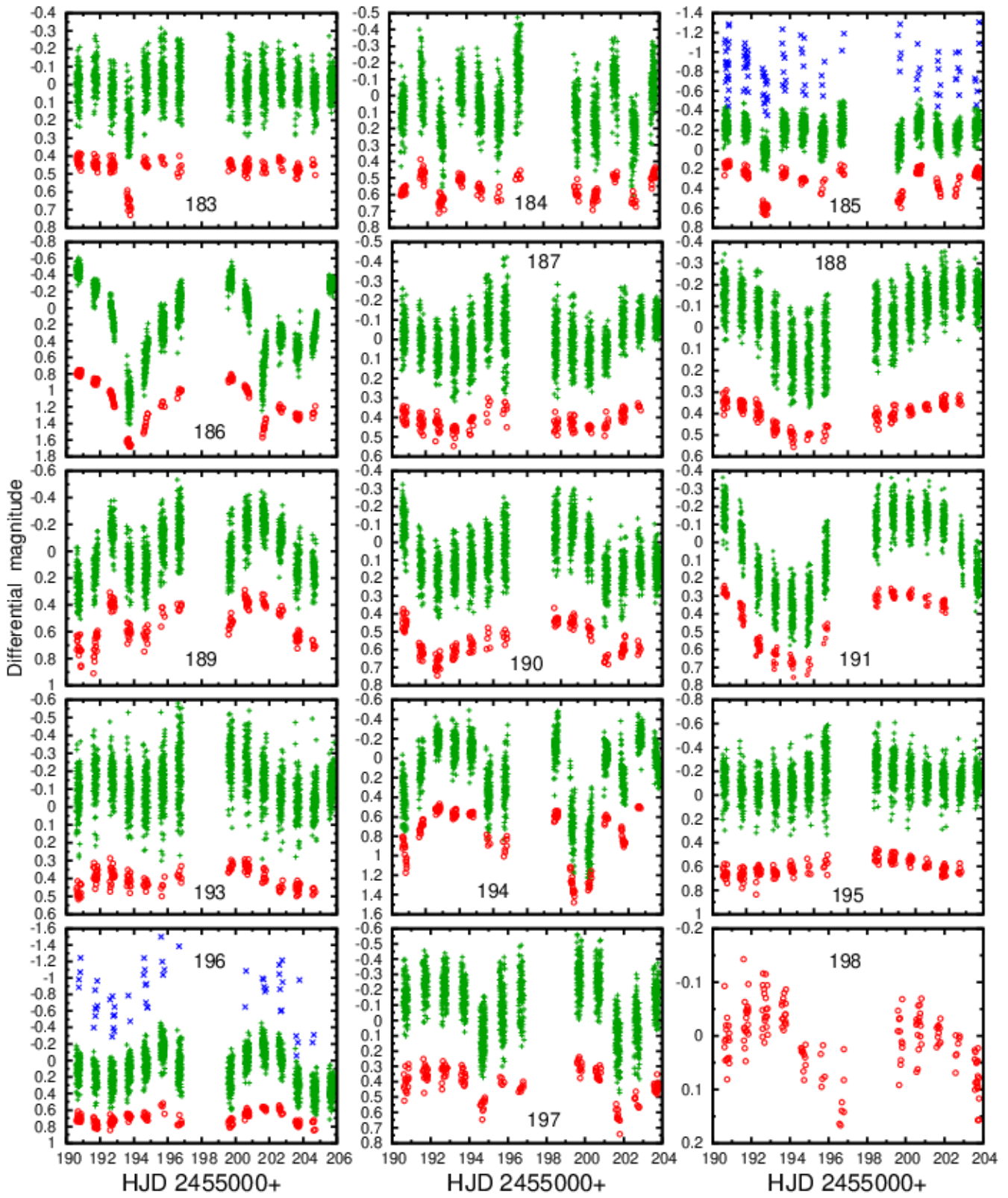


Figure A2 – continued

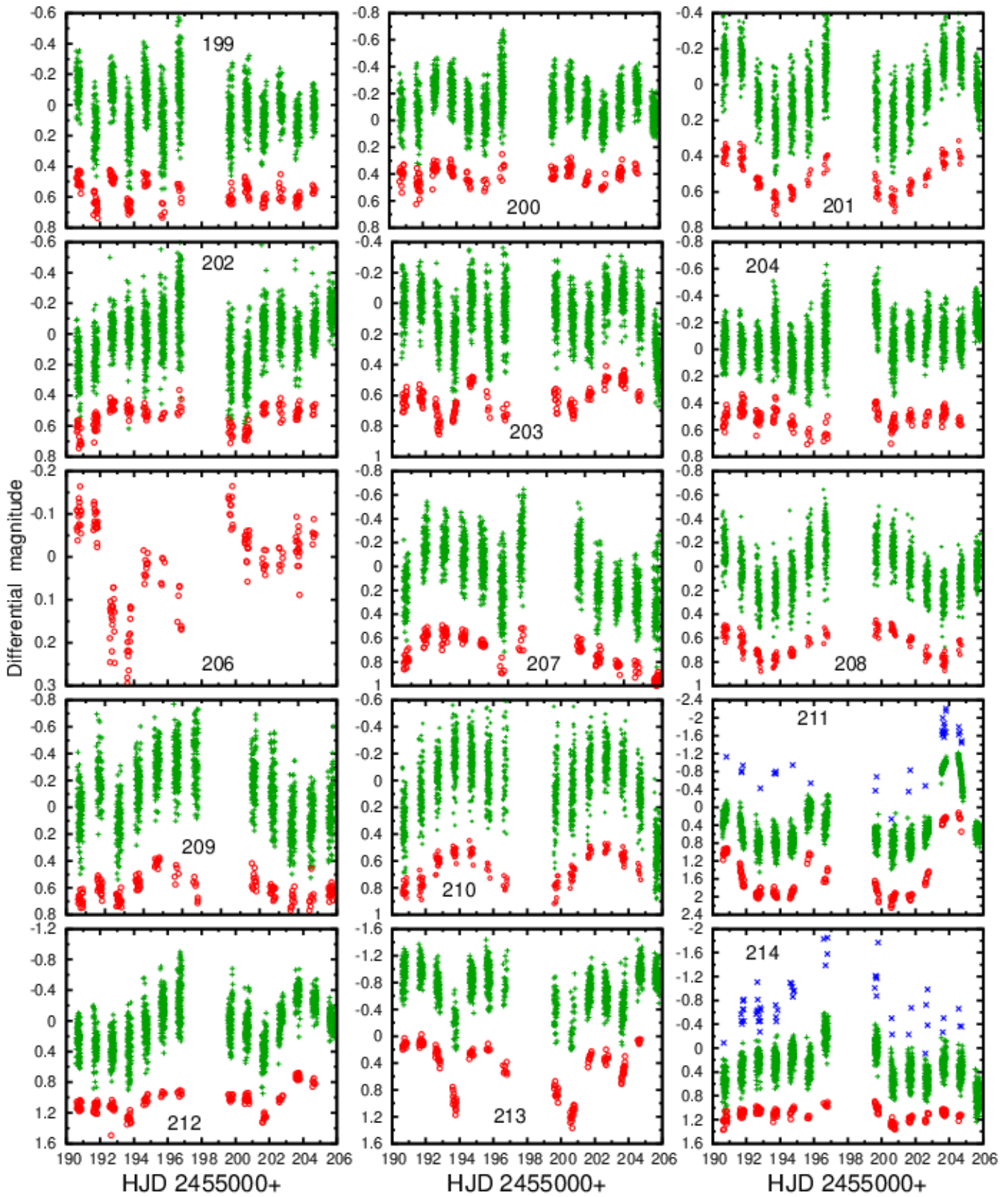


Figure A2 – continued

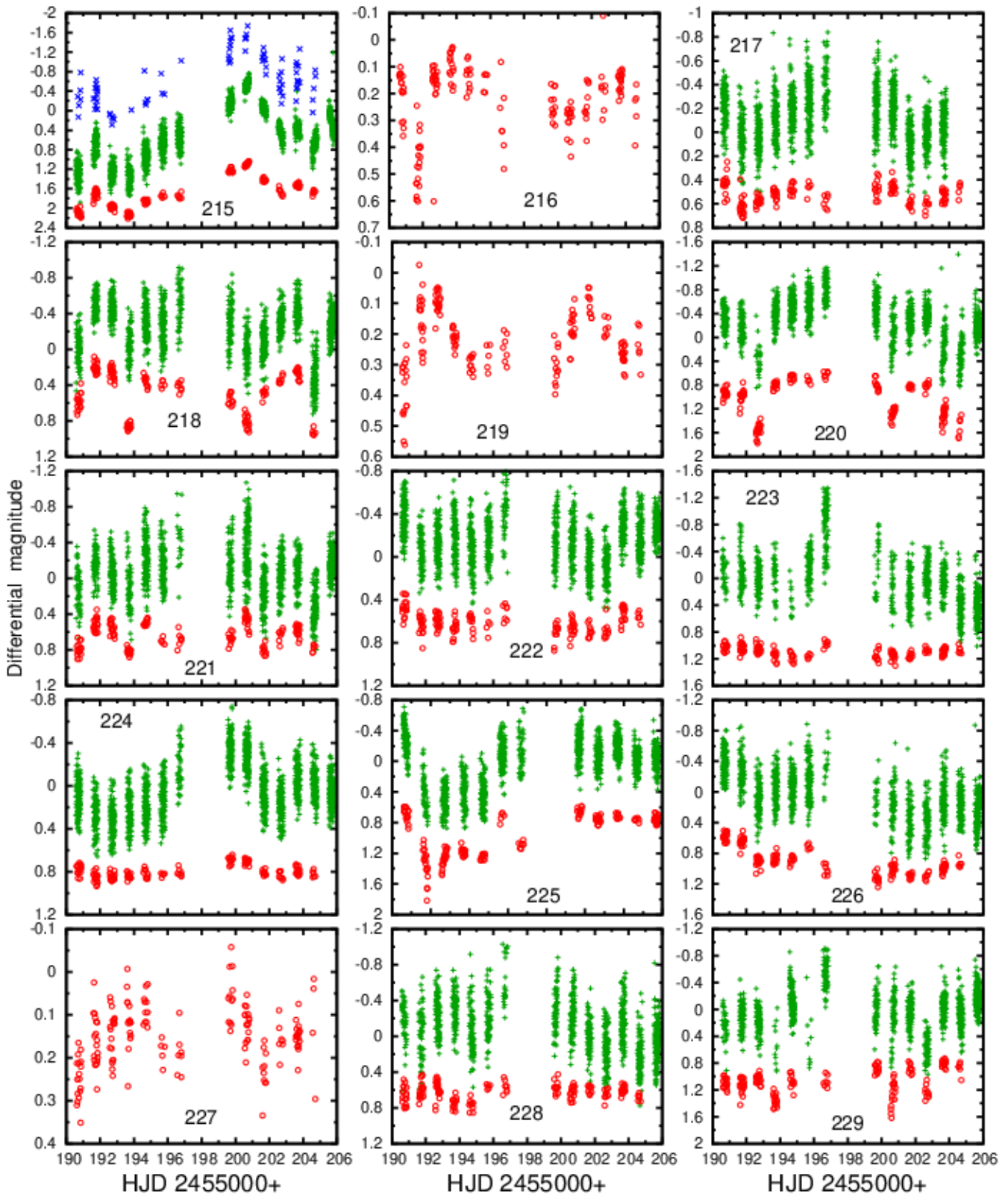


Figure A2 – continued

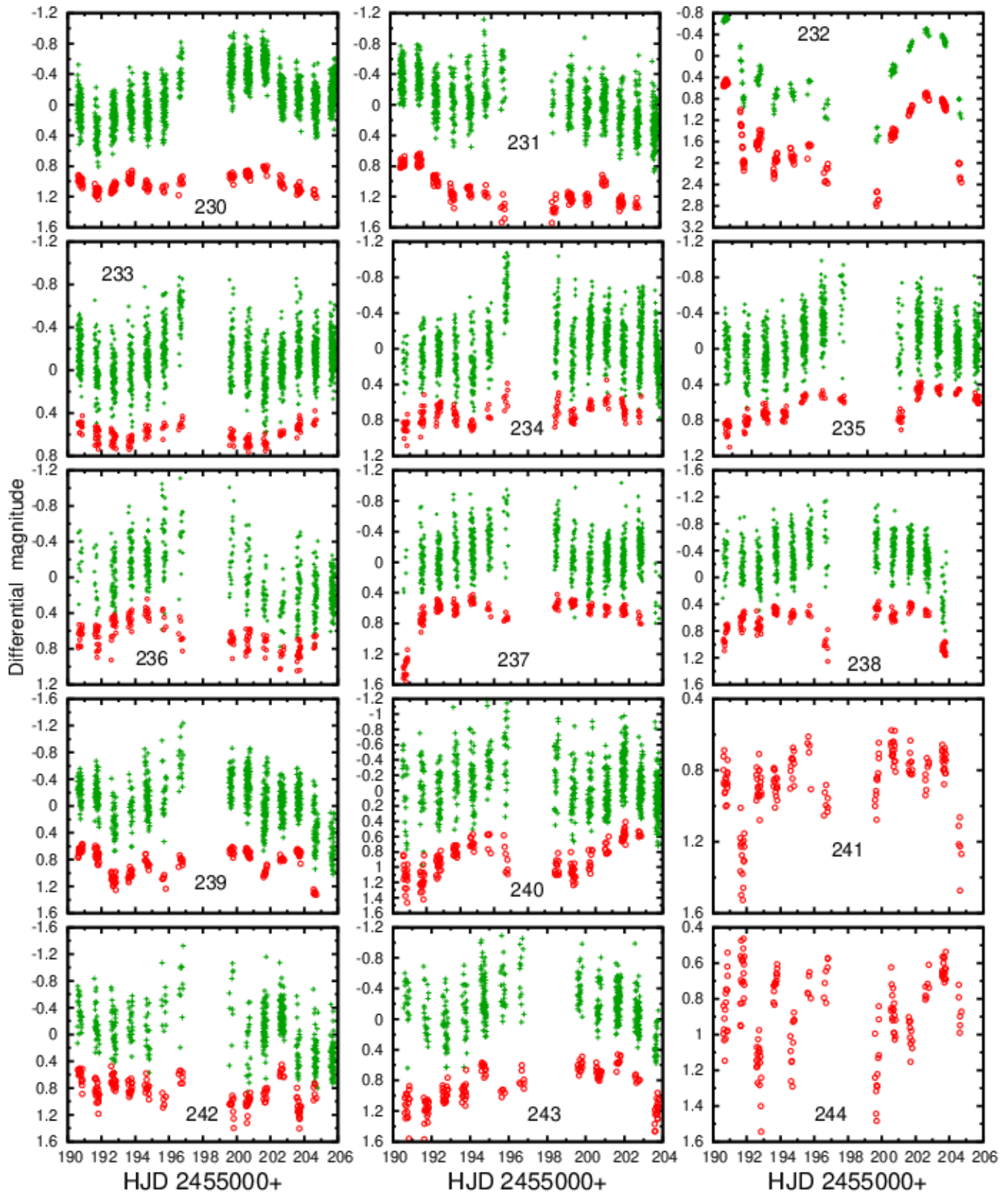


Figure A2 – continued

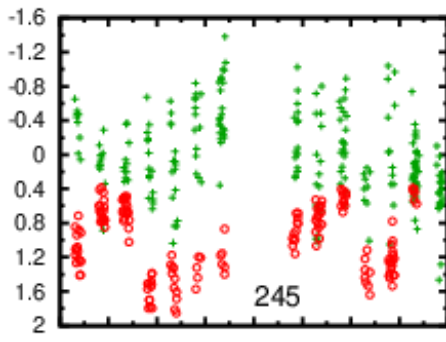


Figure A2 – continued